ABSTRACT

BEHROOZ, MEHRNOOSH. Acid Mine Drainage at Ore Knob Tailings Pile– Hydrologic and Geochemical Characterization and Bioremediation. (Under the direction of Professor Robert C. Borden).

Acid Mine Drainage (AMD) is produced in the vadose zone of the Ore Knob Mine tailings pile (Ashe County, NC) by oxidation of sulfide minerals and subsequent transport of the AMD to the water table within the pile. Surface water from the upstream watershed enters the pile through a series of pools or wetlands on the pile perimeter and rapidly transports the AMD through the pile to the downstream embankment face. Water discharges the embankment face as a series of seeps or springs with high levels of dissolved Fe, SO_4, acidity, Cu, and Zn and impairs water quality in 1.5 km of Ore Knob Branch and 4.7 km of Peak Creek feeding the New River. In this work, a detailed hydrological and chemical characterization was performed to better understand the physical and chemical processes controlling AMD generation within the tailings pile. This information was then used to develop a remediation process that could be used to treat AMD within the tailings pile without the high capital and operating costs associated with traditional treatment approaches.

Spatial variations in the physical and hydraulic characteristics of the Ore Knob tailings cause large variations in water and oxygen transport, with associated changes in the amount and concentration of AMD produced. Tailings in the upstream areas are finer grained, with lower air filled porosity and oxygen diffusivity, which reduces the rate of sulfide mineral oxidation. In downstream areas near the embankment face, the original tailings were coarse grained, with lower water retention and high oxygen diffusivity, increasing the oxidation rate. However, weathering processes have increased the fine grained fraction in the oxidized zone and hardpan layer, increasing water retention and lowering

oxygen diffusivity. The greater thickness of the downstream oxidized zone combined with increased water retention due to weathering may have significantly reduced acid generation in these areas.

The water budget model DRAINMOD was calibrated using soil physical properties and meteorological data and used to estimate recharge rates on the tailings pile surface and upstream watersheds that drain into the pile. This information was then used to calibrate the groundwater flow model, MODFLOW, to help understand water movement within the pile and the impact of different remediation alternatives on water distribution and movement. Recharge rates were higher in the coarse grained areas and lower in fine grained areas. Infiltrating water transports AMD constituents from the vadose zone where they are discharged to the water table within the pile. Surface water that enters the pile from upstream areas then transports the AMD constituents to the downstream embankment face where these constituents are discharged to surface water.

A pollutant load analysis using the recharge analysis results and average long term monitoring results showed that over 89% of the Fe, SO_4, acidity, and Al released to the Ore Knob Branch are produced in the vadose zone of the pile. The total annual load of acidity discharged from the Ore Knob tailings pile is estimated to be over 220 tons/yr. Given the very high levels of dissolved Fe and acidity produced within the pile, traditional end-of-pipe treatment approaches will have very high capital and operating costs. An affordable passive treatment method is needed to treat AMD within the pile before it is discharged to the surface.

A 20 month long in situ pilot test was conducted to evaluate the surface application of waste glycerol (WG) to reduce release of acid mine drainage (AMD) constituents from mine tailings. Beneficial characteristics of the WG include high aqueous solubility, high organic content, and high alkalinity. Four columns were packed with fine grained sulfide rich tailings and incubated in the field under ambient temperature and precipitation conditions. Columns were periodically pumped to maintain unsaturated condition. In the two replicate untreated control columns, diffusion of oxygen into the tailings resulted in large increases in dissolved Fe, SO_4, Mn, Mg, Al, Zn, and hydrogen peroxide acidity with an associated drop in pH. In the two replicate treated columns, WG was blended into the top 0.18 m of tailings seven months after the columns were established, resulting in large reductions in Fe, SO_4, hydrogen peroxide acidity, Al, Cu, and Mn. Observed pollutant reductions resulted from a combination of processes including: (a) neutralization of acidity by the KOH present in the WG (b) reduction of SO_4 to H_2S with subsequent precipitation of dissolved metals, and potentially (c) consumption of oxygen, slowing oxidation of the tailings.

Acid Mine Drainage at Ore Knob Tailings Pile – Hydrologic and Geochemical Characterization and Bioremediation

by
Seyedeh Mehrnoosh Behrooz

A dissertation submitted to the Graduate Faculty of
North Carolina State University
in partial fulfillment of the
requirements for the degree of
Doctor of Philosophy

Civil Engineering

Raleigh, North Carolina

2012

APPROVED BY:

Robert C Borden Committee Chair	Morton Barlaz
Kumar Mahinthakumar	Dean L. Hesterberg

BIOGRAPHY

Mehrnoosh Behrooz is a graduate research assistant at North Carolina State University fulfilling the requirements for her Ph.D. in Environmental Engineering with a minor in Soil Science under supervision of Professor Robert C Borden. She is originally from Tehran, Iran. Mehrnoosh has a M.Sc. in water and wastewater treatment from Sharif University of Technology and a B.Sc. in Chemical Engineering from University of Tehran.

ACKNOWLEDGMENTS

I would like to express a special gratitude to Dr. Robert C Borden for his kindness, endless support, and his precious lessons not only in professional and technical fields but also in personal life.

I appreciate Dr. Barlaz, Dr. Kumar and, Dr. Hesterberg for accepting to be in my doctoral committee and evaluating my research.

I would like to thank Dr. Aziz Amoozegar, David Black, Lisa Lentz, Guillermo Rodriguez, and Roberto Garcia for their help and support in sample and data analysis.

I appreciate Ronda Underwood for her help and dedication during sample collection and analysis.

I also would like to thank the North Carolina Department of Natural Resources, U.S. Environmental Protection Agency, and United Soybean Oil for the financial and technical support they provided for this project.

TABLE OF CONTENTS

LIST OF TABLES vi
LIST OF FIGURES vii
CHAPTER 1 1
1. OVERVIEW 1
1.1 Introduction and Site History 1
1.2 Chemistry of Acid Mine Drainage Generation 2
1.2.1 Acid Producing Reactions 2
1.2.2 Secondary Mineral Precipitation 3
1.2.3 Hardpan Formation 4
1.3 Acid Mine Drainage Prevention and Treatment 4
1.4 Research Hypothesis and Objectives 7
1.5 Thesis Content 8
CHAPTER 2 9
2. PHYSICAL, HYDROLOGIC, AND AQUEOUS CHEMICAL CHARACTERIZATION OF THE ORE KNOB TAILINGS PILE (ASHE COUNTY, NORTH CAROLINA, USA) 9
2.1 Introduction 9
2.2 The Ore Knob Mine and Tailings Pile 11
2.3 Methods 15
2.4 Tailings Physical and Hydrologic Characteristics 19
2.5 Effect of Weathering on Physical and Hydraulic Characteristics 22
2.6 Water Flow through the Tailings Pile 27
2.7 Modeling Recharge and Water Flow through the Tailings Pile 29
2.8 Subsurface and Surface Water Quality 34
2.8.1 Ground Water 34
2.8.2 Surface Water 36
2.9 Pollutant Budgets 39
2.10 Discussion and Conclusions 41
CHAPTER 3 43
3. WASTE GLYCEROL ADDITION TO REDUCE AMD PRODUCTION IN UNSATURATED MINE TAILINGS 43
3.1 Introduction 43

3.2 Materials and Methods 45
3.3 Experimental Results 48
3.3.1 Column Installation and Material Properties 48
3.3.2 Major Anions and Cations in the Column Effluent 49
3.3.3 Mineral Precipitation 61
3.4 Potential Field Application 63
3.5 Conclusions and Applications 66
CHAPTER 4 68
4. GEOCHEMICAL CHARACTERIZATION 68
4.1 Introduction 68
4.2 Methods 68
4.3 X-Ray Diffraction Results 69
4.4 Acid Extraction Results 71
CHAPTER 5 74
5. SUMMARY AND CONCLUSION 74
CHAPTER 6 77
6. FUTURE WORK 77
REFERENCES 79
APPENDIX 90
Appendix A- Aquatic Geochemistry 91
Appendix B- Experimental Columns 94
Appendix C- DRAINMOD Software 103
Appendix D- MIN3P Software 107

LIST OF TABLES

Table 2.1 Vadose zone permeability results 21

Table 2.2 Physical properties of fine grained (MW10) and coarse grained (MW13) Tailings 25

Table 2.3 Average dissolved pollutant budget for Ore Knob Mine tailings pile 39

Table 4.1 Detected minerals and related chemical formula.....67

Table S.A.1 Appendix A– Average composition of saturated pore water in tailings pile.....88

Table S.A.2 Appendix A– Average parameter values in surface water monitoring stations within the Peak Creek watershed.....89

Table S.B.1 Appendix B– Pore water and leachate composition in Control Columns– Replicate A 92

Table S.B.2 Appendix B– Pore water and leachate composition in Control Columns– Replicate B 94

Table S.B.3 Appendix B– Pore water and leachate composition in Treated Columns– Replicate A 96

Table S.B.4 Appendix B– Pore water and leachate composition in Treated Columns– Replicate B 98

LIST OF FIGURES

Fig. 2.1 Map of operation area, Mill site, and Tailings pile. Excavated tailings from the mine shaft at operations area were processed at the mill site and tailings were pumped to a valley forming the 22 acre tailings pile 12

Fig. 2.2 **a** Topographic map of tailings pile watershed showing four major subwatersheds (A, B, C, and D) and surface water monitoring locations. Contours are in feet above mean sea level **b** Infrared aerial photograph of the tailings pile showing monitor well locations 14

Fig. 2.3 Embankment face of the Ore Knob tailings pile.....14

Fig. 2.4 Depth of oxidized tailings in the Ore Knob tailings pile 20

Fig. 2.5 Silt-clay percent and hydraulic conductivity in different locations at Ore Knob tailings pile (error bars are the range of observed values) 21

Fig. 2.6 Water retention capacity for fine grained (MW10) and coarse grained (MW13) tailings in different depth based on visual appearance of the tailings.....23

Fig. 2.7 Variation in total porosity, water content, and effective oxygen diffusivity versus depth in fine grained (MW10) and coarse grained (MW13) tailings.....25

Fig. 2.8 Average water table profile through the tailings pile.....28

Fig. 2.9 Variation in runoff, evapotranspiration, deep recharge in coarse grained (MW13), fine grained (MW10) and watershed areas for driest, average and wettest years.....31

Fig. 2.10 Simulated water table elevations in tailings pile for Alternative B. Contour interval is meters above mean sea level.....33

Fig. 2.11 Cumulative frequency distribution for vadose zone thickness under existing conditions (Alternative B) and after plugging the concrete pipe and construction of the bypass channel 34

Fig. 2.12 **a** Ferric hydroxide precipitates at downstream of the embankment face, **b** Ore Knob Branch before confluence with Peak Creek, **c** Ore Knob Branch confluence with Peak Creek 38

Fig. 3.1 Schematic of experimental columns 46

Fig. 3.2 Variation in **a** total organic carbon (TOC), **b** dissolved oxygen (DO), **c** redox potential (Eh), **d** pH, **e** acidity, **f** iron (Fe), **g** manganese (Mn), **h** magnesium (Mg), **i** sulfate (SO_4), **j** hydrogen sulfide (H_2S), **k** aluminum (Al), **l** copper (Cu), **m** zinc (Zn), and **n** silica (Si) at 0.5 m below surface in experimental columns over time.....50

Fig. 3.3 Variation in **a** total organic carbon (TOC), **b** dissolved oxygen (DO), **c** redox potential (Eh), **d** pH, **e** acidity, **f** iron (Fe), **g** manganese (Mn), **h** magnesium (Mg), **i** sulfate (SO_4), **j** hydrogen sulfide (H_2S), **k** aluminum (Al), **l** copper (Cu), **m** zinc (Zn), and **n** silica (Si) in column effluent (1.2 m depth) in experimental columns over time 51

Fig. 3.4 Profiles of **a** total organic carbon (TOC), **b** dissolved oxygen (DO), **c** redox potential (Eh), **d** pH, **e** acidity, **f** iron (Fe), **g** manganese (Mn), **h** magnesium (Mg), **i** sulfate (SO_4), **j** hydrogen sulfide (H_2S), **k** aluminum

(Al), **l** copper (Cu), **m** zinc (Zn), and **n** silica (Si) versus depth at one year after WG addition 52

Fig. 3.5 Carbon content of the tailings in control and treated columns at the end of the study.....54

Fig. 3.6 Average mass discharged from control and treated columns in 14 months following substrate addition. Error bars are maximum value observed 58

Fig. 3.7 Comparison of contaminant concentrations in the treated columns and control columns during the treatment period (June 2008 to August 2009). Graphs include minimum, maximum, upper quartile, lower quartile and average of each data set 59

Fig. 3.8 Variation in treatment efficiency over time following WG addition.....61

Fig. 3.9 Average saturation index of potential mineral precipitates in control and treated columns in the second summer after WG addition at 1.0 m below ground surface. Error bars are average of minimum and maximum saturation indices 62

Fig. 4.1 Abundance of different minerals versus depth at fine grained (MW10) and coarse grained (MW13) locations (Relative Intensity, RI = 100 intensity peak of mineral/total intensity of the strongest peaks of detected minerals in spectrum).....70

Fig. 4.2 Concentration of S, Fe, Al, Ca, Si, Zn, K, Mg, Cu and Mg versus depth based on acid extraction of fine grained grain (MW10) and coarse grained

(MW13) tailings....72

Fig. S.C.1 Drainmod input file for the fine grained tailings of the Ore Knob Tailings pile....106

Fig. S.C.2 System design input file for the fine grained tailings of the Ore Knob tailings pile....106

Fig. S.C.3 Soil water characteristic input file for the fine grained tailings of the Ore Knob tailings pile....107

CHAPTER 1

1. OVERVIEW

1.1 Introduction and Site History

Oxidation of sulfide minerals in mine tailings impoundments and waste piles releases H^+, SO_4, Fe, and other metals to the tailings pore water. Depending on the type of minerals present in the ore body, a variety of the elements (e.g., Ni, Pb, Hg, Al, Cu, Co, and Cr) can be discharged into the environment. Low pH pore water, along with dissolved constituents, can migrate out of the tailings and into adjacent aquifers and surface waters, detrimentally affecting these resources.

The Ore Knob deposit was discovered before the Civil War. Between 1871 and 1883, it was worked intensively, yielding 11,500 t of copper ore from 11 openings and ore main shaft. Further mining activity was limited until the mine was reopened in the late 1950s. From 1957 to 1962, Appalachian Sulfides, Inc. operated a mine and processing facility at the site. The extracted ore was ground in a processing facility located in the Little Peak Creek watershed. Copper, gold, and silver were extracted using a froth flotation and cyanide leaching process. Most waste tailings were pumped to a large tailings impoundment located on Ore Knob Branch. However, a portion of the tailings were dumped in a small hollow adjacent to the processing facility. Acid mine drainage from the processing area and associated waste piles has impaired 1.5 km of Ore Knob Branch and 4.7 km of Peak Creek

feeding the New River. However, water quality conditions in the Little Peak Creek are outside the scope of this study.

1.2 Chemistry of Acid Mine Drainage Generation

1.2.1 Acid Producing Reactions

Oxidation of sulfidic minerals causes production of water with low pH, high metals, and high sulfate concentration known as Acid Mine Drainage (AMD). Parker and Robertson (1999) reported release of different toxic elements including As, Pb, Cu, Zn, Cd, Mn, and Ni from oxidation of different sulfidic minerals. The primary reactions controlling the oxidation of pyrite are presented by Singer and Stumm (1970).

$FeS_2 + 3.5O_2 + H_2O \rightarrow Fe^{2+} + 2SO_4^{2-} + 2H^+$ Reaction 2.1

$Fe^{2+} + O_2 + H^+ \rightarrow Fe^{3+} + 0.5H_2O$ Reaction 2.2

$FeS_2 + 14Fe^{3+} + 8H_2O \rightarrow 15Fe^{2+} + 2SO_4^{2-} + 16H^+$ Reaction 2.3

$Fe^{3+} + 3H_2O \rightarrow Fe(OH)_3 + 3H^+$ Reaction 2.4

$2FeS_2 + 15/2O_2 + 7H_2O \rightarrow 2Fe(OH)_{3(s)} + 4SO_4^{2-} + 8H^+$ Reaction 2.5

The process starts with oxidation of pyrite with dissolved oxygen and production of ferrous iron (Reaction 2.1). Ferrous iron is further oxidized to ferric iron which becomes a strong oxidant of pyrite (at pH < 3.5- Reaction 2.3). Some studies reported the rate of reaction 2.2 to be slow in acidic media (McKibben and Barnes 1986; Singer and Stumm 1970). At mildly acidic to neutral pH, iron hydroxide precipitates. Reaction 2.5 shows the

overall reaction of pyrite oxidation. Different studies show the same reaction series for various sulfide minerals. When present, certain iron oxidizing bacteria (*Acidithiobacillus ferrooxidans*) can accelerate the rate of iron sulfide oxidation by a factor of 10^6 compared to abiotic conditions (Gonza´lez-Toril et al. 2003; Singer and Stumm 1970).

1.2.2 Secondary Mineral Precipitation

A variety of different minerals may precipitate when AMD is produced from sulfide oxidation including sulfates and hydroxysulfates (e.g., jarosite, gypsum), oxides and hydroxides (e.g., goethite, ferrihydrite), and silicates (e.g., kaolinite). Processes leading to secondary mineral precipitation include oxidation and/or hydrolysis of the dissolved cations (e.g., Fe^{+2}, Fe^{+3+}, Al^{+3}), reaction with acid buffering minerals, mixing with neutral or alkaline waters, and concentration of the mine water due to evaporation (Nordstrom and Alpers 1999). Secondary mineral formation can temporarily consume acidity based on the following reaction:

$$\text{cations}^{n+}_{(aq)} + \text{anions}^{n-}_{(aq)} + nH^{+}_{(aq)} + nH_2O_{(l)} \rightarrow \text{secondary solids-}nH_2O_{(s)} \qquad \text{Reaction 2.12}$$

Secondary minerals can sorb or coprecipitate significant quantities of trace elements including metals and metalloids. This phenomenon immobilizes elements in AMD and acts as an important natural attenuation mechanism (Berger et al. 2000; Nordstrom and Alpers 1999). However, if these secondary minerals later dissolve, acidity and co-precipitated contaminants can be released to the environment (Lottermoser, 2007).

1.2.3 Hardpan Formation

Hardpans form from precipitation of secondary minerals in the interface of the oxidized and reduced zone and can potentially reduce oxidation of underlying sulfide minerals. Furche et al. (2007) reported that cemented layers in sulfide-bearing mine tailings slowed the downward movement of the oxidation front, and a reduced wind and water erosion of the tailings surface. Blowes et al. (1991) found that precipitation of gel materials reduced the tailings porosity, decreasing oxygen diffusivity and slowing the downward ingress of gaseous oxygen. However, Johnson et al. (2000) described a possible decrease in the efficiency of hardpan layers as gas barriers, when lower volume minerals precipitated, increasing the air-filled porosity.

1.3 Acid Mine Drainage Prevention and Treatment

AMD production can be reduced by excluding either oxygen or moisture (or both) (Johnson and Hallberg 2005). Flooding with water (e.g., wet cover) and sealing abandoned mine tailings can be used to reduce contact between oxygen and reactive minerals. Dry covers are used to reduce water infiltration and can also be used to limit oxygen entry. However, ongoing maintenance of these covers is necessary in prevent cracking and resulting acid generation (Swanson et al. 1997). Acid neutralizing materials can also be blended with the tailing to limit AMD production.

Once produced, AMD can be treated by adding alkaline material to raise the pH, followed by aeration to produce $Fe(OH)_3$ and then settling to remove solids before discharge

to surface water. However, this requires substantial infrastructure for chemical addition, aeration, and sedimentation, and on-going costs for chemicals, power, and sludge removal/disposal.

Various neutralizing agent are used including limestone ($CaCO_3$), soda ash (Na_2CO_3), caustic soda (NaOH), and anhydrous ammonia (NH_3). Limestone is inexpensive and will initially increase the pH of mine waters. However under aerobic conditions, limestone becomes armored with metals hydroxide, reducing efficiency. Anoxic limestone drains containing biodegradable organic material can be used to keep dissolved iron in the Fe^{+2} form, reducing armoring. However, the organic material must be replenished to maintain performance (Skousen et al. 1993). Hydrated lime ($Ca(OH)_2$) is easy to use, safe and relatively inexpensive. However, the volume of the sludge produced is higher than when using limestone (Skousen et al. 1993). Soda ash has a high reagent cost and produces sludge with poor settling properties. Caustic Soda (NaOH) is effective in treating AMD, because of its high solubility, ease of dispersion in water, and large amount of alkalinity released. However, significant disadvantages of NaOH include high cost, danger involved with handling, poor sludge properties, and freezing problems in cold weather. Anhydrous ammonia is effective in treating AMD with high levels of Fe and Mn. However, this material is also dangerous and has negative effects on downstream aquatic life (Skousen et al. 1993).

Anaerobic bioremediation processes can be used to reduce sulfate (SO_4) and immobilize heavy metals in the subsurface if a carbon and energy source is available to drive SO_4 reduction by Sulfate Reducing Bacteria (SRBs). Naturally-occurring SRBs use hydrogen (or organic acids) released from fermentation of complex substrates as an electron donor and

SO_4 as an electron acceptor, consuming H^+ and producing hydrogen sulfide (H_2S) in the following reaction:

$$2H^+ + SO_4^{2-} + 4H_2 \rightarrow H_2S + 4H_2O \qquad \text{Reaction 2.13}$$

Sulfide produced in this reaction will react with a variety of metals ions (e.g., Fe, Ni, Zn, Cd, Pb, Cu, Hg), forming less soluble precipitates. Three general approaches have been used to bring biodegradable organic carbon into contact with the AMD to stimulate SO_4 reduction: (1) engineered bioreactors; (2) treatment wetlands; and (3) permeable reactive barriers (Skousen et al. 1993; Waybrant et al. 2002). While each of these methods can be effective, they all have significant capital costs for the initial construction and periodic maintenance for good performance.

1.4 Research Hypothesis and Objectives

AMD production is controlled by a complex interaction of physical, chemical, and biological processes (Blowes et al. 1992; Evangelou and Zhang 1995; Lottermoser 2007). The total pollutant load produced within the tailings pile is controlled by the rate of oxygen entry into the pile (Jaynes et al. 1984; Nicholson et al. 1989; Pantelis and Ritchie 1991; Yanful 1993). Essentially all of the oxygen that enters the pile reacts with sulfidic minerals producing dissolved Fe, SO_4, and acidity. The primary source of oxygen entering the tailings pile is assumed to be gaseous diffusion through the tailings pile surface. The oxygen diffusion rate is controlled by the air filled porosity and the oxygen concentration gradient. However, the oxygen concentration gradient is controlled by the rate of oxygen consumption in the different layers.

Numerous interacting processes control the temporal and spatial variations in air filled porosity and oxygen reaction rates. Higher water infiltration rates will more rapidly transport pollutants through the pile to the embankment face. However, higher infiltration rates may also reduce the air filled porosity, reducing oxygen transport and pollutant generation. The higher surface area of fine grained sediments present in the upstream portion of the tailings pile increase the oxygen reaction rate, increasing AMD production (Lottermoser 2007). However these fine grained sediments also retain more water, reducing the air filled porosity and oxygen diffusion rate. On a micro–scale, oxygen reaction rates are controlled by geochemical conditions and bacterial activity at the mineral surface. However, if a coating of oxidized material develops on the particle surface, the rate of oxygen diffusion through this coating may control the overall oxidation rate. On a macro–scale, the water

infiltration rate will be controlled by the presence of cemented layers and hardpans (Blowes et al. 1991). However, these hardpans are believed to develop from precipitation of secondary phases, which will be influenced by the rate of water infiltration.

Objectives of this research are to: (a) improve our understanding of the processes controlling AMD production from the Ore Knob Tailings pile and similar sulfidic waste piles throughout the world; and (b) develop a method to treat AMD within the tailings pile without the high capital and operating costs associated with traditional treatment approaches.

1.5 Thesis Content

Chapter 2 presents the results of a detailed hydrological and geochemical characterization of the pile, conducted to help understand the interconnection between the physical, hydrologic, and meteorological characteristics of the site and AMD production. In chapter 3, a new method for treating mine tailings is evaluated where waste glycerol is applied to the tailings surface and used to treat AMD constituents within the tailings pile. Chapter 4 presents results of a geochemical characterization of the tailings sediments. Conclusions and recommendations for future work are presented in Chapters 5 and 6.

CHAPTER 2

2. PHYSICAL, HYDROLOGIC, AND AQUEOUS CHEMICAL CHARACTERIZATION OF THE ORE KNOB TAILINGS PILE (ASHE COUNTY, NORTH CAROLINA, USA)

2.1 Introduction

Exposure of sulfide minerals to a moist, oxidizing environment often produces acid mine drainage (AMD) (Nordstrom and Alpers 1999; Singer and Stumm 1970) contaminants, including Al, As, Cd, Cu, Mn, Ni, Pb, and Zn (Parker and Robertson 1999). AMD may be released from a variety of sources including the mine itself, spoil mounds, and mineral tailings, severely impacting surface and groundwater resources. The U.S. Environmental Protection Agency (U.S. EPA 2004) identified 156 hardrock mining sites with total cleanup costs up to $24 billion, including 19 National Priorities List sites with potential remediation costs of over $50 million each.

Sulfide oxidation and acidity generation in tailings piles is often controlled by oxygen availability. In the saturated zone, oxygen transport is low since the oxygen diffusion rate in water is four orders of magnitude less than in air (Weast 1976). In the vadose zone, oxygen is primarily supplied by diffusion and advection through gas filled pores (Jaynes et al. 1984; Nicholson et al. 1989; Pantelis and Ritchie 1991; Yanful 1993). Since AMD generating reactions occur on the surface of sulfide minerals (Singer and Stumm 1970), mining processes that generate fine particles can increase the surface area exposed to oxygen and

water, potentially increasing acid generation. However, fine grained sediments also retain more water, reducing the gas filled porosity and acid generation rates (Lottermoser 2007). Near the tailings pile surface, the reduced sulfide content due to previous weathering of sulfide minerals exposes less reactive surfaces to oxygen, reducing acid generation. The thickness of this surface oxidized zone will gradually increase over time, slowing oxygen diffusion into the pile (Gunsinger et al. 2006). However, rapid water infiltration can potentially leach weathering products, exposing unoxidized mineral surfaces, and thus increasing oxidation rates (Gunsinger et al. 2006). In some cases, hardpans may develop as secondary minerals precipitate during infiltration through tailings (Blowes et al. 1991; Boorman and Watson 1976; McGregor et al. 1998; McSweeney and Madison 1988; Tasse et al. 1997). When the hardpan has smaller pores than the surrounding material, water may be retained, reducing the gas filled porosity, oxygen diffusion, and oxygen contact with sulfide minerals (Blowes et al. 1991; Gilbert et al. 2003; Johnson et al. 2000).

Acidity generation in tailings may also be influenced by mineralogy, moisture content, microbial activity, and temperature. The relative resistance of different minerals to oxidation varies due to differences in crystal structure and iron content (Schmiermund 2000). Generally, sulfide minerals containing large amounts of iron (e.g., pyrite, marcasite, and pyrrhotite) produce much more acidity than minerals lacking iron (e.g., sphalerite, galena, and covellite) (Lottermoser 2007; Plumlee 1999). Water serves as both the reaction medium and as an important reactant (Evangelou and Zhang 1995; Rose and Cravotta 1998). In arid environments, oxidation rates may be 2–3 times lower than rates in humidity cells due to reduced moisture content and larger particle size (Fennemore et al. 1998). Sulfur oxidizing

and ferrous iron oxidizing bacteria can catalyze the kinetic reaction of pyrite oxidation and increase the oxidation rate 30–300 fold (Nordstrom and Alpers 1999). Abiotic and biotic oxidation rates are temperature dependent and slow at the reduced temperatures associated with some mine sites (Escobar et al. 2009).

2.2 The Ore Knob Mine and Tailings Pile

Ore Knob, near Jefferson (Ashe County), North Carolina, is the location of a massive fissure type sulfide deposit. The steeply dipping vein varies from 2.4 to 5.5 m thick and extends over 1220 m along the contact between the Carolina gneiss and the adjoining muscovite – biotite schist (Rankin and Stuckey 1943). Pyrrhotite, pyrite, chalcopyrite, quartz, biotite, and amphiboles are the principal minerals in the vein (Kinkel 1967; Rankin and Stuckey 1943). From 1957 to 1962, Appalachian Sulphides, Inc. operated the mine and processing facility at the site (Fig 2.1), extracting copper, gold, and silver using a froth flotation and cyanide leaching process (Kinkel 1967; Rankin and Stuckey 1943). Most waste tailings were pumped to an impoundment located on Ore Knob Branch. A drop inlet and 61 cm (24 inch) reinforced concrete pipe (RCP) were installed to provide drainage from the upstream end of the impoundment, through the dam, discharging into Ore Knob Branch. Over time, the embankment forming the dam was progressively raised to provide additional storage for the accumulated tailings, forming a 9 ha tailings pile with a maximum tailings depth of 21 m at the center of the embankment face. The surface elevation near the embankment face is approximately 6 m higher than near the drop inlet, causing water to pool

in this area, forming a small pond – wetland. The drop inlet is located about 490 m from the face of the tailings. However, the outlet of the pipe has been covered by tailings, probably as a result of slope failure on the tailings embankment face.

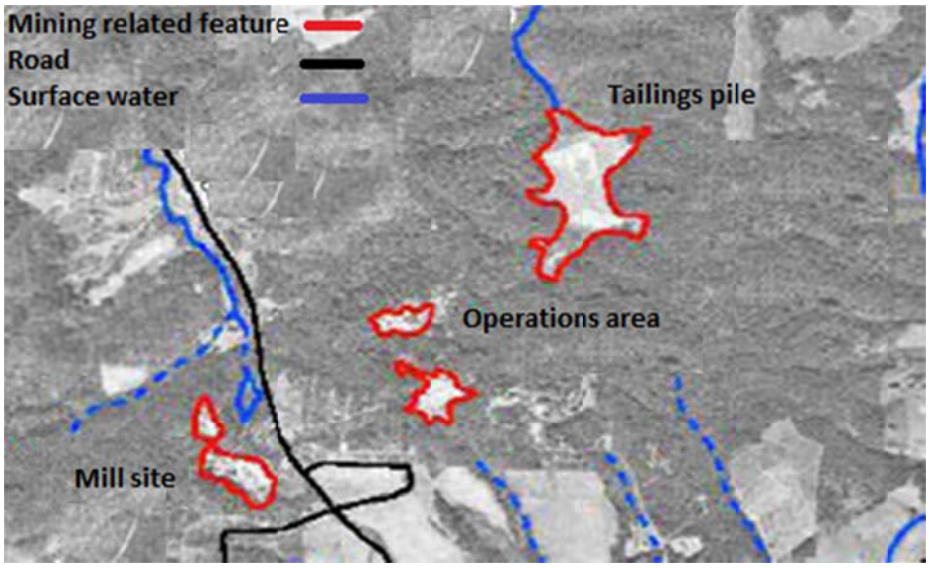

Fig. 2.1 Map of operation area, Mill site, and Tailings pile. Excavated tailings from the mine shaft at operations area were processed at the mill site and tailings were pumped to a valley forming the 22 acre tailings pile

Chapter 4 presents a mineralogic and geochemical characterization of these tailings based on X–ray diffraction (XRD) and acid extraction measurements. Briefly, the tailings throughout the pile contain pyrrhotite, troilite, mackinawite, pyrite, quartz, and aluminosilicate minerals. Extraction of the sediment with HCl/HNO_3 and H_2O_2 following U.S. EPA method 3050 B and analysis by ICP–AES indicate that the tailings also contain 1.4–2.9 mg/g Zn and 0.8–2.2 mg/g Cu. Potential acidity of tailings collected below the water table varied from 900 to 1100 Kg/ton with an acid neutralization potential of 13 to 47 Kg H_2SO_4 per ton.

Fig. 2.2a shows a topographic map of the watersheds that contributes flow to the tailings pile along with surface water sampling locations. Water flowing through the tailings pile originates as surface runoff, baseflow, and groundwater from four primary tributaries (A, B, C, and D) and rainfall that infiltrates directly through the tailings pile surface and small undifferentiated areas directly adjoining the pile (central area). The mine shaft and multiple mine adits are located in the upstream portion of watershed A, so water released from the mine flows downstream and enters the tailings pile. Where each tributary (A, B, C, and D) enters the pile, small pools or wetlands have formed where water is temporarily stored prior to infiltration into the pile. The infiltrated water migrates through the pile as groundwater, eventually discharging as a series of springs and seeps on the down gradient embankment face. Fig. 2.3 shows the highly eroded embankment face. The bedrock underlying the impoundment is highly metamorphosed, containing alternating layers of muscovite schist and quartz-biotite granitic gneiss. The bedrock permeability is one to two orders of magnitude lower than the tailings, so most water is believed to flow through the tailings and/or discharge pipe. The site has a humid continental climate with average annual precipitation = 124 cm. Precipitation is fairly uniform throughout the year, varying from 8.3 cm per month in December to 12.4 cm/month in May. The average monthly temperature varies from 0 to 20°C (data from http://www.nc.climate.ncsu.edu for Station: 314496 – Jefferson 2 E, NC located 9 km from the pile). Fig. 2.2b is a 1998 color infrared aerial photograph of the pile (NCDOT 2010) and shows the location of six monitoring wells that were installed to characterize seepage through the pile.

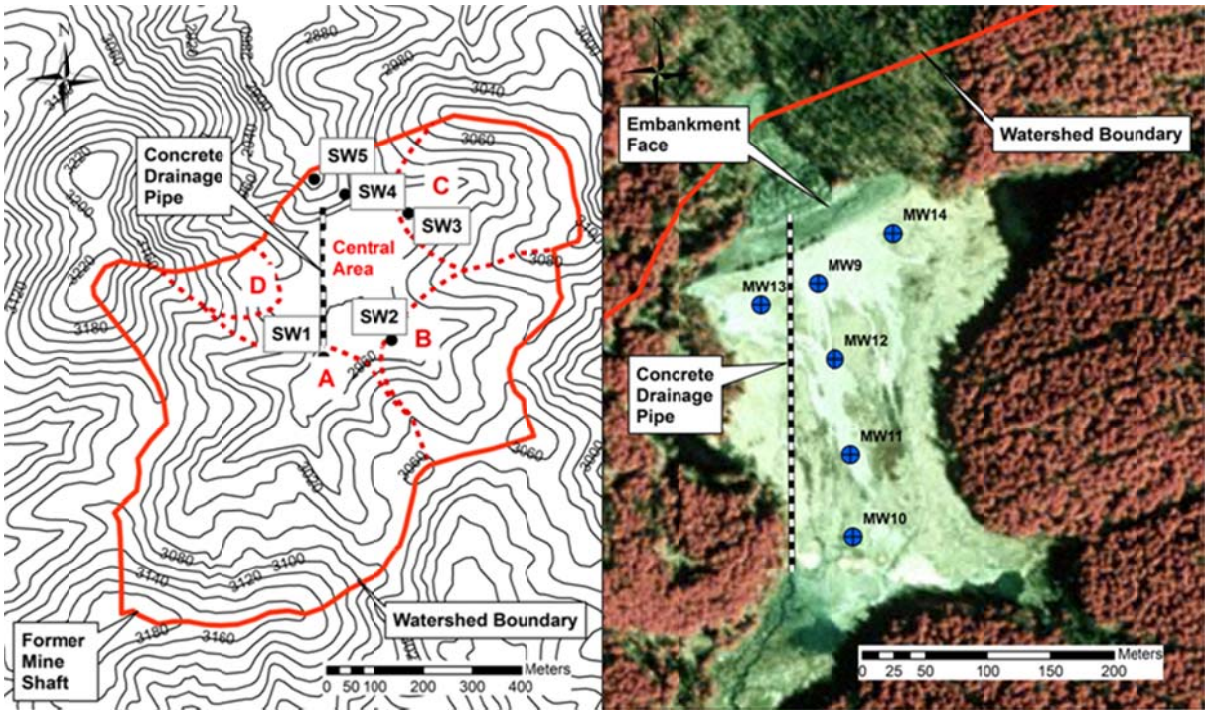

Fig. 2.2 a Topographic map of tailings pile watershed showing four major subwatersheds (A, B, C, and D) and surface water monitoring locations. Contours are in feet above mean sea level. **b** Infrared aerial photograph of the tailings pile showing monitor well locations

Fig. 2.3 Embankment face of the Ore Knob tailings pile

In 2008, the U.S. EPA began an Emergency Response removal action to stabilize the Ore Knob tailings dam, including excavation of sediment from a downstream sedimentation basin, construction of a channel to divert storm water around the pile, filling four ponds/wetland around the perimeter of the pile, and regrading the embankment face to reduce the slope and control erosion. In 2009, U.S. EPA placed the site on the National Priorities List for eventual cleanup. The overall objective of the research presented in this chapter was to improve our understanding of the major physical characteristics of the Ore Knob tailings pile that control the transport and reaction of water, oxygen, and pollutants within the pile. This information will be used to identify the most efficient approaches for long term management of the pile. In this chapter, results of a detailed physical and hydrologic characterization of the pile are presented and used to develop a model of saturated water flow through the pile. This information can later be used to develop quantitative models of pollutant generation and transport within the vadose zone of the pile.

2.3 Methods

Six soil borings were obtained by hollow stem auger drilling within the tailings pile for collection of soil samples and installation of monitoring wells (Fig. 2.2b). The thickness of the oxidized layer and depth to the reduced layer and hardpan were determined by visual observation during monitoring well installation and from standard penetration test results. Hand auger borings were also installed at additional locations to provide information on spatial variations in oxidized layer thickness. Particle size analysis was conducted using a

Beckman Coulter LS 13–320 laser particle size analyzer equipped with a Universal Liquid Module.

The hydraulic conductivity of the saturated zone was estimated by conducting falling head slug tests in each of the monitoring wells. The pressure response versus time data from the slug tests were analyzed using Hvorslev's method (Schwartz and Zhang 2002). The infiltration capacity of the tailings pile surface was measured immediately adjoining four monitoring wells using a double ring infiltrometer. At each location, saturated hydraulic conductivity (K_{sat}) was measured using a compact constant head permeameter (CCHP) (Amoozegar 1989).

Undisturbed samples on unconsolidated material were collected using an Uhland sampler. Blocks of consolidated material from the hardpan layers were excavated, shaped, and sealed in 7.6 cm diameter cylinders with paraffin for analysis. Saturated hydraulic conductivity of each sample was measured using the constant head method (Klute and Dirksen 1986). Moisture retention curves were measured on a pressure plate apparatus while applying suction, and monitoring change in moisture content (Klute 1986). Water retention of each material was measured on undisturbed samples at 0–0.4 bar and on disturbed samples at 0.5 – 15 bar (Klute 1986). The measured pressure saturation curves were fit to the Brooks – Corey (1964) model using an automated calibration procedure that minimized the root mean square error (RMSE) between simulated and measured water saturation (Patil et al. 2009). The effective saturation (S_e) was calculated by:

$$S_e = [(\theta - \theta_r)/(n - \theta_r)] = (\psi/\psi_b)^{\lambda} \qquad \text{for } \psi < \psi_b$$

$$S_e = 1 \qquad \text{for } \psi \geq \psi_b$$

where θ is the soil water content (V_{water} cm^3/V_{total} cm^3), θ_r is the residual soil water content (V_{water} cm^3/V_{total} cm^3), n is total porosity ($V_{void}cm^3/V_{total}cm^3$), ψ is capillary pressure of water (cm), ψ_b is bubbling pressure (cm), and λ is pore size distribution index. Saturation pressure and saturation permeability curves for soils from the upland watershed were estimated using the Rosetta software (Schaap et al. 2001), based on relationships developed by Van Genuchten (1980) and Mualem (1976) and the particle size distribution (NRCS 2008).

Water samples from monitoring wells were collected using diffusion bag samplers constructed of 2.54 cm (1 inch) diameter regenerated cellulose dialysis membrane inside an outer protective layer of LDPE mesh. Samplers were installed near the top, middle, and bottom of the saturated zone in each well to monitor vertical variations in water quality. New dialysis membranes were used during each sampling event and filled with deionized water prior to installation. A rubber balloon packer was placed between the top and middle samplers and between the middle and bottom samplers. The balloon packers were intended to reduce mixing in the wells, allowing individual zones to be monitored. However, physically removing the samplers and packers from the wells caused significant mixing and may have limited the effectiveness of this sampling technique in isolating different zones. The samplers were allowed to equilibrate for one week.

Surface water was monitored on eight separate dates between March 2007 and August 2008. All samples were collected as grab samples. Whenever possible, samples were collected by fully submerging the sample bottle below the water surface and sealing with no headspace. However, at many of the sampling stations, the water was not deep enough to fully submerge the bottle. The water sample was then transported a few feet to the sampling

vehicle where the water samples were passed through a 0.45 μm filter and then placed in individual sample bottles with appropriate preservatives.

The pH, dissolved oxygen (DO), Eh, and temperature were measured in the field immediately after sample collection. DO was measured using colorimetric test kits (CHEMetrics) with a detection limit of 0.1 mg/L; pH, Eh, and temperature were measured using a field meter with a Ag/AgCl reference electrode. Hot acidity (mg/L as $CaCO_3$) was measured by boiling the sample in the presence of hydrogen peroxide and sulfuric acid and then titrating to pH=8.2 with sodium hydroxide to measure acidity associated with dissolved metals (Clesceri 1989). Samples for metals and sulfate analysis were filtered in the field by pumping through a 0.45 μm disposable cartridge filter. Metals were preserved by acidification to pH < 2 with 2N nitric acid. No preservative was added to the samples being analyzed for sulfate, which could have allowed a small amount of sulfate to be removed by sorption to precipitated iron oxide residues. Dissolved metals were analyzed on a Perkins Elmer Plasma II ion coupled plasma atomic emission spectrometer (ICP–AES) following methods equivalent to SW–846 6010C (detection limit = 0.06–0.09 mg/L). Sulfate was analyzed by ion chromatography following methods equivalent to SW–846 9056 (detection limit = 2.5 mg/L). All samples were stored on ice at 4°C for transport to the laboratory. Blank, duplicate, and spiked samples were analyzed during every sampling event.

2.4 Tailings Physical and Hydrologic Characteristics

There are significant spatial variations in the physical and hydraulic characteristics of the tailings sediment. Sediments at the up gradient end of the tailings pile are much finer grained than the material closer to the embankment face. The tailings are believed to have originally been discharged near the embankment, causing more coarse grained material to settle out near the embankment and finer grained material to be deposited upstream, near the drop inlet.

Visual observations indicate the presence of an upper, oxidized zone overlying a deeper reduced zone throughout the tailings pile. The oxidized layer varies in thickness from 0.1 – 0.3 m in the fine grained sediments near the drop inlet to 0.8 – 1 m in the coarse grained sediment near the embankment face (Fig. 2.4). Within the oxidized zone, there is a surficial layer of soft, yellow to light brown, fine grained material that grades into a more densely packed, partially oxidized, dark brown layer. Occasional inclusions of unoxidized material were observed in test pits. Below the oxidized zone, the material transitions to a grey hardpan layer, which is underlain by loose unconsolidated sediment. Within the reduced layer, there is a gradual transition in color and cementation with depth, from a relatively soft, light grey material to a dark gray, cemented hard pan. Below this hard pan, the vadose zone is much softer and dark blue-gray to black. Standard penetration test blow counts (corrected) vary from 5–10 blows per foot (bpf) in the oxidized zone to 50–100 bpf in the hardpan, to 5–15 bpf in the reduced coarse grained sediment. The reduced fine grained sediment below the hardpan was very soft and would not support the weight of the hammer. The grains of the

coarse reduced tailings appear to have been mechanically fractured, with ragged edges and angular shapes. The specific gravity of the reduced tailings varied from 3.2 to 3.6 (ASTM D 854–06).

The hydraulic conductivity of the saturated tailings was determined by conducting rising head slug tests in each monitoring well and analyzing the results following Hvorslev's method (Schwartz and Zhang 2002). Fig. 2.5 shows the spatial variation in hydraulic conductivity and silt-clay content (weight % passing #200 sieve). Hydraulic conductivity increased from MW10 near the drop inlet to MW9 near the embankment face, consistent with the decline in silt-clay content.

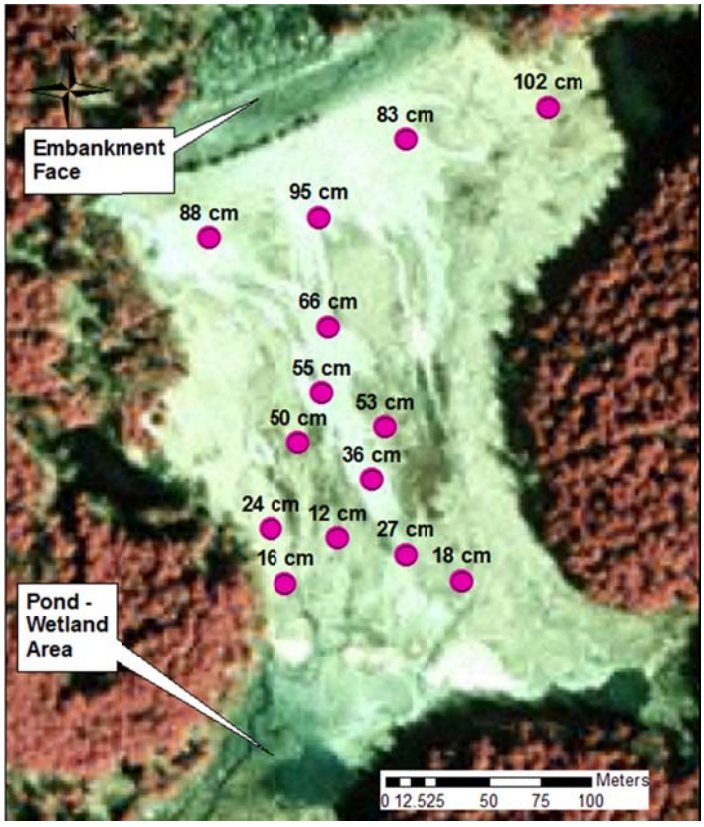

Fig. 2.4 Depth of oxidized tailings in the Ore Knob tailings pile

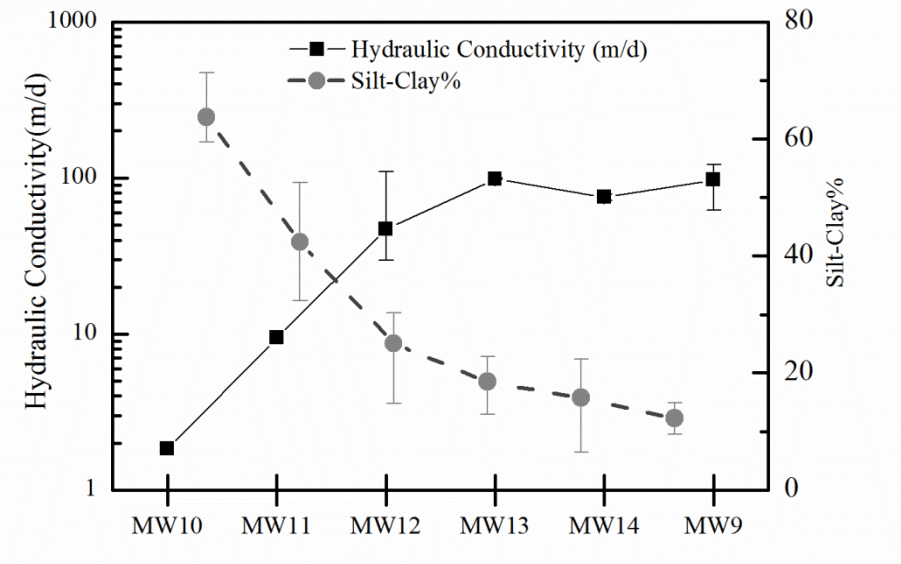

Fig. 2.5 Silt-clay percent and hydraulic conductivity in different locations at Ore Knob tailings pile (error bars are the range of observed values)

The effective permeability of the vadose zone sediments immediately adjoining four monitoring wells (MW10, MW11, MW12, MW13) were measured using three different techniques: (1) saturated infiltration rate was measured in the field using a double ring infiltrometer (Bouwer 1986); (2) saturated hydraulic conductivity was measured in the field using a CCHP; and (3) saturated hydraulic conductivity was measured on cores of hardpan material in the laboratory using constant head method (Klute and Dirksen 1986). Results of the vadose zone permeability testing are summarized in Table 2.1.

The three testing methods generated relatively consistent results. Infiltration rates were highest near the embankment face and declined towards the drop inlet, consistent with the decline in sediment grain size. Saturated hydraulic conductivity (K_{sat}) values in the yellow-brown layer measured with the CCHP showed much less variability.

Table 2.1 Vadose zone permeability results
NA – not analyzed

Method	Field double ring infiltration rate (cm/d)		Saturated hydraulic conductivity (cm/d)			
			Field measurement with CCHP		Constant head lab permeameter	
Layer	Oxidized, yellow/brown	Reduced, gray	Oxidized, yellow/brown	Reduced, gray	Oxidized, yellow/brown	Hard pan, gray
MW13	237	173	79	71	105	197
MW12	153	130	75	31	NA	NA
MW11	112	59	82	42	NA	NA
MW10	30	27	56	43	NA	49

Both the double ring infiltration and CCHP results indicate a modest decline in permeability from the oxidized to the reduced zone above the hard pan. However, the lab permeameter results indicate an increase in permeability in the hard pan layer. Overall, there is no evidence that oxidation of the tailings or formation of the hardpan resulted in a major change in permeability.

2.5 Effect of Weathering on Physical and Hydraulic Characteristics

A more detailed characterization of the surficial sediments was conducted at two locations (MW10 and MW13) to evaluate the impact of weathering on water and oxygen transport. Pressure-saturation curves were measured on undisturbed soil samples obtained at several depths at MW10 and MW13 (Fig. 2.6). The major physical and hydraulic characteristics of the tailings at each location are summarized in Table 2.2.

In the upstream location (MW10), sediment characteristics were relatively consistent with depth, indicating that weathering processes have not had a major impact on the physical

and hydraulic characteristics of the tailings. Throughout the profile, the sediments are fine grained (D_{50} = 40 to 150 µm), with a relatively constant fine fraction (D_{10} = 3 to 11 µm) and porosity (0.43 to 0.48). All of the pressure-saturation curves at MW10 followed the same general pattern (Fig. 2.6), indicating a consistent pore size distribution.

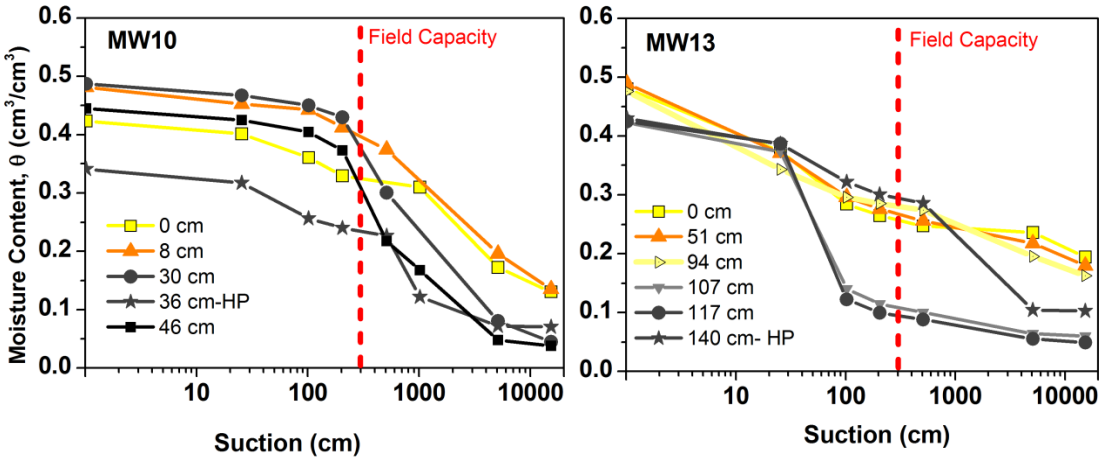

Fig. 2.6 Water retention capacity for fine grained (MW10) and coarse grained (MW13) tailings in different depth based on visual appearance (color) of the tailings

At the downstream location (MW13), there are significant differences in the physical and hydraulic characteristics with depth. Below 0.5 m, the tailing are relatively coarse grained (D_{50} = 239 to 407 µm). However, from 0 to 0.5 m below the ground surface, weathering has increased the amount of fine grained material (D_{10} = 1 to 4 µm), resulting in a broader pore size distribution. This is reflected in the steady decline in moisture content with increasing capillary suction in the MW13 oxidized sediments (Fig. 2.6). In the less extensively weathered material immediately above the hardpan, there is much less fine grained material (D_{10} = 105 to 154 µm), resulting in a narrow pore size distribution and

abrupt breaks in the pressure-saturation curves (Fig. 2.6). The hardpan layer contains more fine grained material (D_{10} = 54 μm), with a pressure-saturation curve that is intermediate between the shallow oxidized tailings and deeper reduced material.

Differences in the physical characteristics of the sediment at MW10 and MW13 are reflected in air filled porosity and effective oxygen diffusivity at each location. Fig. 2.7 shows profiles of total porosity and moisture content versus depth measured in cores at MW10 and MW13 measured in July 2009 (Table 2.2). Effective diffusivity of oxygen through the unsaturated tailings was computed using a relationship developed by Reardon and Moddle (1985). Air filled porosity was computed as the difference between the total porosity and volumetric moisture content.

At MW10, the large amount of fine grained material resulted in a relatively high moisture content (0.32-0.37), low air filled porosity (0.1 – 0.13), and low oxygen diffusivity throughout the profile. At MW13, the variations in sediment characteristics with depth resulted in large variations in air filled porosity and oxygen diffusivity. In the oxidized zone, the larger amount of fine material causes more water to be retained, reducing the air filled porosity and effective diffusivity. In the reduced zone above the hardpan (1.1 – 1.2 m), the much lower field capacity of this material allows the water to drain away, resulting in a higher air filled porosity and high effective diffusivity (note difference in diffusivity scale for MW10 and MW13). However, in the hardpan, the increase in fine material causes more water to be retained, reducing the effective oxygen diffusivity. Deeper in the pile, the tailings are saturated, resulting in very low oxygen diffusivity.

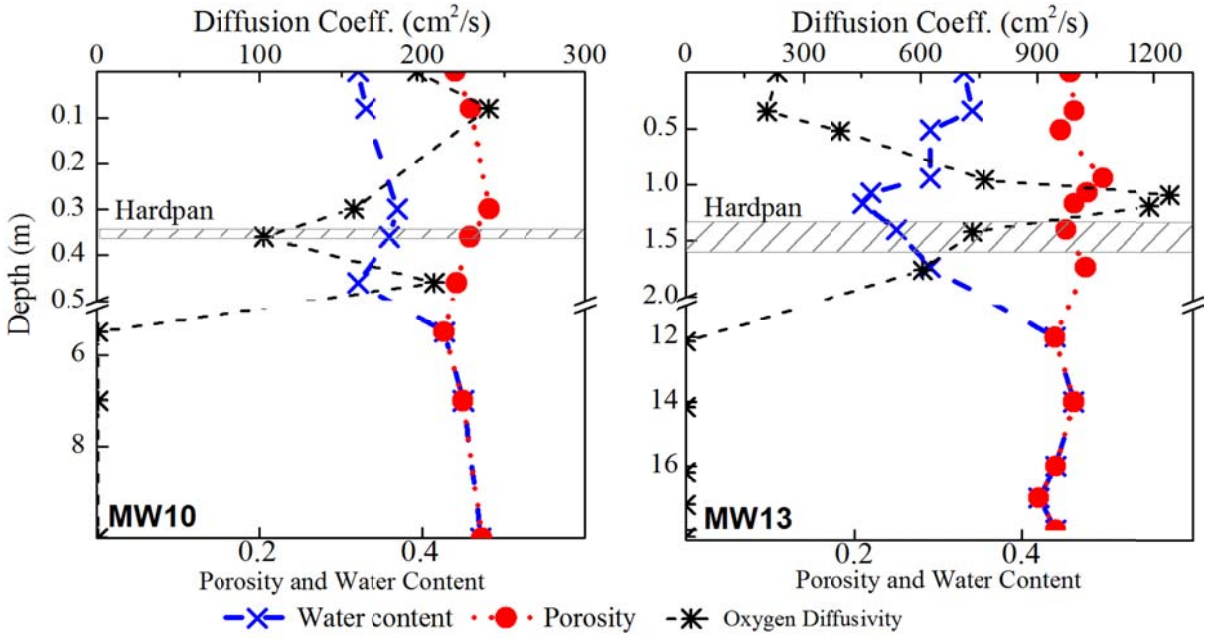

Fig. 2.7 Variation in total porosity, water content, and effective oxygen diffusivity versus depth in fine grained (MW10) and coarse grained (MW13) tailings

Table 2.2 Physical properties of fine grained (MW10) and coarse grained (MW13) tailings
NA= not available, Ox=oxidized, Red=reduced, y=yellow, br=brown, or=orange, gr=gray, d=dark, p=pale, B=below, WT=water table, har=hardpan

		Depth	Color	D_{10}	D_{50}	Silt+ Clay	Porosity (n)	Ambient Water Content (θ)	Ambient Air Filled Porosity (Φ)	Irreducible water content (θ_{wr})	Pore Size Distribution Factor (λ)	Bubbling Pressure (ψ_b)
MW10 - Fine tailings	Unit	m	-	mm	mm	%		-	-	-	-	cm
	Oxidized- yellow	0	25YR-8/8	3	91	38	0.44	0.32	0.12	0.13	0.23	24.64
	Oxidized Brown-Orange	0.08	7.5YR-5/8	7.0	78.9	37	0.46	0.33	0.13	0.14	0.19	30.53
	Reduced-Gray	0.30	10Y-3/1	11	61	48	0.48	0.37	0.11	0.05	0.23	37.82
	Hardpan	0.36	25YR-3/1	9	153	29	0.46	0.36	0.10	0.07	0.25	20.58
	Below Hardpan	0.46	7.5Y-4/3	4	40	62	0.44	0.32	0.12	0.04	0.23	31.51
	Below WT	5.5	7.5Y-4/3	6	45	59	0.43	0.43	0.00	NA	NA	NA
	Below WT	7	7.5Y-4/3	3	30	85	0.45	0.45	0.00	NA	NA	NA
	Below WT	10	7.5Y-4/3	1.6	12.4	99	0.47	0.47	0.00	NA	NA	NA
MW13 - Coarse tailings	Oxidized yellow	0	5YR-8/6	3	90	36	0.46	0.33	0.13	0.19	0.40	7.28
	Oxidized Brown-Orange	0.34	7.5YR-5/8	1	31	64	0.46	0.34	0.12	NA	NA	NA
	Oxidized- Dark Brown	0.51	10YR-4/6	4	383	30	0.45	0.29	0.16	0.18	0.32	5.39
	Oxidized- Pale Yellow	0.94	5Y-8/6	85	379	8	0.50	0.29	0.21	0.12	0.41	15.00
	Pale Gray	1.07	25YR-8/1	105	316	5	0.48	0.22	0.26	0.06	0.88	21.46
	Reduced- Dark Gray	1.17	5Y-3/1	154	350	4	0.46	0.21	0.25	0.05	0.97	22.76
	Hardpan	1.40	7.5Y-2/1	54	389	10	0.45	0.25	0.20	0.10	0.23	16.16
	Below Hardpan	1.73	7.5Y-4/3	90	366	8	0.48	0.29	0.19	NA	NA	NA
	Below WT	12	7.5Y-2/1	78	239	8	0.44	0.44	0.00	NA	NA	NA
	Below WT	14	7.5Y-2/2	41	407	12	0.46	0.46	0.00	NA	NA	NA
	Below WT	16	7.5Y-2/1	83	248	8	0.44	0.44	0.00	NA	NA	NA
	Below WT	17	7.5Y-2/2	114	313	5	0.42	0.42	0.00	NA	NA	NA
	Below WT	18	7.5Y-2/1	50	257	11	0.44	0.44	0.00	NA	NA	NA

2.6 Water Flow through the Tailings Pile

Water flowing through the tailings pile originates as surface runoff and baseflow from four primary tributaries, several small undifferentiated areas, and rainfall that infiltrates directly through the tailings pile surface. Where the primary tributaries enter the pile, the water table rises to the ground surface and small pools or wetlands have formed. Water is temporarily stored in these pools prior to infiltration, then migrates through the pile as saturated flow, eventually discharging as a series of springs and seeps on the down gradient embankment face. The original concrete drainage pipe is still present within the pile and flow can sometimes be observed entering the drop inlet. However, the pipe outlet is periodically blocked by sediment. During some periods, large amounts of water can be observed discharging from a large hole in the embankment face, indicating that the pipe is carrying a substantial flow. However during other periods, the hole becomes blocked with accumulated sediment and there is no evidence of a concentrated discharge. As a result, the fraction of flow transported as groundwater seepage vs. that carried by the pipe varies considerably, with no consistent pattern.

Water table (WT) elevations in each monitoring well were measured monthly from July 2007 to August 2008 by manual monitoring and using continuously recording pressure transducers. In general, WT elevations were reasonably constant over the monitoring period. Water level fluctuations were greatest in MW10, closely adjoining the up gradient pond/wetland. Water levels in MW10 responded relatively rapidly to rainfall events, indicating a good hydraulic connection between the pond and the WT in the tailings pile. For

all other wells, water levels were relatively constant and declined gradually due to an extended drought.

Fig. 2.8 shows a profile extending from MW10 through the tailings pile to the embankment face. Water table elevations are average values over the monitoring period. Bedrock and land surface elevations are based on results from soil borings. In the vast majority of the tailing pile, the WT is deep (2 – 10 m below ground surface) with no evidence of perched water tables. The hydraulic gradient between MW10 and MW11 is very small, suggesting some water is being transmitted through this area by the concrete drainage pipe. From MW11 to MW9 near the embankment face, the hydraulic gradient is much greater, consistent with more rapid groundwater flow in this area. The WT elevation in MW14 was consistently higher than in MW9 and MW13 indicating a hydraulic gradient from the east to west, possibly due to recharge from tributary C.

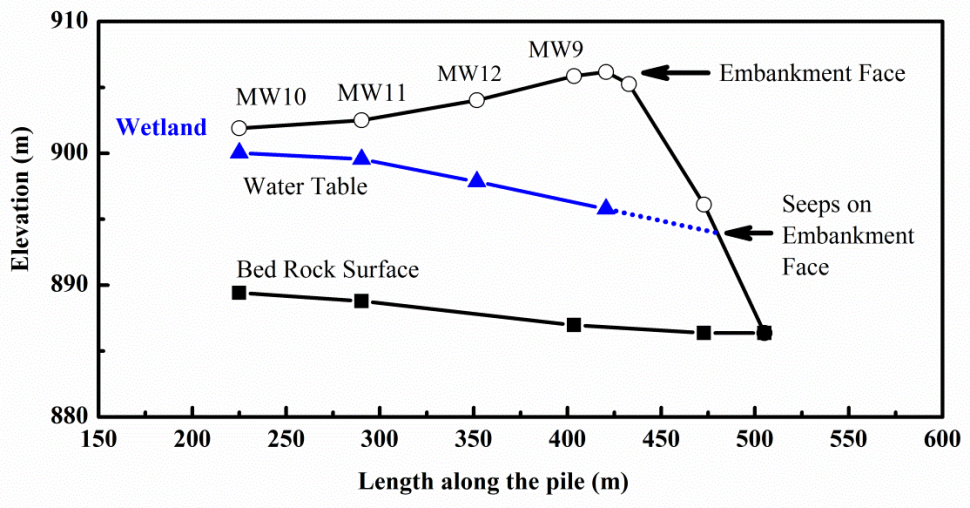

Fig. 2.8 Average water table profile through the tailings pile

Average groundwater flow velocities between well pairs were calculated based on the average hydraulic gradient and average permeability. Calculated groundwater velocities were 0.1 m/d from MW10 to MW11, 3.7 m/d from MW11 to MW12, and 7.9 m/d from MW12 to MW9. The high groundwater velocity from MW12 to MW9 was due to the large amount of water recharging the pile from the tributaries and the high permeability of the tailings. The low velocity calculated between MW10 and MW11 may be due to a significant amount of flow being carried through this zone by the concrete pipe. Alternatively, the actual velocity may be higher than the calculated velocity, if the measured hydraulic conductivity (K) in MW10 (K = 2 m/d) is not representative of this portion of the tailings pile.

2.7 Modeling Recharge and Water Flow through the Tailings Pile

Efficient management of AMD requires a quantitative understanding of water movement through the tailings pile. In this section, surface recharge and stream flow entering the pile were estimated and used to calibrate a groundwater flow model and evaluate the effect of different management strategies on water table position.

Surface runoff and recharge were estimated for the period from when the mine closed in 1960 to 2009, using the water balance model DRAINMOD (Skaggs 1982; Skaggs and Tabrizi 1981), which performs a continuous water balance in the soil profile. DRAINMOD was used to simulate daily evapotranspiration (ET), surface runoff, and deep recharge for three different areas: (1) coarse grained tailings near MW13, (2) fine grained tailings near MW10, and (3) watershed soils contributing stream flow to the pile. Model input included

meteorological data, pressure saturation curves, and hydraulic conductivity at varying depths (Skaggs and Tabrizi 1981). The hydraulic characteristics of the watershed soil were estimated from the particle size distribution (NRCS 2008), following procedures described by Saxton et al. (1986). Daily rainfall, temperature, and evapotranspiration were estimated from monitoring data collected at site ID#314496 – Jefferson 2 E, located 9 km away at 844 m above sea level (State Climate Office of North Carolina 2010).

Fig. 2.9 shows estimated annual ET, recharge, and surface runoff from the coarse grained (MW13), fine grained (MW10), and watershed areas for driest year, wettest year, and long term average for the period from 1960 to 2009. Runoff was generally not a major fraction of the overall water budget. ET was highest in the up gradient watershed due to the extensive vegetative cover. Near MW13, the coarse grained tailings allowed rapid recharge, reducing ET and runoff. The relatively high average annual recharge into the tailings, 64 – 86 cm/yr, rapidly transports acidity produced within the vadose zone to the water table surface.

Saturated flow through the tailings pile was simulated using MODFLOW (Harbaugh et al. 2000). The tailings pile was represented as a 7 layer grid. The permeability distribution was estimated from slug tests on the monitoring wells (Fig. 2.5). The transition from tailings to bedrock was estimated from the observed bedrock elevations and surrounding topography. Seeps along the embankment face were represented as drains. Recharge rates into the tailings surface were estimated from the calculated infiltration. All runoff and baseflow from tributaries B, C, and D entered the pile as recharge from the ponds/wetlands at each location.

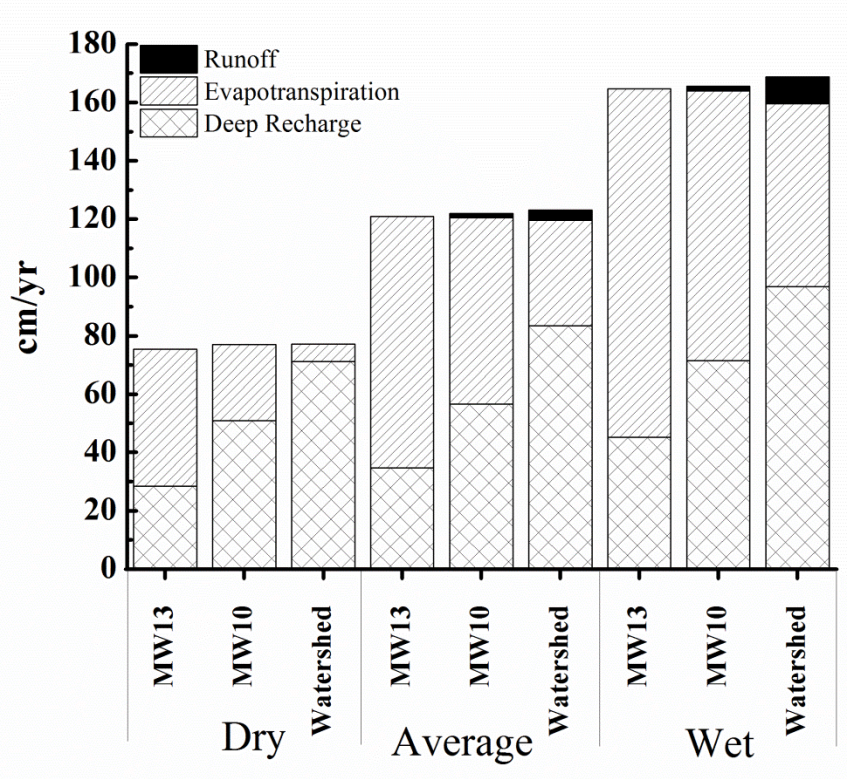

Fig. 2.9 Variation in runoff, evapotranspiration, deep recharge in coarse grained (MW13), fine grained (MW10) and watershed areas for driest, average and wettest years

During the initial model testing, it was apparent that MODFLOW could not be accurately calibrated to match the observed water levels in the pile due to the low permeability of the tailings in the upstream area. The simulated water table (WT) elevations at the upstream end of the pile were much too high and the WT was too low in the middle and downstream ends of the pile. Two potential alternatives were identified to explain the error in model calibration and were evaluated using MODFLOW. Under Alternative A, the hydraulic conductivity (K) in the upstream area was assumed to be 20 times higher than the value measured in MW10. Alternative A provided an adequate match to the observed WT data (mean calibration error = 0.20 m, root mean squared error (RMSE) = 0.86 m). However,

the very high K value used in the simulation is not reasonable in light of the fine grained material present throughout the area.

Under Alternative B, a portion of the flow was assumed to be carried from the upstream area to the middle of the pile by the concrete pipe and/or natural soil underneath the pile. This effect was represented in the model by a single row of high permeability cells. Fig. 2.10 shows simulated water table elevations in the tailings pile under the Alternative B assumptions. Overall, Alternative B provided a slightly better fit to the observed WT data (mean error = - 0.08 m, RMSE = 0.66 m) and accurately matched the locations where water ponds above the tailings surface. Most water enters the pile from these ponds and discharges as seeps along the embankment face. More importantly, Alternative B is much more reasonable given the flow observed to enter the concrete pipe, but not to discharge from the pipe. Unfortunately, there is no way to directly verify the validity of Alternative B.

As part of the emergency response action, U.S. EPA will plug the concrete drainage pipe and excavate an emergency bypass channel/spillway into the tailings to carry storm water from tributary A around the eastern edge of the pile, crossing tributaries B and C, and ultimately discharging into Ore Knob Branch downstream of the pile. The effect of plugging the concrete pipe and constructing of the bypass channel was simulated using MODFLOW by representing the channel as a drain.

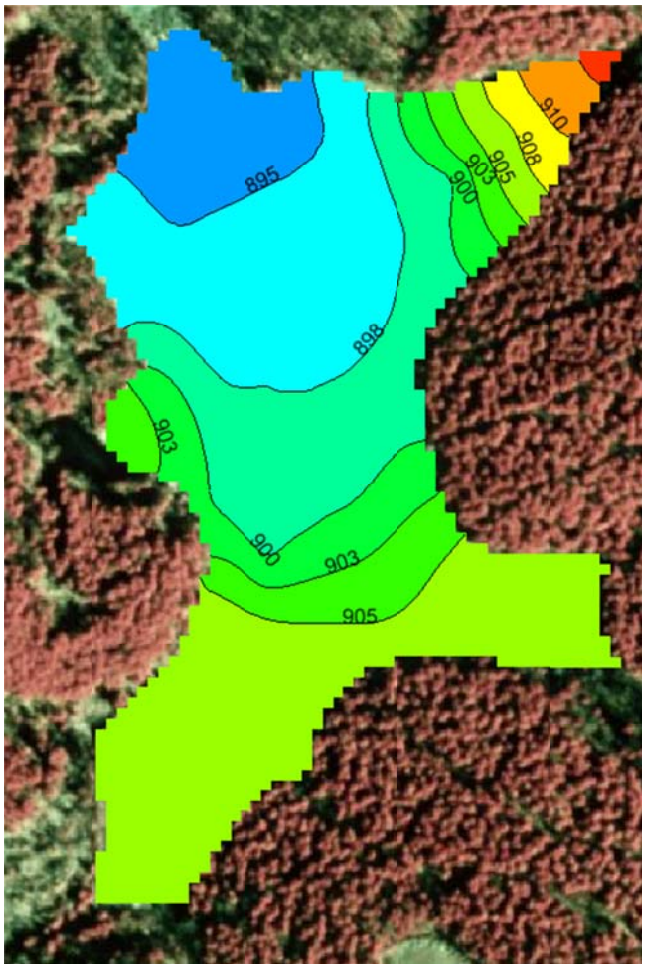

Fig. 2.10 Simulated water table elevations in tailings pile for Alternative B. Contour interval is meters above mean sea level

Fig. 2.11 shows simulated vadose zone thickness for existing conditions and after plugging the pipe and construction of the bypass channel. Under existing conditions, the vadose zone thickness is zero (WT is above the tailings surface) for 44% of the pile, 0 to 2 m thick for 7% of the pile, and over 2 m thick for 49% of the pile. After plugging the concrete pipe and completion of the bypass channel, seepage at the embankment face should be reduced by about 58%, and the portion of the pile saturated to the land surface should be

reduced by 0.6 ha to 37% of the pile surface. However, the bypass channel is expected to have minimal impact on the water table elevations near the embankment face. Diverting flow around the pile may slow the transport of acidity out of the pile. However, the increase in unsaturated tailings could potentially increase overall acidity production by allowing greater oxygen penetration into the pile.

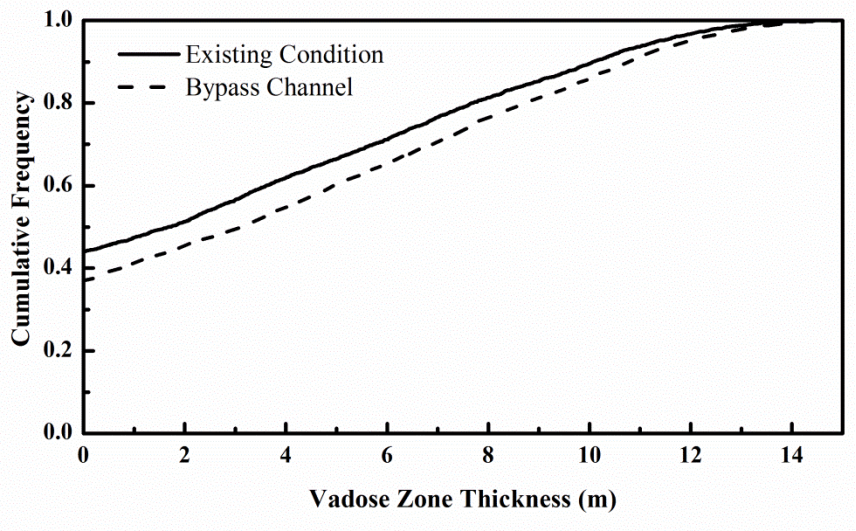

Fig. 2.11 Cumulative frequency distribution for vadose zone thickness under existing conditions (Alternative B) and after plugging the concrete pipe and construction of the bypass channel

2.8 Subsurface and Surface Water Quality

2.8.1 Ground Water

Six fully screened groundwater monitoring wells were sampled on five separate occasions in 2007–2008 to monitor temporal and spatial variations in geochemical parameters. Average values for each of the monitored groundwater parameters are presented

in Table S.A.1 in Appendix A. Bromide (Br), nitrite (NO_2), nitrate (NO_3), and phosphate (PO_4) were below detection in all samples and are not shown in Table S.A.1. The field Eh measurements are corrected to a standard hydrogen electrode so the values are approximately 240 mV higher than are commonly reported for 'uncorrected' electrodes. DO was measured in the field using disposable Chemetrics ampoules. Measured hot acidity values closely matched theoretical values (1–6% difference) estimated using a relationship developed by Kirby et al. (2005) which accounts for acidity associated with Fe(II), Fe(III), Mn, Al, and free protons (H^+).

As groundwater migrates down gradient through the tailings pile, dissolved Fe, SO_4, and acidity increase dramatically. During migration from MW10 to MW9, SO_4 increases by 967 mg/L as S and Fe increases by 1786 mg/L, a ratio of 1.20 moles of SO_4 per mole Fe, consistent with the oxidation of pyrrhotite in the tailings pile. Sulfate concentrations measured by ion chromatography are very similar to total S concentrations measured by ICP–AES, indicating that essentially all of the dissolved S is present as SO_4, with non-detectable levels of other sulfur species. In the down gradient wells (MW13, MW9, and MW14), pH values are moderate (5.8 to 6.1), even though the groundwater contains extremely high levels of hot acidity. In samples with high acidity levels (> 500 mg/L), more than 98% of the acidity was typically associated with Fe^{2+}. Free protons (H^+) are not released until Fe^{+2} reacts with oxygen, when the AMD is discharged at the land surface.

Groundwater samples were collected and analyzed for aluminum (Al), arsenic (As), cadmium (Cd), cobalt (Co), chromium (Cr), copper (Cu), nickel (Ni), lead (Pb), and zinc (Zn). Concentration of As, Cd, Co, Cr, Ni, and Pb were below analytical detection limits in

all samples (0.06–0.09 mg/L). Zn concentrations increased from up gradient to down gradient wells, following the same general trend as SO_4. Cu concentrations were relatively low all samples, varying between 0.06 and 0.11 mg/L. Average Al concentrations were below 0.2 mg/L in MW10, MW11, MW12, and MW14 and below 1.0 mg/L in MW13 and MW9. The slightly elevated aluminum values in MW13 and MW9 are likely associated with the slightly lower pH in these wells, which increased the effective solubility of Al. Ca was the cation present at the highest concentration (excluding Fe), followed by Mg, K, and Na. Silica (Si) concentrations were lowest in the up gradient wells (5–10 mg/L), gradually increasing to 30–40 mg/L in the down gradient wells.

In every well, there is a consistent trend of declining Eh and DO with depth, indicating more reducing, anaerobic conditions with depth below the WT. DO values are highest in the most up gradient well, possibly due to influx of oxygenated water from the up gradient pond/wetland. In all of the down gradient wells, pH was lowest, and Fe, SO_4, and acidity were highest in the top sample interval. This is consistent with recharge of concentrated AMD through the vadose zone. Readers should be aware that some mixing probably occurs in the monitoring wells, so the observed differences between the top, middle, and bottom samples are probably the minimum that actually occurs within the pile.

2.8.2 Surface Water

Surface water was periodically monitored at four locations surrounding the tailings pile (SW1, SW2, SW3, SW4, and SW5) (Fig. 2.2 a) and at two downstream locations (SW6 and SW7). SW1 is located at the large pond wetland at the upstream end of the tailings pile.

There are several mine adits in the upper portion of the SW1 watershed, some of which were treated with anoxic limestone drains in the 1980s. Analytical results for SW2 were similar to SW3. However, SW2 was sampled much less frequently and will not be discussed further. SW3 is located at a small pond on the eastern edge of the tailings pile near the embankment face. There are no known mine discharges in the SW3 watershed. SW4 monitors a large seep on the eastern edge of the embankment face and is believed to be representative of concentrated acid seeps discharging from the tailings pile. SW5 is located on Ore Knob Branch, a short distance downstream from the pile, and includes all seepage from the tailings pile and water that may have passed through the concrete drainage pipe in the tailings pile. SW6 is located on Ore Knob Branch, 1.2 km downstream from the tailings pile and immediately upstream of the confluence with Peak Creek. SW7 is located on Peak Creek a short distance upstream of where it joins with Ore Knob Branch and is representative of background water quality.

Fig. 2.12 shows surface water a: discharging from embankment face, b: Ore Knob Branch before confluence with Peak Creek, and c: Ore Knob Branch at confluence with Peak Creek. All of these surface water monitoring locations were sampled on eight separate dates between March 2007 and August 2008. Average values and standard deviations for each of the parameters are presented in Table S.A.2 in Appendix A. The pH was well below the surface water quality standard of 6 in all sampling stations within the Ore Knob Branch watershed. The only station that met the pH standard was SW8, which is a background station not impacted by the mine.

Fig. 2.12 a Ferric hydroxide precipitates at downstream of the embankment face **b** Ore Knob Branch before confluence with Peak Creek **c** Ore Knob Branch confluence with Peak Creek

Dissolved Fe, SO_4, and hot acidity concentrations discharging from the tailings pile (SW4 and SW5) are much higher than water entering the pile, indicating that most acidity is produced within the pile. Average dissolved Fe concentrations in SW1 were 62 mg/L, compared to 11–12 mg/L in well MW10, which is located a short distance down gradient within the tailings pile. The substantial decline in dissolved Fe from SW1 to MW10 suggests that some dissolved Fe is being removed as water infiltrates into the tailings pile. In contrast, SO_4 increased dramatically from 275 mg/L in SW1 to 1700–1900 mg/L in MW10. The cause of this dramatic increase is not understood. Dissolved Fe and SO_4 levels in SW1 are significantly higher than in SW3, indicating that the upstream mine and adits do contribute substantial amounts of AMD.

Surface water discharging from the tailings pile (SW4 and SW5) contains extremely high concentrations of Fe, SO_4, and acidity. As this water migrates downstream along Ore Knob Branch to SW7, the pH decreases to 3.1, due to oxidation of Fe^{+2} and the formation of

$Fe(OH)_3$ and H^+. At the point where Ore Knob Branch discharges into Peak Creek (SW6), the stream still carries 290 mg/L of acidity (as $CaCO_3$).

Surface water samples were collected and analyzed for Al, As, Cd, Co, Cr, Cu, Ni, Pb, and Zn. Arsenic, Cd, Co, Cr, Ni, and Pb were below the analytical detection limit in all samples, and will not be discussed further. Average Cu concentrations entering the tailings pile from the upstream watershed were very high (1–2 orders of magnitude above the NC surface water standard of 0.007 mg/L). Cu concentrations discharging from the tailings pile were lower, but still over 40 times the surface water standard. There was only a small decline in Cu during transport downstream through Ore Knob Branch, indicating little Cu attenuation other than dilution. Zn concentrations entering the pile were high and increased due to AMD production within the pile.

2.9 Pollutant Budgets

An overall pollutant budget was developed for the tailings pile to evaluate the relative contributions of water and pollutants entering from the upstream mine impacted areas (watershed A on Fig. 2.2), un-impacted areas (watersheds B, C, and D on Fig. 2.2), and infiltration through the tailings pile surface. Average flow rates from each of these contributing areas were calculated using the runoff, ET, and recharge estimates generated by DRAINMOD. Pollutant loads in surface water were calculated as the average flow rate for each watershed times the average pollutant concentration. Watershed C, which contains SW3, does not contain any mine related affects and was assumed to be representative of

other watersheds (B and D) that do not contain mine adits or spoil piles. The pollutant load generated by recharge through the tailings pile surface was calculated as the difference between the surface water load entering the pile from the upstream watershed and the combined load discharging to Ore Knob Branch.

Results of the pollutant budget analysis are presented in Table 2.3. Recharge through the tailings pile surface contributes 14% of the total discharge, but carries most of the pollutants. Watershed A, which contains the mine adits, releases 26 t/yr of acidity, while 221 t/yr of acidity are generated by oxidation within the tailings pile. The only exception to this overall trend is copper, where calculated load discharging from the pile is essentially the same as the load entering the pile in the surface water, indicating that little or no copper is released from the pile. This is consistent with the low copper concentrations measured in monitoring wells in the pile.

Table 2.3 Average dissolved pollutant budget for Ore Knob Mine tailings pile

	Average concentration in surface water entering pile (mg/L)			Total pollutant load (kg/yr)		
	Mine impacted (SW1)	Unimpacted (SW3)	Combined discharge (SW5)	Upstream watershed	Recharge through pile surface	Combined discharge
Flow (m^3/d)	580	510	1300			
Acidity	170	110	930	26,000	220,000	250,000
Fe	62	12	410	7,500	100,000	110,000
SO_4	280	140	1,500	40,000	370,000	410,000
Mn	1.2	0.2	3.9	140	900	1,000
Al	1.0	2.1	9.8	260	2,400	2,600
Cu	0.5	0.3	0.3	80	0.5	75
Zn	0.7	0.2	1.4	87	280	370

2.10 Discussion and Conclusions

A pollutant budget analysis indicates that over 89% of the dissolved Fe, SO_4, aluminum, and acidity released to Ore Knob Branch are produced in the vadose zone of the pile. These AMD constituents are rapidly transported through the pile by surface water from the upstream watershed. Given the tremendous mass of acidity produced within the pile (approximately 220 tons per year), long term treatment of the discharge is not practical.

Significant spatial variations in the physical and hydraulic characteristics of the tailings cause large variations in air filled porosity and effective oxygen diffusion into the tailings pile. Tailings in the upstream areas are finer grained, with lower air filled porosity and oxygen diffusivity. The original tailings in the downstream areas are coarser grained, with lower water retention and high oxygen diffusivity. However, weathering processes have increased the fine grained fraction in the oxidized zone and hardpan layer, increasing water retention and lowering oxygen diffusivity. The thickness of the downstream oxidized zone combined with the increased water retention due to weathering may have significantly reduced acidity generation in the downstream areas.

Due to concerns over the stability of tailings pile slope and concerns over potential overtopping of the embankment during large flood events, U.S. EPA is regrading the embankment face and constructing a diversion channel around the tailings pile. These changes are expected to substantially reduce water flow through the pile, reducing the vector that transports AMD into Ore Knob Branch. However, these modifications will also lower the water table in upstream portions of the pile where acidity production is now relatively low. It is not clear whether lowering the water table in the upstream areas will significantly

increase acid production since the tailings in this area are fine grained and retain substantial water even when the water table is low. A quantitative model capable of simulating saturated unsaturated flow, oxygen transport, and geochemical reactions is required to address this issue.

CHAPTER 3

3. WASTE GLYCEROL ADDITION TO REDUCE AMD PRODUCTION IN UNSATURATED MINE TAILINGS

3.1 Introduction

Mining can produce enormous quantities of waste rock and mill tailings that may contain reactive sulfide minerals (Moncur et al. 2005). These wastes are often deposited in impoundments or piles where they are exposed to atmospheric oxygen (O_2) and infiltrating rainwater, leading to the formation of acid mine drainage (AMD). The adverse effects of AMD can continue for centuries after mining has ended (Blowes et al. 1992; Nordstrom and Alpers 1999; Pyatt and Grattan 2001).

AMD can be treated by a variety of methods. While both chemical and biological AMD treatment methods can be effective, they often require ongoing maintenance, substantial land area, and produce metal containing sludge that must be managed (Coetser et al. 2006). Instead of treating AMD after it is produced, tailings piles can be managed to prevent AMD production by reducing contact between the tailings and oxygen. Common approaches for reducing oxygen contact include installation of clay or synthetic caps and flooding the pile with water. Organic covers have also been proposed as an oxygen consuming barrier to prevent AMD production (Germain et al. 2003). In theory, a wide variety of electron donors can be used including wood chips, sawdust, composted municipal sewage sludge, poultry manure, and leaf compost (Waybrant et al. 2002; Zagury et al. 2006). In test cells packed with mine tailings, Hulshof et al. (2006) observed a 80–99.5% reduction

in Fe concentrations when woodchips and pulp waste were blended into the upper 1 m compared to untreated controls.

In this study, we report on the use of waste glycerol (WG), a byproduct of biodiesel production, to reduce release of metals, sulfate, and acidity from unsaturated tailings at the Ore Knob Mine, a former copper–zinc mine located in western North Carolina. From 1957 to 1962, Appalachian Sulphides, Inc. operated a mine and processing facility at the site. Most waste tailings were pumped to an impoundment located on Ore Knob Branch, eventually forming a 9 ha tailings pile with a maximum tailings depth of 21 m at the center of the embankment face. The hydrological and geochemical characteristics of the pile have been described by Behrooz and Borden (2012). Oxidation of pyrrhotite and related sulfide minerals in the vadose zone of the Ore Knob Mine tailings pile produces AMD, which is rapidly transported through the pile by infiltrating surface water. Annual pollutant loads (kg/yr) released by the pile are estimated to be 220,000 acidity, 100,000 Fe, 370,000 SO_4, 900 Mn, 2,400 Al, and 280 Zn.

Rapid growth in biodiesel production has increased the availability of WG, which typically contains large amounts of soluble organic material (glycerol, methanol, and other soluble constituents) and significant amounts of alkalinity from residual base added as a catalyst in the transesterification process (Colucci et al. 2005). The WG could be tilled into the surface of tailings piles to treat and/or prevent AMD production. As the dissolved WG is transported deeper into the tailings with infiltrating rainfall, the residual base would neutralize acidity while the soluble organic components could consume oxygen as it diffuses into the tailing and serve as electron donor for SRBs to reduce sulfate to sulfide precipitating

dissolved metals. The effectiveness of WG in reducing AMD production was examined in–situ in a 20 month column study.

3.2 Materials and Methods

Four experimental columns were installed in December 2007 at Ore Knob tailings pile (Behrooz and Borden 2012) and were loaded with reduced tailings believed to have limited prior exposure to oxygen. The experimental columns were allowed to equilibrate for 3 months before sampling began in March 2008. Each column was 1.37 m long by 0.3 m diameter PVC pipe with approximately 0.17 m of pipe projecting above the ground surface to contain precipitation that fell on the column. Fig. 3.1 shows the structure of the experimental columns.

The columns were buried in the tailings pile in an attempt to replicate in–situ temperature variations. Platinum electrodes were installed at 0.25, 0.50, 0.75 and 1 m below the tailings surface to monitor changes in Eh, following methods developed by Fiedler et al. (2007). Suction lysimeters were installed at the same four depths to monitor changes in pore water chemistry. A slotted PVC pipe covered with 0.2 m of gravel and a fiberglass mesh was installed at the bottom of each column to collect any accumulated liquid. The suction lysimeters were sampled with a vacuum pump following methods described by Chaimberg et al. (1992). Water samples from the bottom of the columns were collected with a peristaltic pump and passed through a 0.45 μm Whatman filter to remove particulate material. All

samples were placed on ice immediately after collection and transported to the laboratory within 24 hours for analysis.

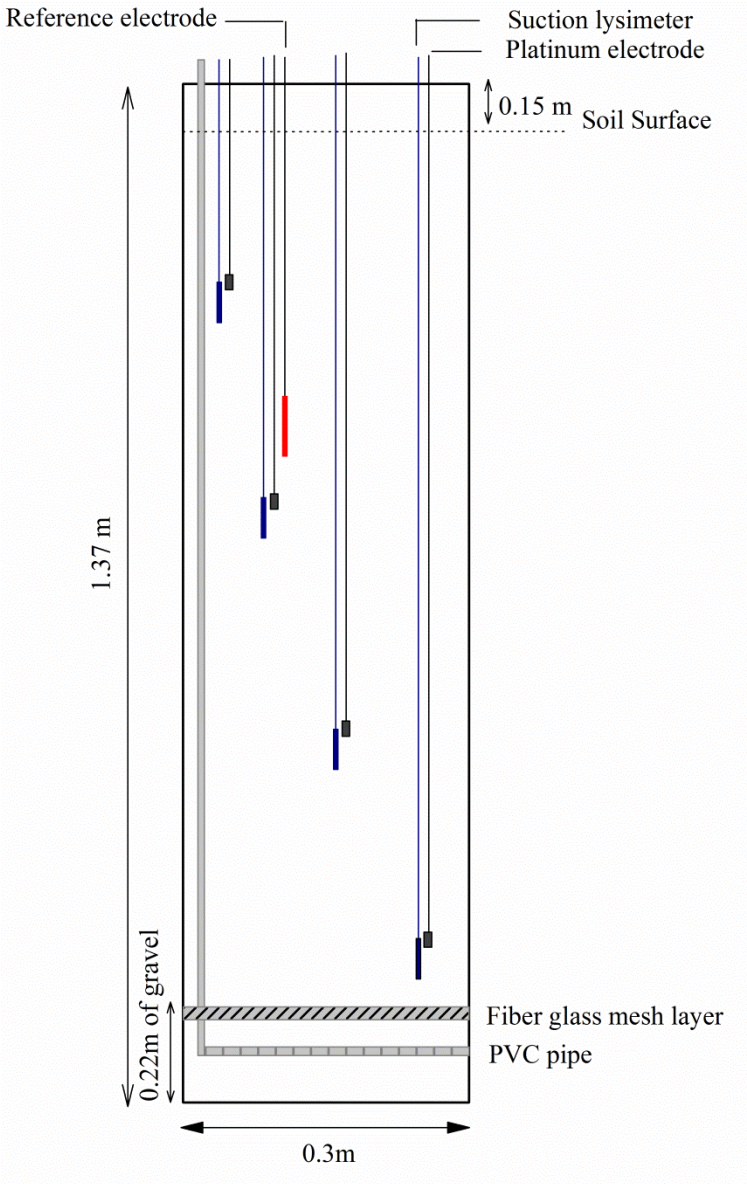

Fig. 3.1 Schematic of experimental columns; platinum electrodes and suction lysimeters were placed in 0.25 m intervals

Experimental columns were monitored periodically over the 20 month experimental period. Dissolved oxygen (DO), H_2S, pH, and redox potential (Eh) were measured in the field. DO and H_2S were measured using visual Chemetrics kits. The Eh was measured using a voltmeter, a platinum electrode, and a gel–filled Calomel reference electrode (Fiedler et al. 2007). The pH of infiltrated was measured using a handheld meter with an ACCUMET combination electrode, which was calibrated prior to each use at pH = 4, 7, and 10. The total organic carbon (TOC) was measured using a Shimadzu TOC analyzer (ASI–L TOC Autosampler). Alkalinity of WG was measured following Standard Methods 2320–B4D (APWA 1989). The chemical oxygen demand (COD) of the WG was measured following method 8000 U.S. EPA (U.S. EPA 1980). Dissolved Al, Cu, Ca, Mg, Mn, Na, Pb, Co, Ni, Cr, K, Si, and Zn in pore water were analyzed by inductively coupled plasma atomic emission spectroscopy (ICP–AES) with a Perkins Elmer Plasma II Ion Coupled Plasma Argon Emission Spectrometer (ICP–AES) following methods equivalent to U.S. EPA method SW–846 6010C. Dissolved Pb, Ni, and Co were always below detection limits (less than 0.05 mg/L) and will not be discussed further. Dissolved anions (SO_4, NO_3, NO_2, PO_4, Cl, and Br) were analyzed using ion chromatography (Dionex IC) following methods equivalent to U.S. EPA method SW–846 9056. NO_3^-, NO_2^-, PO_4^{-3}, Cl^-, and Br^- were below detection limits (less than 2.5 mg/L) in all samples. Carbon content of the tailings was measured using a Perkin Elmer 2400 CHN Elemental Analyzer. Hot acidity was measured by boiling the sample in the presence of hydrogen peroxide and sulfuric acid and then titrating to pH=8.2 with sodium hydroxide to measure acidity associated with dissolved metals (Clesceri 1989).

Physical properties of tailings, including porosity, air–filled porosity, and hydraulic conductivity were measured by Behrooz and Borden (2012) on fresh, unoxidized tailings collected from 0.5 m below the ground surface immediately adjoining the test columns. The tailings were characterized by x–ray diffraction (XRD) and extraction of the sediment with HCl/HNO_3 and H_2O_2 following U.S. EPA method 3050 B, followed by ICP–AES analysis.

After seven months of operation to establish baseline conditions, 2.5 kg of WG were applied to the surface of two replicate columns; two columns remained as replicate controls. The amount of WG applied was estimated to consume any oxygen entering the surface of the column over a 12 month period, assuming an oxygen diffusion depth of 0.25 m and an air filled porosity of 10%. The WG was applied by removing the top 0.18 m of tailings, blending it with 2.5 kg of WG, and then adding the mixed WG tailings back to the surface of the column. The experimental columns were installed in December 2007 and then monitored in March, April, May, and June 2008 to establish baseline conditions. The WG was applied in June 2008. Both treated and control columns were monitored in July 2008, August 2008, June 2009, and August 2009. The columns were frozen from December 2008 to February 2009 and could not be sampled.

3.3 Experimental Results

3.3.1 Column Installation and Material Properties

The columns were packed with reduced tailings, believed to have limited prior exposure to oxygen. These tailings have a D_{50} = 40 μm, D_{10} = 4 μm, particle density of 3.03,

bulk density of 1.69, porosity of 0.44, saturated hydraulic conductivity (K_{SAT}) of 4.6×10^{-6} m/d (Behrooz and Borden 2012). However, these properties could have been altered over the experimental period by oxidation or WG addition. The tailings used to pack the columns had a pH of 4.3 (Sobek et al. 1978), an acid neutralization potential of -2 kg H_2SO_4/t and a potential acidity of 900 kg H_2SO_4/t (Sobek et al. 1978). X–ray diffraction measurements indicate the tailings are principally albite, quartz, and chlorite with smaller amounts of pyrrhotite and pyrite. Extraction of the sediment with HCl/HNO_3 and H_2O_2 following U.S. EPA method 3050 B and analysis by ICP–AES indicates the tailings also contain 4.1×10^3 mg/kg of Zn and 1.1×10^3 mg/kg of Cu.

The WG used to treat the columns had a chemical oxygen demand (COD) of 1.1×10^6 mg/kg, and a total organic carbon content (TOC) of 3.5×10^5 mg/kg. The WG contained 1×10^5 mg/kg of alkalinity as $CaCO_3$ and 2.9×10^4 mg/kg of K, presumably from the KOH used in the biodiesel production. Al, Ca, Cu, Fe, Mg, Mn, Na, NO_3, PO_4, SO_4, S, Si, Cl, and Br were all below detection (< 0.05 mg/g).

3.3.2 Major Anions and Cations in the Column Effluent

Variations in parameter concentration versus time are shown for 0.5 m below the tailings surface (Fig. 3.2) and for the column effluent (Fig. 3.3). Fig. 3.4 shows profiles of contaminant concentrations versus depth in the four columns one year after WG addition. Complete pore water and leachate monitoring results are provided in Appendix B (Tables S.B.1 to S.B.4. On some dates, there was not enough liquid sample to analyze for all of the parameters, so the number of samples analyzed for each column varies. There was also an

extended period between 61 and 274 days when the columns were frozen and could not be sampled.

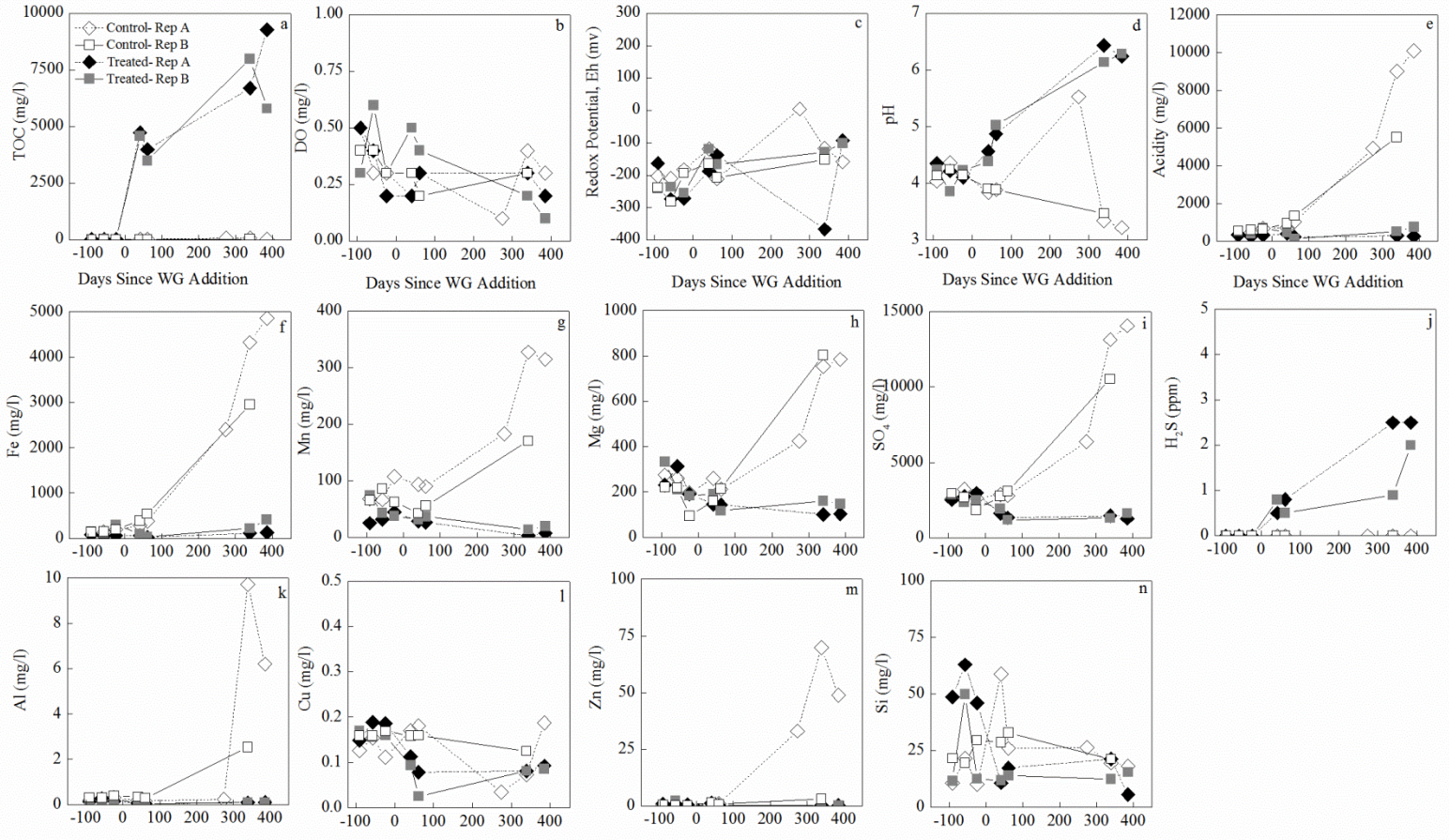

Fig. 3.2 Variation in **a** total organic carbon (TOC), **b** dissolved oxygen (DO), **c** redox potential (Eh), **d** pH, **e** acidity, **f** iron (Fe), **g** manganese (Mn), **h** magnesium (Mg), **i** sulfate (SO_4), **j** hydrogen sulfide (H_2S), **k** aluminum (Al), **l** copper (Cu), **m** zinc (Zn), and **n** silica (Si) at 0.5 m below surface in experimental columns over time

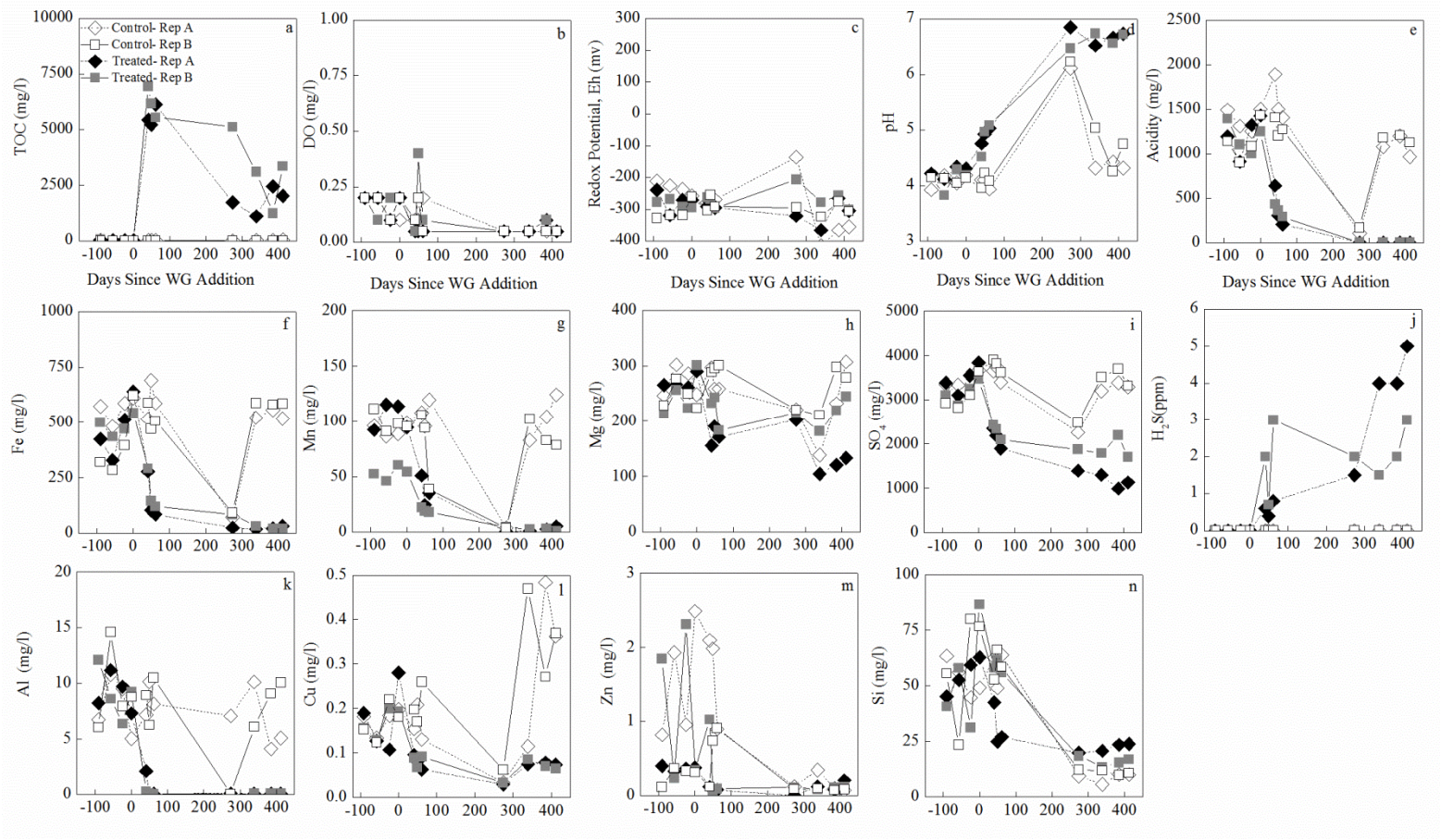

Fig. 3.3 Variation in **a** total organic carbon (TOC), **b** dissolved oxygen (DO), **c** redox potential (Eh), **d** pH, **e** acidity, **f** iron (Fe), **g** manganese (Mn), **h** magnesium (Mg), **i** sulfate (SO_4), **j** hydrogen sulfide (H_2S), **k** aluminum (Al), **l** copper (Cu), **m** zinc (Zn), and **n** silica (Si) in column effluent (1.2 m depth) in experimental columns over time

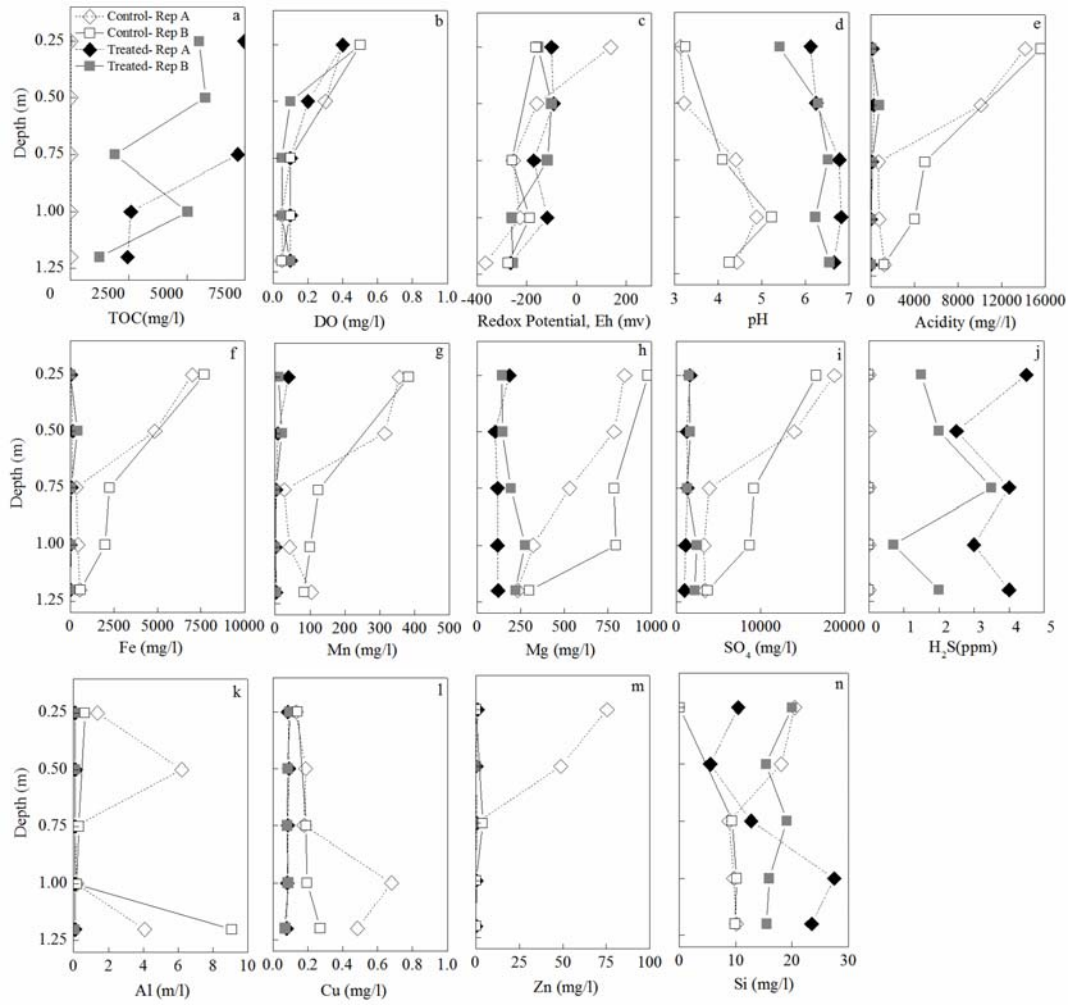

Fig. 3.4 Profiles of **a** total organic carbon (TOC), **b** dissolved oxygen (DO), **c** redox potential (Eh), **d** pH, **e** acidity, **f** iron (Fe), **g** manganese (Mn), **h** magnesium (Mg), **i** sulfate (SO_4), **j** hydrogen sulfide (H_2S), **k** aluminum (Al), **l** copper (Cu), **m** zinc (Zn), and **n** silica (Si) versus depth at one year after WG addition

TOC values were near the analytical detection limit (10 mg/L) over the monitoring period. In the treated columns, TOC increased to roughly 5,000 mg/L immediately after WG addition in the 0.5 m samples (Fig. 3.2a) and column effluent (Fig. 3.3a), indicating that some portion of the WG rapidly penetrated the full length of the columns (Fig. 3.4a). At one

year after WG addition (Fig. 3.4a), high TOC concentrations remained throughout the treated columns. If the WG was uniformly distributed throughout the column, the TOC concentration would have increased to approximately 22,000 mg/L, suggesting that most of the organic material was not present in solution. The rapid penetration of relatively high TOC concentrations throughout the column was somewhat surprising since the average hydraulic residence time (HRT) in the columns was more than a year. The rapid WG penetration could be due to: a) heterogeneities in the columns; b) the high density of WG (1.3 grams/mL); or c) the intermittent nature of groundwater recharge where pulses of water migrate through the vadose zone following rainfall events.

Fig. 3.5 shows the total carbon distribution in the column sediment at the end of the experiment. It was not possible with the analytical method employed to distinguish between organic and inorganic carbon. However, all water samples were undersaturated with respect to $FeCO_3$, $CaCO_3$, and $MgCO_3$, suggesting that most of the carbon in the sediment was organic. The carbon content of the treated 0.5, 0.75, and 1.0 m samples were elevated compared to the control columns, consistent with some penetration of carbon throughout the column. However, the carbon content of the 0.25 m treated samples were much higher, indicating that most carbon was retained in the upper portion of the columns.

As part of the data analysis, we attempted to perform a mass balance on the carbon added to the column in the form of WG and recovered in the column effluent and solid tailings. The total TOC discharged in the treated columns effluent was 70 g or 8.5% of the carbon added in the WG, consistent with retention of most TOC within the columns.

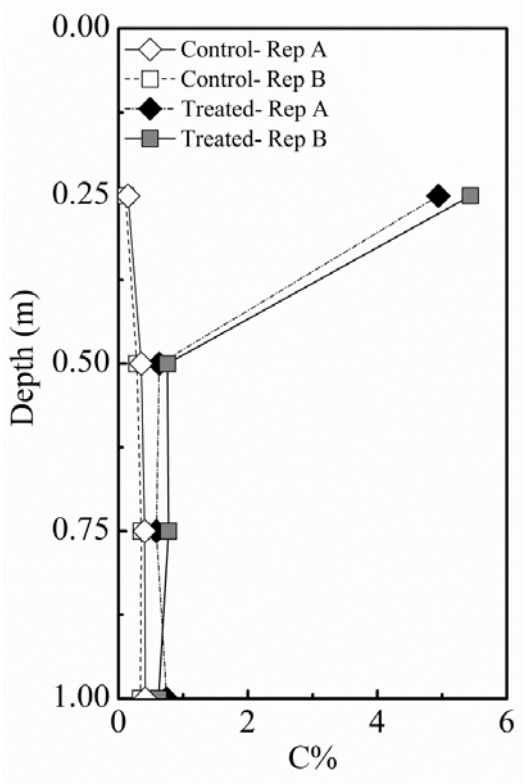

Fig. 3.5 Carbon content of the tailings in control and treated columns at the end of the study

The highest carbon concentrations in the tailings were measured in sediment samples collected from 0.25 m below the surface. If these samples are assumed to be representative of all material from 0 to 0.25 m in the column, the carbon content of this zone was increased by approximately 1.56 kg or roughly twice the carbon added in the WG (0.82 kg organic carbon). Clearly, the addition of 0.82 kg of carbon should not increase the tailings carbon content by 1.56 kg. This apparent error is likely due to assuming the carbon is uniformly distributed throughout the upper 0.25 m of the column. If the carbon content of the sediment was much lower near the surface, this would explain the apparent mass balance error. Overall, the carbon analysis results indicate that only a small amount of organic carbon was

released in the column effluent and a large amount of carbon was still present near the tailings surface, 15 months after WG application.

Dissolved oxygen (DO) and redox potential (Eh) followed the same general pattern in both treated and control columns. There was a small decline in DO with time in both the 0.5 m and effluent samples (Fig. 3.2b and 3.3b), presumably due to oxygen consumption by oxidation of sulfide minerals. The Eh remained essentially constant (≈ –300 mv) in the effluent samples, but slowly increased in the 0.5 m samples, due to the gradual oxidation of the surficial tailings. The similarity in DO and redox measurements across the control and treated columns suggests that WG addition did not measurably reduce oxygen penetration into the columns. However, it is difficult to reliably measure oxygen concentrations less than 0.5 mg/L, so WG may have somewhat reduced oxygen availability.

While oxygen penetration in the treated and control columns may have been similar, acidity production and the resulting pH were dramatically different. Prior to WG addition, the pH of the columns varied between 4.0 and 4.5 and acidity varied between 1,000 and 1,500 mg/L. In the control columns, acidity increased dramatically with time in the 0.5 m samples with an associated decline in pH (Fig. 3.2d and 3.2e). In the control column effluents (Fig. 3.3d and 3.3e), acidity was relatively constant with a small increase in pH. In the treated columns, acidity remained constant or increased slightly with time at 0.5 m below the surface and declined to < 1 mg/L in the column effluent (Fig. 3.2e and 3.3e). The pH followed a similar trend, increasing to between 6 and 7 from 0.5 m to the column effluent one year after WG addition (Fig. 3.4d). The increase in pH immediately after WG addition is likely associated with the KOH present in the WG. The larger pH increase and acidity decline in

the second year may be associated with oxygen and/or SO_4 consumption by the added organic material. An exception to these overall trends was monitoring data collected in March immediately after the spring snow melt (274 days after WG addition). When first sampled after snowmelt, all the columns appeared to be saturated with cold water. In the control columns, saturation with cold water resulted in a large increase in pH and decline in acidity. However, by the following June (day 232), acidity and pH had returned to the levels observed the previous summer.

In the control columns, the large increase in acidity in the shallow 0.5 m samples corresponds with a similar increase in dissolved iron (Fe) and sulfate (SO_4), presumably due to oxidation of pyrrhotite and pyrite. There were also substantial increases in manganese (Mn), magnesium (Mg), aluminum (Al), and zinc (Zn) in these samples, released from the tailings by oxidation and/or low pH. In control column effluents, Fe, Mn, Mg, SO_4, and Al remained relatively constant with time due to the long HRT and slow flushing of dissolved salts through the column. Similar to pH and acidity, there were large apparent drops in Fe, Mn, SO_4, and Al immediately after spring snowmelt.

In the treated columns, results were dramatically different. In the shallow 0.5 m samples, dissolved Fe, Mn, Mg, Al, and Zn remained relatively constant. SO_4 declined from 2500-3000 mg/L to below 1500 mg/L. These declines were likely associated with reduced production of SO_4 and/or reduction of SO_4 to H_2S by SRBs (Fig. 3.2j). The highest H_2S levels were observed in the second summer, presumably due to growth of SRBs over time and increased reduction of SO_4 to H_2S at higher temperatures.

In the treated column effluents, there were large declines in Fe, Mn, SO_4, and Zn coincident with hydrogen sulfide (H_2S) production. There were smaller decreases in sodium (Na), potassium (K), and calcium (Ca) with time in the control or treated columns effluents (Appendix B, Tables S.B.1 to S.B.4). Given the long HRT of the columns, the observed declines in Fe, Mn, and Zn were probably not due to reduced oxidation of the surficial tailings, but due to reduction of SO_4 to H_2S and precipitation as metal sulfides. Na, K, and Ca do not commonly precipitate as sulfides, so these cations were not as effectively removed.

The beneficial effects of organic substrate addition are most apparent in chemical profiles at one year after WG addition (Fig. 3.4). TOC remains high throughout the treated column profile. While the DO profiles are similar, redox potential is somewhat higher in the shallowest control samples. This results in very high acidity, Fe, Mn, and SO_4 in the shallowest control samples with corresponding low pH due to intense oxidation at the tailings surface. The high acidity and low pH results in high levels of Mg and Zn. In the shallow treated column samples, acidity, Fe, Mn, Mg, SO_4, Al, Cu, and Zn remain low, indicating much more limited oxidation of the tailings. Deeper in the treated columns, Fe, Mn Al, and Zn declined.

Fig. 3.6 shows the total mass discharged from the control and treated columns after WG addition. The large increase in TOC in the treated column effluents corresponds to large reductions in acidity, Fe, Mn, Al, and Cu. In the 12 months following WG addition, 6–10% of the applied TOC was recovered in the treated column effluents. The WG applied to the treated columns provided 250 g of alkalinity as $CaCO_3$, which exceeds the acidity discharged

in the untreated control columns, indicating that the residual base (KOH) was a major component of the treatment process.

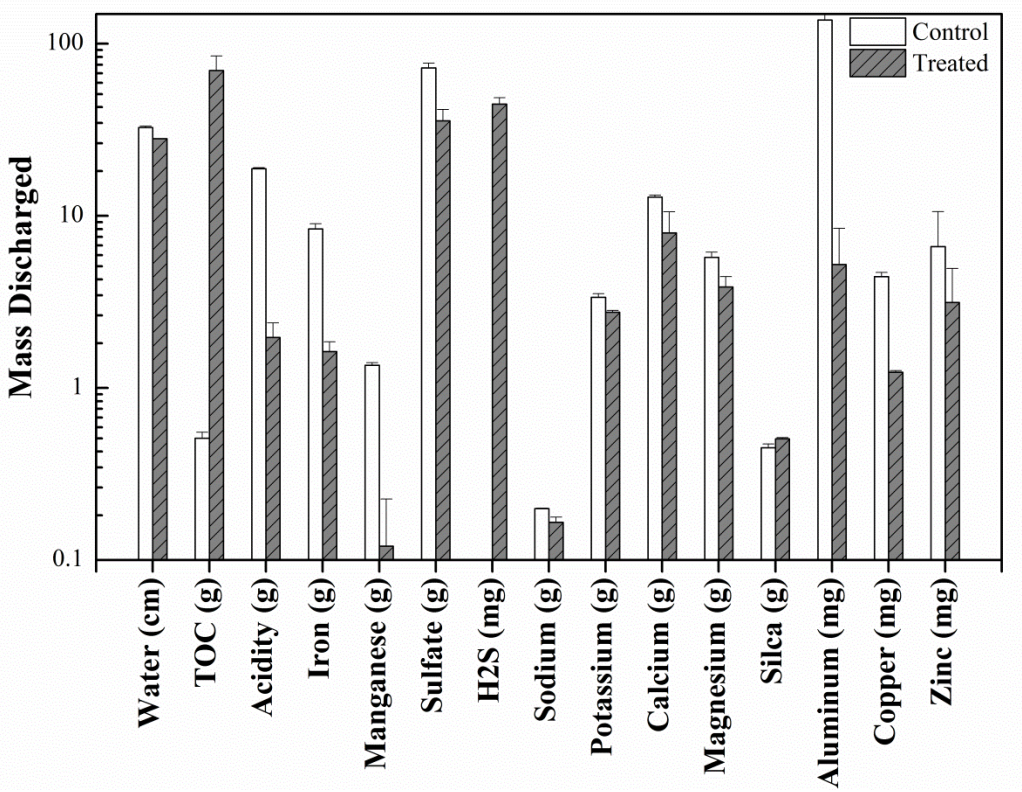

Fig. 3.6 Average mass discharged from control and treated in 14 months following substrate addition. Error bars are maximum value observed

Fig. 3.7 shows average parameter concentrations for the five sampling dates after WG addition for the treated columns (A and B) and control columns (A and B). With the exception of TOC, concentrations of all major parameters decreased following WG addition. In comparison, concentrations of most parameters increased in the untreated controls. Same day contaminant concentrations in the treated column effluents were reduced by the following amounts compared to the untreated controls (± one standard deviation): 86 ±12%

for acidity, 83 ±18% for Fe, 48 ±9% for SO_4, 97 ±6% for Al, 84 ±16% for Mn, 67 ±13% for Cu, 29 ±74% for Zn, 33 ±11% for Ca, 30 ±8% for Mg, 11 ±24% for Na, and 13±10% for K. Removal efficiencies for most major parameters increased with time, reaching a maximum in the second summer after WG addition (Fig. 3.8).

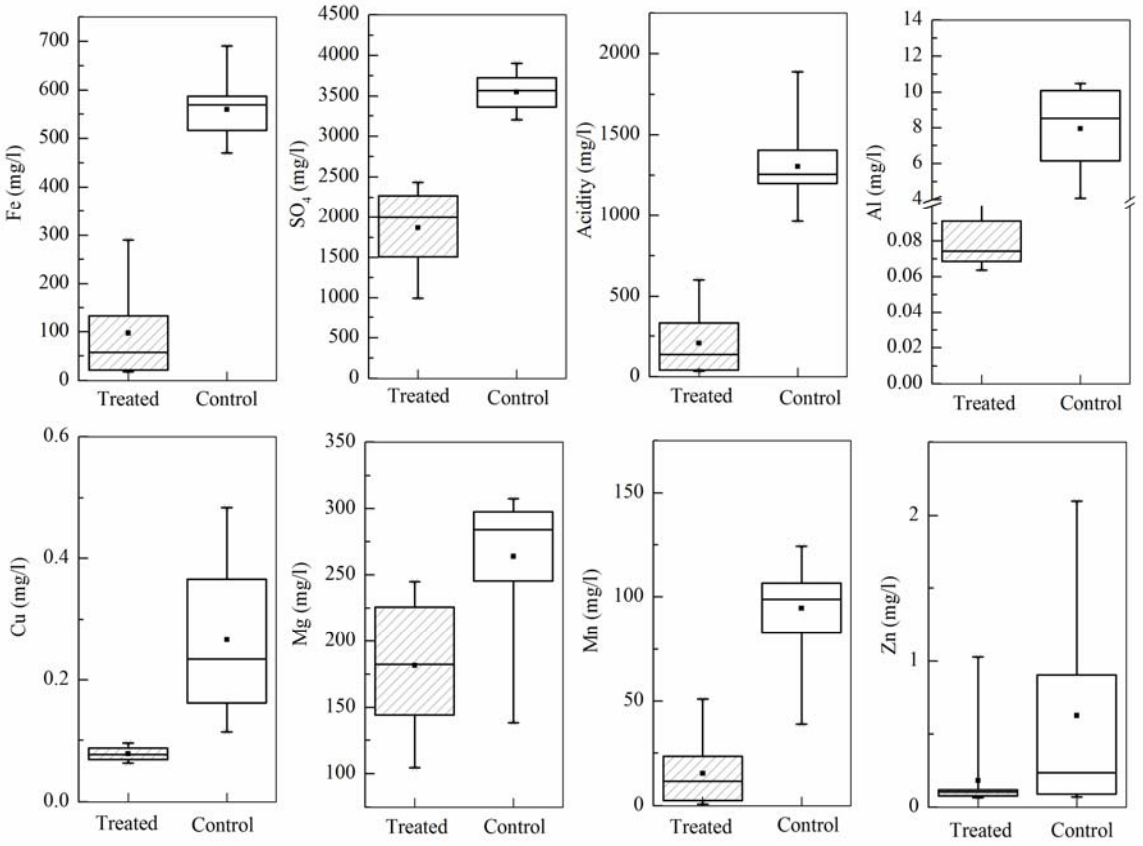

Fig. 3.7 Comparison of contaminant concentrations in the treated columns and control columns during the treatment period (June 2008 to August 2009). Graphs include minimum, maximum, upper quartile, lower quartile and average of each data set

3.3.3 Mineral Precipitation

The PHREEQC geochemical modeling program with an internal PHREEQC database (Parkhurst and Appelo 1999) was used to calculate the saturation index (SI) for potential mineral precipitates. SI is defined as the base ten log of the ion activity product (IAP) divided by the mineral solubility product (Ksp) (SI = log (IAP/Ksp), so a SI value of 1 indicates the dissolved mineral concentration is a factor of ten above saturation. The anomalous data collected immediately after spring snowmelt was not included in this analysis since it was likely associated with a short–term event and may not be representative of longer term trends. A charge balance was computed for each sample as a quality control check. With the exception of a few samples collected from the treated columns during active H_2S production, average charge balance errors were 4 – 5%. In the few cases where the charge balance error exceeded 10%, these samples were excluded from the analysis.

Fig. 3.9 shows the average and range of SI for different minerals at 1.0 m below the ground surface in the treated and control columns. The control columns were somewhat supersaturated with quartz (SI = 0.2 – 1.1) throughout the profile. The shallow sampling ports in the control columns were also slightly supersaturated with gypsum (SI = 0 – 0.14), while the deeper ports were consistently supersaturated with alunite. Gypsum saturation is consistent with the very high sulfate concentrations observed in the 0.5 m samples. By the second summer, the deeper pore waters were also saturated with gibbsite, potassium (K) mica, and kaolinite.

In the two summer months immediately after WG addition, the treated columns were undersaturated with respect to most minerals (except quartz). However during the following

summer, the increase in H_2S caused the bottom sampling ports in the treated column to be strongly supersaturated with a variety of sulfide minerals (amorphous FeS, mackinawite, pyrite, and sphalerite), while the increase in pH caused the bottom sampling ports to be supersaturated with aluminum minerals (alunite, gibbsite, calcium montmorillonite, illite, potassium feldspar, potassium mica, and kaolinite). Precipitation of some aluminum minerals may be slow, and solutions may remain supersaturated with some aluminosilicates for extended periods (Nagy et al. 1991). However, sulfide precipitation is expected to be relatively rapid, removing dissolved Fe and Zn (Rickard 1995).

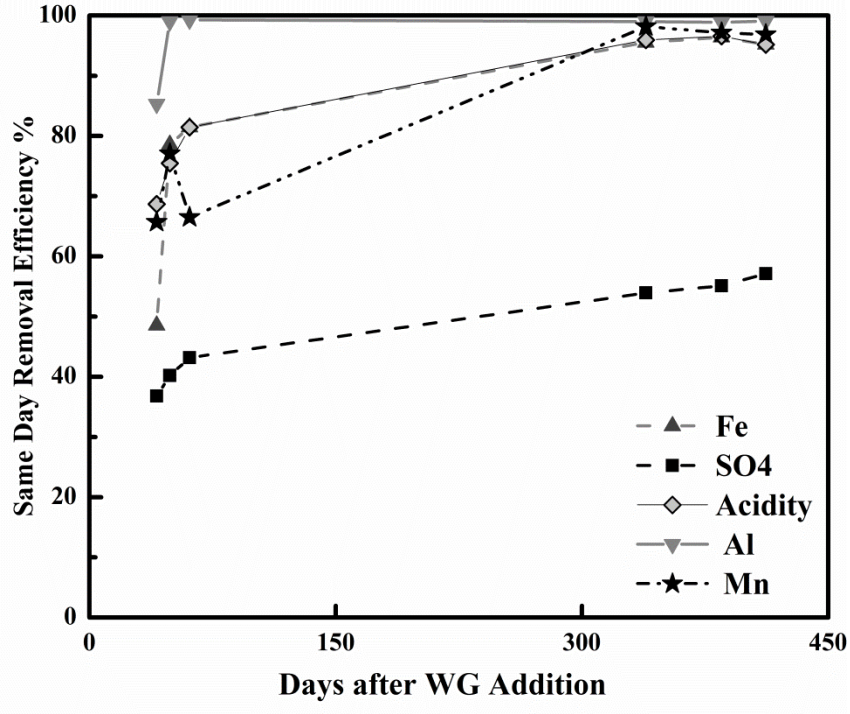

Fig. 3.8 Variation in treatment efficiency over time following WG addition

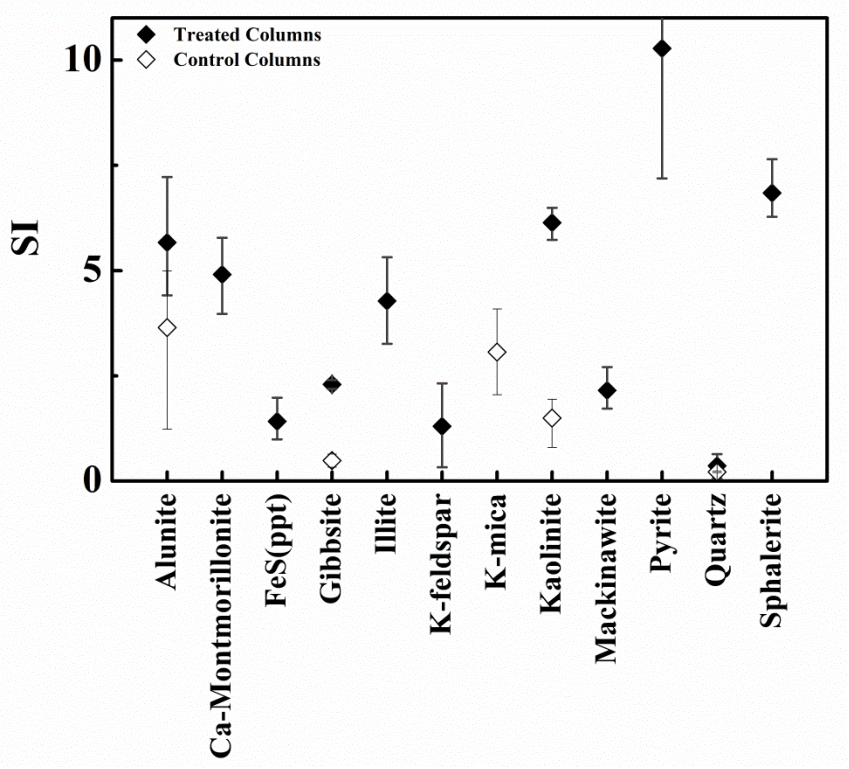

Fig. 3.9 Average saturation index of potential mineral precipitates in control and treated columns in the second summer after WG addition at 1.0 m below ground surface. Error bars are average of minimum and maximum saturation indices

3.4 Potential Field Application

Waste glycerol (WG) could potentially be used to reduce AMD production from mine tailings by spraying the material onto the tailings surface, and then tilling it into the tailings using a disc harrow or similar implement. WG and associated fermentation products that migrate deeper into the tailings could then reduce concentrations of AMD constituents that have already been produced. In humid areas, natural rainfall infiltration would carry the WG deeper into the tailings. However in arid areas, surface irrigation may be required.

As reported above, 2.5 kg of WG was blended into the surface of 0.3 m diameter columns containing mine tailings (application rate = 35 kg/m^2) and was effective in reducing concentrations of major AMD constituents in the column effluents. Acidity was reduced by an average of 86%, Fe by 83%, Al by 97%, Mn by 84%, and Cu by 67%, when compared with same day concentrations in the untreated controls. Observed removal efficiencies for acidity, Fe, and Al were similar to those achieved in well operated, passive treatment systems employing alkalinity addition, aeration, and sedimentation (PIRAMID Consortium 2003). Anaerobic bioreactors using solid organic substrates can achieve similar removal efficiencies. Zagury et al. (2006) reported removal efficiency of up to 100% for Fe, 99% for Mn, 99% for Cd, 99% for Ni, and 94% for Zn in batch experiments using a variety of organic substrates. In pilot scale bioreactors filled with spent mushroom compost conditioned with gypsum and limestone, Dvorak et al. (1992) observed over 95% reductions in Al, Cd, Fe, Mn, Ni, Zn, and acidity. However, bioreactors require significant land area for construction and must be regularly replenished with fresh organic substrate to maintain treatment performance.

Acidity is released from tailings piles when oxygen (O_2) reacts with pyrite (FeS_2) releasing Fe^{+2}, SO_4, and acidity. Once released from the pile, the AMD will react with additional oxygen causing the Fe^{+2} to precipitate as $Fe(OH)_3$ with the following overall reaction.

$$3FeS_2 + 11.25O_2 + 10.5H_2O \rightarrow 6H_2SO_4 + 3Fe(OH)_3 \qquad \text{Reaction3.1}$$

WG can treat and/or reduce acidity through two major processes. Large amounts of residual alkalinity (0.1 kg of $CaCO_3$ / kg WG used in this project) are present in the some WG products due to the KOH or NaOH used in biodiesel production and will neutralize H_2SO_4 that has already been produced. Glycerol, methanol, and other dissolved organic material in the WG provide 1.1 kg of COD per kg of WG, which can reduce oxygen before it reacts with FeS_2 or reduce the SO_4 back to sulfide, causing Fe^{+2} to precipitate. Based on the stoichiometry of equation 1, the overall effect of these two processes would be to reduce acidity generation by approximately 2 kg of acidity as $CaCO_3$ per kg of WG. As of August 2011, WG cost \$0.11 – 0.18 /kg in bulk quantities (http://www.icispricing.com/, downloaded March 1, 2012). If only the residual base in the WG is considered, the alkalinity in WG would cost \$1.1 – 1.8 \$/kg $CaCO_3$, which is much higher than other common alkalis. However, if the apparent beneficial effects of the soluble organic carbon in reducing AMD production are considered, WG will reduce acidity production by 0.055 – 0.09 \$/kg of acidity, a much lower cost than other materials.

Using the same application rate as in the column experiments and a conservative cost of \$0.18/kg WG, treatment of the 9 ha Ore Knob tailings pile would cost \$550,000 (\$62,000 per ha) plus costs for transportation to the site, spray application, and tilling into the tailings surface. This cost is substantial, but much lower than the \$11,000,000 that will be expended by U.S. EPA for short–term management of the site (U.S. EPA 2010). Costs could possibly be reduced further by using a smaller amount of WG. In the column experiment, most of the organic carbon added to the tailings was still present at the end of one year, indicating that the amount of material added was much greater than that required for short–term treatment.

Behrooz and Borden (2012) reported that the Ore Knob Tailings pile was currently releasing approximately 220,000 kg/yr of acidity. Treating this acidity would require ≈110 t of WG per year at a cost of $20,000 per year plus transportation and surface application. The analyses presented above show that WG can be a cost effective alternative to common commercial alkalis. However, the primary benefits of this process would be the ease of application. In the process described above, treatment occurs within the pile, so there is essentially no land required, no permanent treatment facilities (tanks, basins, aeration equipment, etc.), no power required for aerators, pumps or mixers, and no waste sludge or other residuals produced. The process is effective at reducing a variety of contaminants, not effectively removed by alkali addition.

While the process described above can be cost effective, it is not a permanent solution. Additional WG would need to be periodically reapplied to maintain performance. A potentially more efficient approach would be to apply WG prior to installation of a permanent cap. The WG would treat/neutralize acidity already produced in the pile and provide a reservoir of reducing power to control future AMD production.

3.5 Conclusions and Applications

Monitoring data collected during the course of this project demonstrated that surface application of WG effectively reduced pollutant concentrations and total loads for over 15 months, with most carbon still present in the tailings at the end of the monitoring period. WG addition reduced effluent acidity by an average of 86%, Fe by 83%, Al by 97%, Mn by 84%,

and Cu by 67%, compared to same day concentrations in the treated and untreated controls. Treatment likely occurs through a combination of processes including: (a) neutralization of acidity by the KOH present in the WG; (b) reduction of SO_4 to H_2S with subsequent precipitation of dissolved metals, and potentially (c) consumption of oxygen, slowing oxidation of the tailings.

Geochemical modeling indicated that the effluents of the treated columns were supersaturated with amorphous FeS, mackinawite, pyrite, and sphalerite, which could result in relatively rapid removal of Fe and Zn. The column effluents were also supersaturated with alunite, gibbsite, calcium montmorillonite, illite, potassium feldspar, potassium mica, and kaolinite due to the increased pH. However, the slower kinetics of aluminosilicate precipitation could reduce treatment efficiency.

Surface application of WG could potentially be very cost effective for temporary treatment of mine tailings. WG is easy to apply and material costs are comparable to other common alkalis. Major advantages of this approach include no permanent infrastructure or land required, no sludge production, minimal maintenance, and high removal efficiencies for a broad range of contaminants.

CHAPTER 4

4. GEOCHEMICAL CHARACTERIZATION

4.1 Introduction

Soil cores were collected adjoining MW10 and MW13 and analyzed for mineralogic and geochemical characteristics to gain a better understanding of the weathering processes at these two locations.

4.2 Methods

The relative abundance of crystalline minerals was determined by X-Ray powder diffraction using a Rigaku Smart lab X-Ray Diffractometer with a CuKα and a monochromator. Ground samples were step scanned from 5° to 90° 2θ with sampling step of 0.02°. Working conditions were 44 mA and 40 kV. Results were analyzed using PDXL powder diffraction analysis software. In PDXL software, crystalline phases or compounds are identified using a hybrid search/algorithm in a reference database. The hybrid search consecutively identifies phases and it subtracts the intensities of the identified phases from the pattern and starts searching for the next phases.

Trace constituents in the tailings were determined by acid digestion following method U.S. EPA 3050 B using a 1:1 ratio of 12.1 N HCl to 15.8 N HNO_3 and 30% H_2O_2 . Extracted solution was analyzed using inductively coupled plasma atomic emission spectroscopy (ICP-AES) using a Perkins Elmer Plasma II-ICP-AES. This method is designed to extract the

environmentally available metals using HNO_3/H_2O_2 and does not recover silicates and elements bound in silicate structures.

4.3 X-Ray Diffraction Results

Samples of oxidized and reduced tailings from both borings (MW10 and MW13) were analyzed by X-ray diffraction to identify the dominant crystalline minerals and to provide a qualitative indication of the relative abundance of the different minerals. Minerals detected by x-ray diffraction are listed in Table 4.1. To aid in interpreting the weathering patterns, we have grouped these minerals together into five general categories: (1) quartz; (2) aluminosilicates; (3) sulfides; (4) sulfates; and (5) oxides and hydroxides. Graphs showing the relative intensity for the five groups versus depth are presented in Figure 4.1 Fraction Intensity is equal to 100 times the intensity peak of selected mineral/ total intensity of the strongest peaks in spectrum.

At both the fine grained (MW10) and coarse grained (MW13) locations, the overall composition of the tailings is similar in the reduced zone below the water table. At both locations, the reduced tailings are composed of quartz, aluminosilicates and sulfide minerals. The major sulfide minerals are pyrrhotite and pyrite with minor amounts of wurtzite and isocubanite. Aluminosilicates include illite, kaolinite, albite, chlorite and glauconite consistent with weathering of a mixture of quartz and sulfide minerals. At the fine grained location (MW10), the aluminosilicate fraction appears to be somewhat higher, presumably

due to a greater amount of fine grained gangue (worthless material mined with the primary ore) that settled out at this location.

Table 4.1 Detected minerals and related representative chemical formula

Mineral group	Name	Representative chemical formula
Silicate	quartz	SiO_2
Aluminosilicates	illite	$(K,H_3O)(Al,Mg,Fe)_2(Si,Al)_4O_{10}[(OH)_2,(H_2O)]$
	kaolinite	$Al_2Si_2O_5(OH)_4$
	albite	$NaAlSi_3O_8$
	chlorite	$Mg_5Al_2Si_3O_{10}(OH)_8$
	glauconite	$(K,Na)(Fe^{3+},Al,Mg)_2(Si,Al)_4O_{10}(OH)_2$
Sulfides	pyrite	FeS_2
	pyrrhotite troilite mackinawite	FeS
	wurtzite	ZnS
	isocubanite	$CuFe_2S_3$
Sulfates	gypsum	$CaSO_4•2(H_2O)$
	jarosite	$KFe^{3+}{}_3(SO_4)_2(OH)_6$
	carphosiderite	$Fe_3(SO_4)_2\ (OH)_5•2H_2O$
	Piypite	$K_2Cu_2(SO_4)_2O$
Oxide Hydroxide	rancieite	$(Ca,Mn^{2+})Mn^{4+}{}_4O_9•3(H_2O)$
	goethite	FeO(OH)
	meixnerite	$(\ Mg_5\ Al_3\ (OH)_{16}\ )\ ((OH\ )_3\ (H_2O)_4\ )$

In the oxidized zone near the land surface, there are greater differences in the tailings mineralogy between the two different locations. At the coarse grained location (MW13), sulfide minerals are depleted to a depth of 1.0 m with a corresponding increase in sulfates (gypsum and jarosite) and oxides/hydroxides. At the fine grained location (MW10), oxidation is much more limited. Except at the immediate land surface, sulfides are present throughout the profile with reduced amounts of sulfates and oxides/hydrosulfides.

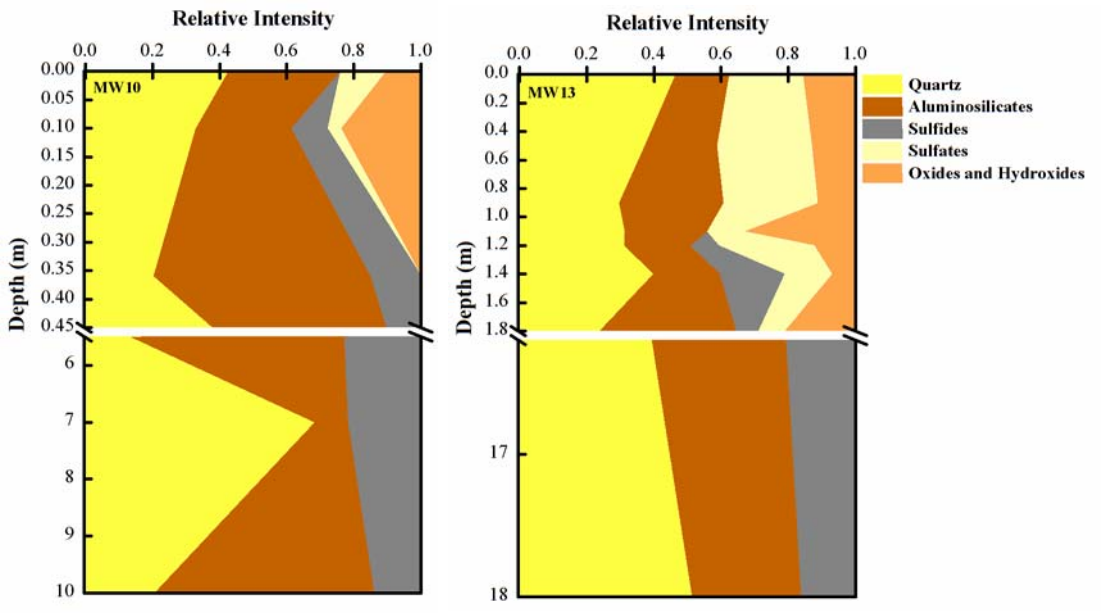

Fig. 4.1 Abundance of different minerals versus depth at fine grained (MW10) and coarse grained (MW13) locations (Relative Intensity, RI = 100 intensity peak hight of mineral/total intensity hight of the strongest peaks of detected minerals in spectrum)

4.4 Acid Extraction Results

The acid extraction results for fine grained (MW10) and coarse grained (MW13) tailings are presented in Fig. 4.2. The dominant extractable elements at both locations are S, Fe, Si, and Al. At the fine grained location, trace element concentrations are relatively consistent with depth, consistent with reduced weathering at this location.

At the coarse grained location, substantial amounts of sulfur, iron, calcium, magnesium and potassium are present in the upper oxidized zone due to precipitation of sulfate minerals, even though the sulfide minerals have been largely depleted. These oxidized sediments are also enriched in copper due to precipitation of piypite in the oxidized zone and

presence of copper sulfide mineral- isocubanite- in the hard pan layer. There is a notable increase in aluminum (illite, albite, and chlorite) and zinc (wurtzite), possibly due to the increased pH at this depth. The relatively low amount of silica observed in the acid extractions is assumed to be due to incomplete recovery of Si with HCl/HNO_3 digestion.

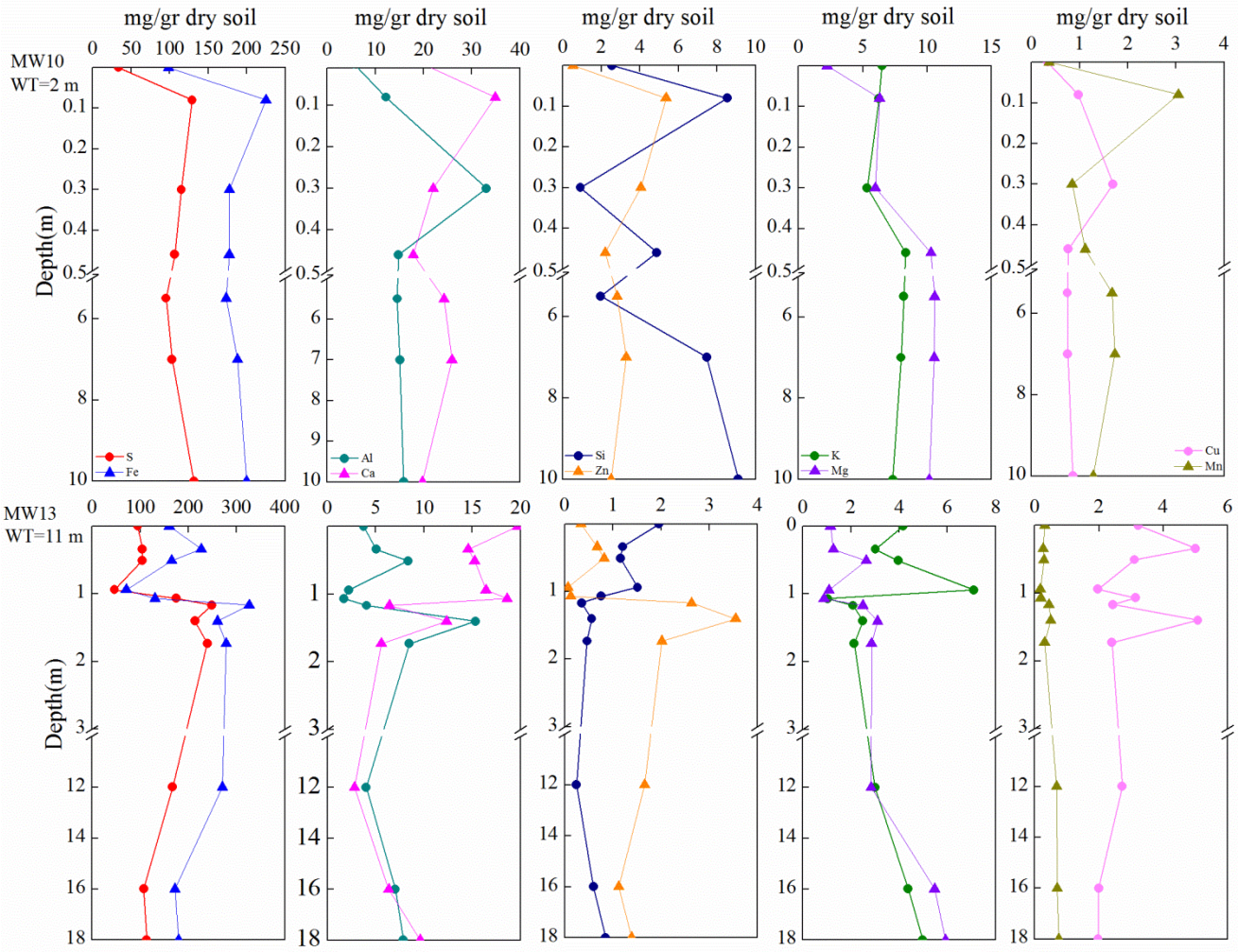

Fig. 4.2 Concentration of S, Fe, Al, Ca, Si, Zn, K, Mg, Cu and Mg versus depth based on acid extraction of fine grained grain (MW10) and coarse grained (MW13) tailings

CHAPTER 5

5. SUMMARY AND CONCLUSION

A detailed hydrologic and geochemical characterization was performed on the Ore Knob Tailings Pile (Ashe County, NC). Significant spatial variations in the physical and hydraulic characteristics of the tailings cause large variations in air filled porosity and effective oxygen diffusion into the tailings pile. Tailings in the upstream areas are finer grained, with lower air filled porosity and oxygen diffusivity. The original tailings in the downstream areas are coarser grained, with lower water retention and high oxygen diffusivity. However, weathering processes have increased the fine grained fraction in the oxidized zone and hardpan layer, increasing water retention and lowering oxygen diffusivity. The thickness of the downstream oxidized zone combined with the increased water retention due to weathering may have significantly reduced acidity generation in the downstream areas.

A hydrological model was calibrated on Ore Knob tailings pile and used to evaluate the U.S. EPA action plan to preserve stability of the embankment face. The proposed diversion of water around the pile is expected to substantially reduce water flow through the pile, reducing the vector that transports AMD into Ore Knob Branch. Although, these modifications will lower the flow through the pile and reduce AMD transport to the downstream, it also lowers the water table in upstream portions of the pile where acidity production is now relatively low. It is not clear whether lowering the water table in the upstream areas will significantly increase acid production since the tailings in this area are

fine grained and retain substantial water even when the water table is low. A quantitative model capable of simulating saturated/ unsaturated flow, oxygen transport, and geochemical reactions is required to address this issue.

A pollutant load analysis using the recharge analysis results and average long term monitoring results show that over 89% of the Fe, SO_4, acidity, and Al released to the Ore Knob Branch are produced in the vadose zone of the pile. Total annual load of acidity discharged from Ore Knob tailings pile is estimated over 220 tons/yr. Given the very high levels of dissolved Fe and acidity produced within the pile, traditional end-of-pipe treatment approaches will have very high capital and operating costs. An affordable passive treatment method is needed to treat AMD within the pile before it is discharged to the surface.

Geochemical characterization of the tailings pile sediments showed that the pH is lowest (3–4) at ground surface and increases with depth. In the most upgradient borings, pH increases to near 7 immediately below the water table (WT) indicating AMD entering from upgradient does not result in a persistent pH decrease. However, further down gradient where there is an extensive unsaturated zone, the increase in pH with depth is more gradual.

Powdered XRD analysis shows the same parent materials in fine and coarse grained areas including; pyrrhotite, troilite, mackinawite, pyrite, quartz, and aluminosilicate. However, weathering pattern has created more intense weathering in the vadose zone of the coarse grained area. Except at the very surface, sulfide minerals are present through the profile in the fine grained area. In the coarse grained area, sulfide minerals are depleted in shallow portions of the vadose zone.

A 20 month long in situ pilot test was conducted to evaluate the surface application of waste glycerol (WG) to reduce release of acid mine drainage (AMD) constituents from mine tailings. WG effectively reduced pollutant concentrations and total loads for over 15 months, with most carbon still present in the tailings at the end of the monitoring period. WG addition reduced effluent acidity by an average of 86%, Fe by 83%, Al by 97%, Mn by 84%, and Cu by 67%, compared to same day concentrations in the treated and untreated controls. Treatment likely occurs through a combination of processes including: (a) neutralization of acidity by the KOH present in the WG; (b) reduction of SO_4 to H_2S with subsequent precipitation of dissolved metals, and potentially (c) consumption of oxygen, slowing oxidation of the tailings.

Geochemical modeling indicates the effluents of the treated columns were supersaturated with amorphous FeS, mackinawite, pyrite, and sphalerite, which could result in relatively rapid removal of Fe and Zn. The column effluents were also supersaturated with alunite, gibbsite, calcium montmorillonite, illite, potassium feldspar, potassium mica, and kaolinite due to the increased pH. However, the slower kinetics of aluminosilicate precipitation could reduce treatment efficiency. Long term monitoring is necessary in order to investigate stability of the precipitated minerals.

CHAPTER 6

6. FUTURE WORK

Spatial variations in the physical and chemical properties of the Ore Knob tailings have a major impact on the depth of weathering and amount of AMD produced. However, there are no good methods for predicting the impact of these variations on AMD production, or how these variations might influence management alternatives.

The U.S. EPA is constructing channels to divert storm water and base flow around the tailings pile to preserve the stability of the embankment face. This diversion is expected to substantially reduce water flow through the pile, reducing the vector that transports AMD into Ore Knob Branch. However, these modifications will also lower the water table in upstream portions of the pile where acidity production is now relatively low. It is not clear whether lowering the water table in the upstream areas will significantly increase acid production since the tailings in this area are fine grained and retain substantial water even when the water table is low. At present, there are no reliable methods for making this assessment.

This research demonstrated that surface application of waste glycerol (WG) was effective in reducing AMD production from fine grained sediments collected in the upstream portion of the waste pile. This same technology is expected to be effective for treating other sites and other portions of the Ore Knob tailings pile. However, the effectiveness and longevity of the treatment will depend on the physical and chemical characteristics of the

tailings. At present, there are no reliable methods for evaluating the effectiveness of WG treatment at other locations with different physical and chemical characteristics.

As a part of this research, geochemical model MIN3P was applied to simulate 1D acid mine drainage generation and treatment in the experimental columns. MIN3P is a multicomponent reactive transport model capable of simulating variably saturated flow (Mayer 1999). The model uses a local mass balance finite volume method using global implicit solution technique (Steefel and Lasaga 1994). This technique considers transport processes and reaction processes simultaneously. The model simulates batch problems and variably saturated flow models by solving coupled reactive transport equations and is capable of simulating advection-dispersion in aqueous phase and diffusion in gas phase.

Major technical challenges were encountered in applying the MIN3P model including: (a) determining the appropriate mineral phases to include in the model simulations; and (b) problems with the numerical stability of the model. Future research should focus on developing improved models and calibration procedures to aid in evaluating remedial approaches for mine tailings.

REFERENCES

Amoozegar A (1989) A compact constant head permeameter for measuring saturated hydraulic conductivity of the vadose zone. Soil Sci Soc Am J 53:1356—1361

Behrooz M, Borden RC (2012) Physical, hydrologic, and aqueous chemical characterization of the Ore Knob Tailings Pile (Ashe County, North Carolina, USA), Mine Water Environ 31(1):3—15, doi:10.1007/s10230.011.0166.0

Berger AC, Bethke CM, Krumhansl JL (2000) A process model of natural attenuation in drainage from historic mining district. Appl Geochem 15:655—666

Berner RA (1978) Rate control of mineral dissolution under earth surface conditions, Am J Science 278: 1235-1252

Blowes DW, Jambor JL, Appleyard EC, Reardon EJ, Cherry JA (1992) Temporal observations of the geochemistry and mineralogy of a sulfide rich mine tailings impoundment. Heath Steele Mines, New Brunswick. Explor Mining Geol 1:251—264

Blowes DW, Reardon EJ, Cherry JA, Jambor JL (1991) The formation and potential importance of cemented layers in inactive sulfide mine tailings. Geochim Cosmochim Ac 55:965—978, doi:10.1016/0016.7037(91)90155.X

Boorman RS, Watson DM (1976) Chemical processes in abandoned sulphide tailings dumps and environmental implications for northeastern New Brunswick. CIM Bull 69:86—96

Bouwer H (1986) Intake rate: cylinder infiltrometer. Method of Soil Analysis, part 1: physical and mineralogical methods, ch 32, 2nd Edit, American Soc of Agronomy, Soil Sci Soc Am, Madison, WI, USA, p 825—844

Brooks RH, Corey AT (1964) Hydraulic properties of porous media. T ASAE 7(1):26—28

Chaimberg M, Carty RH, Scroppo JA (1992) Evaluation of a hydraulically.installed suction lysimeter to obtain representative soil water samples. Environ Progress 11 (3):190—194, doi:10.1002/ep.670110312

Clesceri LS, Greenberg AE, Trussell RR (1989) Acidity hot peroxide treatment. Standard Methods for the Examination of Water and Wastewater, 17th edit, American Public Health Assoc, Washington DC, USA, p 2—33

Coetser SE, Pulles W, Heath RG, Cloete TE (2006) Chemical characterization of organic electron donors for sulfate reduction for potential use in acid mine drainage treatment. Biodegradation 17:169—179, doi:10.1007/s10532.005.7567.3

Colucci JA, Borrero EE, Alape F (2005) Biodiesel from an alkaline transesterification reaction of soybean oil using ultrasonic mixing. J Am Oil Chemists Soc 82:525—530. doi:10.1007/s11746.005.1104.3

Dvorak DH, Hedin RS, Edenborn HM, McIntire PE (1992) Treatment of metal contaminated water using bacterial sulfate reduction: results from pilot scale reactors. Biotechnol Bioeng 40:609—616 doi:10.1002/bit.260400508

Escobar B, Buccicardi S, Morales G, Wiertz J (2009) Bacterial oxidation of ferrous iron and RISCs at low temperatures: their effect on acid mine drainage and bioleaching of sulphide minerals. Adv Mater Res 71—73:433—436

Evangelou VP, Zhang YL (1995) A review: pyrite oxidation mechanisms and acid mine drainage prevention. Crit Rev Env Sci Tec 25:141—199, doi:10.1080/10643389509388477

Fennemore G, Chadneller W, Davis A (1998) Modeling pyrite oxidation in arid environments. Environ Sci Technol 32:2680—2687, doi:10.1021/es970900o

Fiedler S, Vepraskas MJ, Richardson JL (2007) Soil redox potential: Importance, field measurements, and observations. Advances in Agronomy 94:1—54

Furche M, Meima JA, Graupner T, Grissemann Ch, Rammlmair D (2007) Transport in mine tailings: Geophysical monitoring and reactive transport modeling. In: Proc. SGA Meeting, Dublin, Ireland

Germain D, Tassé N, Cyr J (2003) Rehabilitation of mine tailings by simultaneous prevention of oxidation and treatment of acid effluents using a wood waste cover. In: Proc. 6th International Conf on Acid Rock Drainage (ICARD). Australia

Gilbert SE, Cooke DR, Hollings P (2003) The effects of hardpan layers on the water chemistry from the leaching of pyrrhotite tailings material. Environ Geol 44:687—697. doi: 10.1007/s00254.003.0810.5

Gonza´lez-Toril E, Llobet-Brossa E, Casamayor EO, Amann R, Amils R (2003) Microbial ecology of an extreme acidic environment, the Tinto river. Appl Environ Microbiol 69:4853—4865

Gunsinger MR, Ptacek CJ, Blowes DW, Jambor JL (2006) Evaluation of long.term sulfide oxidation processes within pyrrhotite.rich tailings, Lynn Lake, Manitoba. J Contam Hydrol 83:149—170

Harbaugh AW, Banta ER, Hill MC, McDonald MG (2000) MODFLOW.2000, The U.S. Geological Survey Modular Ground Water Model – User Guide to Modularization Concepts and the Ground water Flow Process. USGS OFR 00–92, Washington DC, USA

Hulshof AHM, Blowes DW, Gould WD (2006) Evaluation of in situ layers for treatment of acid mine drainage: A field comparison. Water Res40: 1816—1826

Jaynes DB, Rogowski AS, Pionke HB (1984) Acid mine drainage from reclaimed coal strip mines: 1. model description. Water Resour Res 20:233—42, doi:10.1029/WR020i002 p00233

Johnson DB, Hallberg KB (2005) Acid mine drainage remediation options: a review. Science of the Total Environ 338:3—14

Johnson RH, Blowes DW, Robertson WD, Jambor JL (2000) The hydrogeochemistry of the Nickel Rim mine tailings impoundment, Sudbury, Ontario. J Contam Hydrol 41 (1—2):49—80, doi:10.1016/S0169.7722(99)00068.6

Kinkel AR Jr (1967) The Ore Knob copper deposit North Carolina, and other massive sulfide deposits of the Appalachians. USGS Profess Paper 558, Washington DC, USA

Kirby CS, Cravotta III CA (2005) Net alkalinity and net acidity 2: practical considerations. Appl Geochem 20:1941–1964

Klute A (1986) water retention: Laboratory Methods. In: Method of Soil Analysis; part 1: physical and mineralogical methods, ch 26, 2nd Edit, American Soc of Agronomy, Soil Sci Soc of Am, Madison, WI, USA, p 635— 660

Klute A, Dirksen C (1986) Hydraulic conductivity and diffusivity: laboratory methods. In: Method of Soil Analysis; part 1: physical and mineralogical methods, ch 28, 2nd Edit, American Soc of Agronomy, Soil Sci Soc Am J, Madison, WI, USA, p 687—732

Lasaga AC (1998) Kinetic theory in the earth sciences, Princeton Univ. Press, Princeton, NJ

Lichtner PC (1996) Modeling of reactive flow and transport in natural systems, paper presented at the Rome Seminar on Environmental Geochemistry, Castelnuovo di Porto, Rome

Lottermoser B (2007) Mine Wastes; Characteristics, Treatment, Environmental Impacts. 2nd Edit, Springer, Berlin, Germany, p 37—38

Mayer KU (1999) A numerical model for multicomponent reactive transport in variably saturated porous media. Ph.D. thesis, Department of Earth Sciences, University of Waterloo, Waterloo, Ontario

Mayer KU, Frind EO, Blowes DW (2002) Multicomponent reactive transport modeling in variably saturated porous media using a generalized formulation for kinetically controlled reactions. Water Resour Res 38:13, 1—21

McGregor RG, Blowes DW, Jambor JL, Robertson WL (1998) The solid phase controls on the mobility of heavy metals at the Copper Cliff tailings area. Sudbury, Ontario, Canada. J Contam Hydrol 33:247—271, doi:10.1016/S0169.7722(98)00060.6

McKibben MA, Barnes HL (1986) Oxidation of pyrite in low temperature acidic solutions: Rate laws and surface textures. Geochim Cosmochim Ac 50:1509—1520

McSweeney K, Madison FW (1988) Formation of a cemented subsurface horizon in sulfidic mine waste. J Environ Qual 17 (2):256—262, doi:10.1016/0016.7037(91)90155.X

Moncur MC, Ptacek CJ, Blowes DW, Jambor JL (2005) Release, transport and attenuation of metals from an old tailings impoundment, Appl Geochem 20:639—659, doi:10.1016/j.apgeochem.2004.09.019

Mualem Y (1976) A new model for predicting the hydraulic conductivity of unsaturated porous media. Water Resour Res 12:513—522

Nagy KL, Blum AE, Lasaga AC (1991) Dissolution and precipitation kinetics of kaolinite at 80 degrees C and pH 3 – the dependence on solution saturation state. Am J Sci 291: 649—686

NCDOT (North Carolina Dept of Transportation) (2010) GIS (1998) Color infrared digital ortho mosaics, http://www.ncdot.org/it/gis/DataDistribution/1998colIR/default.html

Nicholson RV, Gillham RW, Cherry JA, Reardon EJ (1989) Reduction of acid generation in mine tailings through the use of moisture retaining cover layers as oxygen barriers. Can Geotech J 26:1—8

Nordstrom DK, Alpers CN (1999) Geochemistry of acid mine waters. In: Plumlee GS, Logsdon, MJ, (Eds) Ohmura N, Sasaki K, Matsumoto N, Saiki H (2002) Anaerobic respiration using Fe^{3+}, S^0, and H_2 in the chemolithoautotrophic bacterium Acidithiobacillus ferrooxidans. J Bacteriol 184:2081—2087

Nordstrom KD, Alpers CN (1999) Geochemistry of acid mine waters. In: Plumlee GS, Logsdon MJ (Eds), The environmental geochemistry of mineral deposits, part A: Processes, Techniques, and Health Issues, Rev Econ Geol 6A:133—160

NRCS (Natural Resources Conservation Service) (2008) Uploaded soil survey data for Ore Knob tailings pile and watershed, version 8, Jan 15–2008, http://websoilsurvey.nrcs. usda.gov/app/WebSoilSurvey.aspx

Pantelis G, Ritchie AIM (1991) Macroscopic transport mechanisms as rate limiting factor in dump leaching of pyritic ores. Appl Math Model 15:136—143, doi:10.1016/0307.904X(92)90005.N

Parker G, Robertson A (1999) Acid Drainage. The Australian Mineral & Energy Environment Foundation, Sydney, Australia, Occasional Paper No 11, p 101—117

Parkhurst DL, Appelo CAJ (1999) User's guide to PHREEQC (version 2)—a computer program for speciation, batch reaction, one dimensional transport, and inverse geochemical calculations, USGS/WRI.99.4259, USGS, Denver, CO, USA

Patil NG, Rajput GS (2009) Evaluation of water retention functions and computer program "Rosetta" in predicting soil water characteristics of seasonally impounded shrink swell soils. J Irrig Drain E.ASCE 135(3):286—294

PIRAMID Consortium (2003) Engineering guidelines for the passive remediation of acidic and/or metalliferous mine drainage and similar wastewaters. European Commission 5th Framework RTD Project EVK1.CT.1999.000021, Passive in-situ remediation of acidic mine / industrial drainage. (PIRAMID). Univ of Newcastle Upon Tyne, Newcastle Upon Tyne, UK

Plumlee GS (1999) The environmental geology of mineral deposits. In: Plumlee GS, Logsdon MS (Eds) The Environmental Geochemistry of Mineral Deposits, part a: processes, techniques and health issues, Soc of Economic Geologists, Littleton, CO, USA, Rev Econ Geol 6A:71—116

Pyatt FB, Grattan PJ (2001) Some consequences of ancient mining activities on the health of ancient and modern human populations. J Public Health Med 23:235—236. doi: 10.1093/pubmed/23.3.235

Rankin HS, JL Stuckey (1943) Copper Deposits of Western North Carolina. TVA and NC Div Mineral Resources, Knoxville, TN, USA

Reardon EJ, Moddle PM (1985) Gas diffusion coefficient measurements on uranium mill tailings: implications to cover design. Uranium 2:111—131

Rickard D (1995) Kinetics of FeS precipitation: part 1. competing reaction mechanisms, Geochim Cosmochim Ac 59 (21):4367—4379, doi:10.1016/0016.7037(95) 00251.T

Rose AW, Cravotta CA III (1998) Geochemistry of coal mine drainage. Coal Mine Drainage Prediction and Pollution Prevention in Pennsylvania, ch 1, PA Dept of Environmental Protection, Harrisburg, PA, USA, http://www.dep.state.pa.us/dep/deputate/ miners/districts/cmdp/chap01.html

Saxton KE, Rawls WJ, Romberger JS, Papendick RI (1986) Estimating generalized soil-water characteristics from texture. Soil Sci Soc Am J 50(4):1031—1036

Schaap M G, Leij FJ, Van Genuchten M Th (2001) Rosetta: a computer program for estimating soil hydraulic parameters with hierarchical pedotransfer functions. J Hydrol 251(3–4):163—176

Schmiermund RL (2000) Non-acidic, sulfate poor, copper enriched drainage from a Precambrian stratabound chalcopyrite/pyrite deposit, Carbon County, Wyoming. Proc, 5th

International Conf on Acid Rock Drainage, Soc for Mining, Metallurgy, and Exploration, Littleton, CO, USA, 2:1059—1070

Schwartz FW, Zhang Hubao (2002) Fundamentals of Ground Water. John Wiley & Sons, New York City, NY, USA, p 273—277

Singer PC, Stumm W (1970) Acidic mine drainage: the rate determining step. Science 167:1121—1123, doi:10.1126/science.167.3921.1121

Skaggs RW (1982) Field evaluation of water management simulation model. T ASAE 25(3):666—674

Skaggs RW, Tabrizi AN (1981) Effect of drainage system design and soil properties on runoff from artificially drained lands. USDA Agricultural Research (Southern Region), New Orleans, LA, USA, p 311—312

Skousen J, Renton J, Evans P, Leavitt B, Brady KBC, Cohen L, Ziemkiewicz P (1997) Neutralization potential of overburden samples containing siderite. J Environ Qual 26:673—681

Sobek AA, Schuller WA, Freeman JR, Smith RM (1978) Field and laboratory methods applicable to overburden and minesoils. U.S. EPA. Report EPA.600/2.78.054

State Climate Office of North Carolina (2010) Uploaded data for 1960—2010, http://www.nc.climate.ncsu.edu

Steefel CI, Lasaga AC (1994) A coupled model for transport of multiple chemical species and kinetic precipitation/dissolution reactions with application to reactive flow in single phase hydrothermal systems, Am J Science 294: 529—592

Swanson DA, Barbour SL, Wilson GW (1997) Dry-site versus wet-site cover design. Proc, 4th International Conf of Acid Rock Drainage, Vancouver, BC. IV: 1595—610

Tasse N, Germain D, Dufour C, Tremblay R (1997) Hard pan formation in the Canadian Malartic mine tailings: implications for the reclamation of the abandoned impoundment. Proc, 4th International Conf of Acid Rock Drainage, CANMET, Ottawa, Canada, 4:1797—1812

U.S. EPA (1980) COD ranges 3–150 mg/L and 20–1500 mg/L COD are U.S. EPA approved (5220 D) for water, wastewater, Federal Register 45(78):26811—26812

U.S. EPA (2010) Action memorandum: Request for a change of scope and removal action ceiling increase at Ore Knob mine site, EPA, Region 4, http://www.epaosc.org/site /site_profile.aspx?site_id=4530

U.S. EPA (US Environmental Protection Agency) (2004) Nationwide Identification of Hardrock Mining Sites. U.S. EPA Report 2004.P.00005, OIG, Washington DC, USA

Van Genuchten MTh (1980) A closed form equation for predicting the hydraulic conductivity of unsaturated soils. Soil Sci Soc Am J 44:892—898, doi:10.2136/sssaj1980 .03615995004400050002x

Waybrant KR, Ptacek CJ, Blowes DW (2002) Treatment of mine drainage using permeable reactive barriers: column experiments. Environ Science Technol 36:1349—1356, doi:10.1021/es010751g

Weast RC (1976) CRC Handbook of Chemistry and Physics. 57th Edit, CRC Press, Cleveland, OH, USA, p 1976—1977

Wösten JHM, Van Genuchten MTh (1988) Using texture and other soil properties to predict the unsaturated soil hydraulic functions. Soil Sci Soc Am J 52: 1762–1770

Yanful EK, Bell AV, Woyshner MR (1993) Design of a composite soil cover for an experimental waste rock pile near Newcastle. New Brunswick, Canada. Can Geotech J 30: 578—587, doi:10.1139/t93.050

Zagury GJ, Kulnieks VI, Neculita CM. (2006) Characterization and reactivity assessment of organic substrates for sulphate reducing bacteria in acid mine drainage treatment. Chemosphere 64:944—954, doi:10.1016/j.chemosphere.2006.01.001

APPENDIX

Appendix A- Aquatic Geochemistry

Table S.A.1 Average composition of saturated pore water in tailings pile; all concentrations are in mg/L

	MW10 Up-gradient			MW11 Middle of Pile			MW12 Middle of Pile			MW13 West near embankment			MW9 Center near embankment			MW14 East near embankment		
	T	M	B	T	M	B	T	M	B	T	M	B	T	M	M	T	M	B
Eh, mV	250	200	170	170	140	120	140	120	120	220	160	140	180	210	210	190	130	99
pH	6.6	6.6	6.5	6.5	6.4	6.3	6.2	6.3	6.4	5.8	6.1	6.1	5.8	6.0	6.0	6.0	6.1	6.1
Temp. (°C)	13	13	13	13	13	13	13	13	13	13	13	12	13	12	12	13	12	12
DO	0.6	0.3	0.1	0.4	0.1	0.0	0.3	0.2	0.0	0.2	0.2	0.0	0.4	0.2	0.2	0.2	0.2	0.0
Acidity	51	36	31	300	270	250	910	830	840	2700	2600	2500	3700	3500	3500	4000	3900	3800
Alk	59	60	62	74	98	83	65	83	78	57	54	54	51	36	36	87	95	99
Al	0.07	0.10	0.12	0.08	0.13	0.09	0.10	0.09	0.11	0.74	0.72	0.76	0.49	0.55	0.55	0.07	0.07	0.07
Ca	468	580	600	570	630	640	600	600	600	300	310	310	470	530	530	590	530	490
Cu	0.07	0.07	0.06	0.07	0.07	0.06	0.07	0.08	0.07	0.07	0.08	0.07	0.07	0.07	0.07	0.07	0.07	0.07
Fe	11	12	12	130	150	150	500	480	480	1400	1400	1400	1800	1800	1800	2400	2000	2000
K	55	63	64	18	20	20	19	28	27	38	39	42	38	40	40	73	73	62
Mg	76	89	89	54	62	63	59	70	69	51	52	51	94	97	97	100	92	88
Mn	1	1	1	2	2	2	6	6	6	14	14	13	14	14	14	21	19	18
Na	24	29	30	7	9	9	9	10	10	4	5	4	9	9	9	7	7	7
Si	5	8	7	31	35	33	33	33	32	10	11	11	31	33	33	28	29	26
Zn	0.15	0.07	0.07	0.09	0.06	0.08	0.10	0.12	0.14	0.16	0.19	0.21	0.22	0.24	0.24	0.23	0.32	0.31
SO_4 as S	560	610	630	640	630	650	910	770	750	1200	1100	1100	1600	1500	1500	1900	1800	1800
Total S	532	580	587	610	610	640	820	710	730	1100	1000	980	1500	1500	1500	1800	1700	1700

T – top monitoring interval; M – middle monitoring interval; B – bottom monitoring interval

Table S.A.2 Average parameter values in surface water monitoring stations within the Peak Creek watershed; all concentrations in mg/L, Sd=standard deviation, T S=total sulfur

	SW1 up-gradient, mine impacted		SW3 up-gradient, no mine impacts		SW4 embankment seep		SW5 overall discharge		SW6 ore knob branch		SW7 Peak Creek (background)	
	Avg	Sd	Avg	Sd	Avg	Sd.	Avg	Sd	Avg	Sd	Avg	Sd
Eh, mV	540	110	490	370	510	210	600	340	590	170	430	240
pH	4.0	1.4	3.8	0.6	3.8	0.9	3.2	0.2	3.1	0.3	7.3	0.9
°C	16	3	16	4	16	2	17	3	18	4	16	3
DO	4	1	3	1	1	1	11	1	7	2	7	3
Acidity	170	44	110	70	2000	1000	930	640	290	70	24	25
Alk	2	3	0	0	0	0	0	1	0	0	15	5
Al	0.96	0.75	2.1	3.2	41	72	10	10	5.2	1.8	0.12	0.09
Ca	43	19	34	35	230	80	160	56	64	35	4	2
Cu	0.54	0.48	0.29	0.31	0.37	0.35	0.28	0.24	0.21	0.14	ND	..
Fe	62	18	12	12	1300	600	400	260	65	38	0	0
K	10	3	8	6	29	15	17	5	9	3	2	2
Mg	6	2	1	1	55	24	26	14	9	4	1	1
Mn	1	0	0	0	8	4	4	2	2	1	0	1
Na	4	3	2	1	5	2	4	2	3	3	3	1
Si	12	6	10	8	13	2	15	4	11	5	5	1
Zn	0.66	0.39	0.22	0.22	3.4	1.7	1.4	0.9	0.57	0.21	0.09	0.02
SO_4 as S	92	30	47	49	1200	600	520	300	210	60	5	4
T S	91	30	60	52	1100	400	480	230	190	50	1	0

Appendix B- Experimental Columns

Table S.B.1 Pore water and leachate composition in Control Columns- Replicate A

Date	Depth	Eh	pH	TOC	DO	H_2S	Acidity	Al	Ca	Cu	Fe	K	Mg	Mn	Na	Zn	S	Si	SO_4
Unit	m	mv	-								(mg/L)								
3/6/08	1.20	-211	3.9	40	0.2	0	1491	6.7	481	0.2	573	118	247	96	15	0.8	1059	63	3351
	1.00	-215	4.4	23	0.1	0	932	0.1	516	0.2	462	127	215	13	8	0.6	854	12	2908
	0.75	-249	4.2	24	0.3	0	689	0.3	741	0.2	259	125	216	24	24	0.6	1022	7	3221
	0.50	-203	4.0	16	0.5	0	351	0.2	433	0.1	69	135	274	68	13	0.4	889	10	2580
	0.25	-12	NA	NA	NA	NA	NA	NA	NA	NA	NA	NA	NA	NA	NA	NA	NA	NA	NA
4/9/08	1.20	-225	4.2	25	0.2	0	1310	10.8	431	0.1	482	116	302	86	13	1.9	1107	56	3341
	1.00	-253	4.5	12	0.1	0	788	0.2	436	0.2	308	98	188	37	5	0.4	700	31	2491
	0.75	-218	4.5	16	0.2	0	950	0.2	397	0.2	365	105	272	53	5	1.0	901	48	2706
	0.50	-210	4.4	11	0.3	0	478	0.2	765	0.2	149	120	261	66	8	0.4	1109	21	3250
	0.25	-203	3.8	22	0.5	0	583	0.2	587	0.1	122	110	201	98	7	0.9	977	17	3158
5/12/08	1.20	-237	4.1	19	0.1	0	1251	9.5	502	0.2	586	125	286	89	18	1.0	1105	45	3568
	1.00	-230	4.3	15	0.1	0	583	0.3	499	0.2	197	119	227	12	10	0.5	844	11	2550
	0.75	-222	4.4	17	0.2	0	606	0.3	427	0.2	165	127	199	26	8	0.6	743	10	2241
	0.50	-183	4.2	12	0.3	0	697	0.3	513	0.1	191	107	195	107	8	0.3	851	10	2607
	0.25	-90	NA	NA	NA	NA	NA	NA	NA	NA	NA	NA	NA	NA	NA	NA	NA	NA	NA
6/5/08	1.20	-257	4.2	28	0.1	0	1501	5.0	564	0.2	610	133	249	99	18	2.5	1210	49	3671
	1.00	-260	4.3	24	0.1	0	633	0.1	473	0.2	301	143	232	13	10	1.0	948	15	2871
	0.75	-263	NA	NA	NA	NA	NA	NA	NA	NA	NA	NA	NA	NA	NA	NA	NA	NA	NA
	0.50	-231	NA	NA	NA	NA	NA	NA	NA	NA	NA	NA	NA	NA	NA	NA	NA	NA	NA
	0.25	-94	NA	NA	NA	NA	NA	NA	NA	NA	NA	NA	NA	NA	NA	NA	NA	NA	NA
7/16/08	1.20	-279	4.1	32	0.1	0	1891	7.2	550	0.2	516	129	297	108	12	2.1	1198	63	3661
	1.00	-284	4.3	23	0.1	0	904	0.2	493	0.2	396	172	242	15	11	0.5	974	66	2908
	0.75	-301	4.7	16	0.1	0	610	0.3	376	0.2	398	116	267	21	15	1.0	951	39	2840
	0.50	-119	3.8	30	0.2	0	721	0.2	481	0.2	281	101	259	93	9	0.8	933	59	2856
	0.25	-103	NA	NA	NA	NA	NA	NA	NA	NA	NA	NA	NA	NA	NA	NA	NA	NA	NA

NA- Not Analyzed

Table S.B.1 Pore water and leachate composition in Control Columns- Replicate A

Date	Depth	Eh	pH	TOC	DO	H_2S	Acidity	Al	Ca	Cu	Fe	K	Mg	Mn	Na	Zn	S	Si	SO_4
Unit	m	mv	-								(mg/L)								
7/24/08	1.20	-285	4.1	20	0.1	0	1501	10.1	546	0.2	690	154	259	96	15	2.0	980	49	3750
	1.00	-283	4.2	24	0.2	0	1038	0.4	606	0.2	230	119	229	15	9	0.5	1079	19	2933
	0.75	-269	4.2	27	0.2	0	1111	0.3	476	0.2	383	139	242	51	12	0.7	986	29	2957
	0.50	-170	NA	NA	NA	NA	NA	NA	NA	NA	NA	NA	NA	NA	NA	NA	NA	NA	NA
	0.25	-37	NA	NA	NA	NA	NA	NA	NA	NA	NA	NA	NA	NA	NA	NA	NA	NA	NA
8/5/08	1.20	-270	3.9	28	0.2	0	1406	8.1	471	0.1	587	127	259	120	17	0.9	998	64	3407
	1.00	-249	4.0	23	0.2	0	1001	0.3	527	0.2	433	170	233	29	10	0.6	986	22	3109
	0.75	-243	4.2	20	0.2	0	1104	0.2	511	0.1	351	116	269	53	9	0.7	1024	38	3252
	0.50	-211	3.9	18	0.3	0	1025	0.2	472	0.2	380	136	211	90	9	0.9	911	26	2810
	0.25	-76	NA	NA	NA	NA	NA	NA	NA	NA	NA	NA	NA	NA	NA	NA	NA	NA	NA
5/10/09	1.20	-414	4.3	33	0.1	0	1080	10.1	566	0.1	522	91	139	83	5	0.3	972	6	3203
	1.00	-189	4.5	45	0.2	0	783	0.2	355	0.4	425	90	167	34	5	0.2	774	5	2274
	0.75	-120	4.4	52	0.2	0	700	0.3	426	0.3	361	133	251	23	7	0.1	949	7	2852
	0.50	-117	3.3	68	0.4	0	9014	9.7	402	0.1	4323	167	754	327	10	69.9	4726	19	13134
	0.25	140	3.2	25	0.6	0	8220	0.5	599	0.2	4481	173	679	314	12	93.8	4715	31	13974
6/25/09	1.20	-365	4.4	16	0.1	0	1200	4.1	547	0.5	557	150	232	104	8	0.1	958	10	3393
	1.00	-226	4.9	16	0.1	0	764	0.2	547	0.7	437	167	322	41	10	0.1	988	10	3267
	0.75	-254	4.4	14	0.1	0	690	0.1	518	0.2	348	202	531	26	11	0.2	951	9	3901
	0.50	-159	3.2	14	0.3	0	10100	6.2	432	0.2	4862	161	785	314	10	48.8	4535	18	14042
	0.25	137	3.1	19	0.4	0	14150	1.4	466	0.1	6994	109	846	356	10	75.3	6432	20	18782
7/22/09	1.20	-355	4.3	50	0.1	0	965	5.1	555	0.4	518	161	308	124	9	0.1	999	10	3297
	1.00	-189	NA	NA	NA	NA	NA	NA	NA	NA	NA	NA	NA	NA	NA	NA	NA	NA	NA
	0.75	-131	NA	NA	NA	NA	NA	NA	NA	NA	NA	NA	NA	NA	NA	NA	NA	NA	NA
	0.50	-202	NA	NA	NA	NA	NA	NA	NA	NA	NA	NA	NA	NA	NA	NA	NA	NA	NA
	0.25	160	NA	NA	NA	NA	NA	NA	NA	NA	NA	NA	NA	NA	NA	NA	NA	NA	NA

Table S.B.2 Pore water and leachate composition in Control Columns- Replicate B

Date	Depth	Eh	pH	TOC	DO	H_2S	Acidity	Al	Ca	Cu	Fe	K	Mg	Mn	Na	Zn	S	Si	SO_4
Unit	m	mv	-								(mg/L)								
3/6/08	1.20	-328	4.2	21.9	0.2	0	1140	6.0	507	0.2	320	133	229	111	8.3	0.1	813	56	2930
	1.00	-341	4.3	21.6	0.2	0	579	0.3	506	0.2	239	120	261	27	9.1	0.2	923	16	2815
	0.75	-295	4.3	20.3	0.3	0	686	0.3	641	0.2	221	144	252	84	16.1	0.8	1021	37	3175
	0.50	-238	4.1	19.7	0.4	0	550	0.3	649	0.2	136	121	220	65	8.7	0.5	1079	21	2937
	0.25	-74	4.2	14.6	0.6	0	580	0.3	760	0.1	64	95	144	124	3.7	1.2	806	15	2692
4/9/08	1.20	-319	4.1	20.0	0.2	0	901	14.6	480	0.1	285	124	277	91	7.0	0.4	936	23	2827
	1.00	-322	4.3	11.7	0.1	0	500	0.2	398	0.2	157	83	148	20	3.1	0.3	644	16	1951
	0.75	-315	4.4	14.8	0.2	0	604	0.3	574	0.2	139	133	185	57	11.8	0.3	833	13	2510
	0.50	-282	4.3	19.8	0.4	0	594	0.3	601	0.2	147	130	217	85	18.0	0.2	859	20	2688
	0.25	18	4.0	21.9	0.7	0	513	0.3	583	0.2	109	98	161	69	5.9	0.2	746	27	2400
5/12/08	1.20	-319	4.1	25.6	0.1	0	1080	7.9	549	0.2	396	151	250	98	9.0	0.3	988	80	3110
	1.00	-326	4.5	16.5	0.2	0	806	0.3	493	0.2	197	137	236	14	10.9	0.2	859	17	2606
	0.75	-265	4.3	12.2	0.2	0	528	0.2	450	0.2	251	122	209	23	17.0	0.2	855	15	2589
	0.50	-193	4.2	11.0	0.3	0	642	0.4	390	0.2	194	110	93	62	7.8	0.2	618	29	1850
	0.25	10	NA	NA	NA	NA	NA	NA	NA	NA	NA	NA	NA	NA	NA	NA	NA	NA	NA
6/5/08	1.20	-261	4.1	19.8	0.2	0	1431	8.8	672	0.2	623	132	224	95	12.1	0.3	1128	77	3645
	1.00	-254	4.3	17.9	0.1	0	1191	0.4	478	0.2	339	115	210	18	8.9	0.2	937	25	2771
	0.75	-258	NA	NA	NA	NA	NA	NA	NA	NA	NA	NA	NA	NA	NA	NA	NA	NA	NA
	0.50	-159	NA	NA	NA	NA	NA	NA	NA	NA	NA	NA	NA	NA	NA	NA	NA	NA	NA
	0.25	-68	NA	NA	NA	NA	NA	NA	NA	NA	NA	NA	NA	NA	NA	NA	NA	NA	NA
7/16/08	1.20	-303	4.0	31.1	0.1	0	1404	8.9	539	0.2	589	174	289	106	12.2	0.1	1301	53	3906
	1.00	-292	4.2	18.8	0.1	0	1049	0.4	479	0.2	494	152	192	25	8.0	0.3	997	21	2991
	0.75	-237	4.1	15.3	0.2	0	1191	0.3	564	0.2	545	165	170	39	5.7	0.2	984	11	3233
	0.50	-165	3.9	20.5	0.3	0	951	0.3	501	0.2	387	110	160	42	7.1	1.4	917	29	2781
	0.25	-102	NA	NA	NA	NA	NA	NA	NA	NA	NA	NA	NA	NA	NA	NA	NA	NA	NA

Table S.B.2 Pore water and leachate composition in Control Columns- Replicate B

Date	Depth	Eh	pH	TOC	DO	H_2S	Acidity	Al	Ca	Cu	Fe	K	Mg	Mn	Na	Zn	S	Si	SO_4
Unit	m	mv	-								(mg/L)								
7/24/08	1.20	-255	4.2	24.6	0.2	0	1201	6.2	624	0.2	470	163	296	94	8.7	0.7	1029	66	3826
	1.00	-269	4.4	21.7	0.1	0	991	0.4	590	0.2	473	130	250	25	9.1	0.3	983	22	3210
	0.75	-206	4.2	16.7	0.1	0	1081	0.3	579	0.2	524	151	108	68	9.3	0.5	977	30	2942
	0.50	-176	NA	NA	NA	NA	NA	NA	NA	NA	NA	NA	NA	NA	NA	NA	NA	NA	NA
	0.25	-29	NA	NA	NA	NA	NA	NA	NA	NA	NA	NA	NA	NA	NA	NA	NA	NA	NA
8/5/08	1.20	-292	4.1	19.4	0.1	0	1271	10.5	623	0.3	506	142	301	39	13.0	0.9	1179	58	3623
	1.00	-301	4.3	21.7	0.1	0	1321	0.3	529	0.2	561	148	257	28	8.1	0.7	1128	24	3492
	0.75	-289	4.0	20.2	0.1	0	996	0.3	485	0.2	492	156	234	33	11.0	0.7	959	18	3241
	0.50	-207	3.9	13.6	0.2	0	1355	0.3	503	0.2	539	170	212	56	9.9	0.7	994	33	3101
	0.25	-128	NA	NA	NA	NA	NA	NA	NA	NA	NA	NA	NA	NA	NA	NA	NA	NA	NA
5/10/09	1.20	-323	5.0	19.9	0.1	0	1180	6.1	511	0.5	587	128	211	102	6.6	0.1	833	12	3518
	1.00	-211	5.2	29.4	0.1	0	1755	0.2	222	0.2	1066	32	28	27	1.0	0.1	931	4	2919
	0.75	-143	3.9	68.5	0.1	0	6989	1.2	423	0.3	3043	180	648	181	9.7	20.3	4076	14	10256
	0.50	-152	3.5	23.8	0.3	0	5519	2.5	423	0.1	2955	216	803	170	12.7	3.0	3500	21	10519
	0.25	180	3.0	43.7	0.7	0	10309	2.7	423	0.1	5053	128	899	343	13.6	108.7	5560	26	16129
6/25/09	1.20	-275	4.3	12.1	0.1	0	1205	9.1	560	0.3	581	155	298	83	8.3	0.1	983	10	3705
	1.00	-187	5.2	26.7	0.1	0	4025	0.2	472	0.2	1999	198	796	100	12.3	0.4	2931	10	8716
	0.75	-259	4.1	11.5	0.1	0	4950	0.3	463	0.2	2262	205	784	124	13.0	4.0	3630	9	9219
	0.50	-167	NA	NA	NA	NA	NA	NA	NA	NA	NA	NA	NA	NA	NA	NA	NA	NA	NA
	0.25	-163	3.3	29.5	0.5	0	15600	0.6	492	0.1	7681	116	979	383	18.0	0.2	5742	0	16652
7/22/09	1.20	-306	4.8	17.6	0.1	0	1126	10.1	533	0.4	586	135	279	79	8.4	0.1	936	11	3326
	1.00	-270	NA	NA	NA	NA	NA	NA	NA	NA	NA	NA	NA	NA	NA	NA	NA	NA	NA
	0.75	-237	NA	NA	NA	NA	NA	NA	NA	NA	NA	NA	NA	NA	NA	NA	NA	NA	NA
	0.50	-194	NA	NA	NA	NA	NA	NA	NA	NA	NA	NA	NA	NA	NA	NA	NA	NA	NA
	0.25	112	NA	NA	NA	NA	NA	NA	NA	NA	NA	NA	NA	NA	NA	NA	NA	NA	NA

Table S.B.3 Pore water and leachate composition in Treated Columns- Replicate A

Date	Depth	Eh	pH	TOC	DO	H_2S	Acidity	Al	Ca	Cu	Fe	K	Mg	Mn	Na	Zn	S	Si	SO_4
Unit	m	mv	-								(mg/L)								
3/6/08	1.20	-239	4.2	21	0.2	0	1190	8.2	571	0.2	424	160	265	92	11.5	0.4	967	45	3395
	1.00	-236	4.5	10	0.1	0	767	0.1	469	0.2	328	117	245	20	7.5	0.2	858	44	2795
	0.75	-199	4.4	16	0.3	0	517	0.1	586	0.2	181	134	236	41	15.8	0.7	834	26	2706
	0.50	-163	4.4	16	0.5	0	325	0.1	559	0.1	87	131	230	25	12.8	0.9	841	49	2524
	0.25	-124	4.1	25	0.6	0	467	0.1	769	0.1	67	115	158	86	4.2	2.7	928	4	2851
4/9/08	1.20	-319	4.1	22	0.2	0	910	11.2	457	0.1	328	118	267	115	5.4	0.3	922	53	3109
	1.00	-317	4.6	14	0.1	0	544	0.2	387	0.2	260	91	211	10	4.3	0.5	710	89	2371
	0.75	-291	4.4	26	0.2	0	460	0.2	597	0.1	79	94	180	22	3.4	0.6	801	44	2407
	0.50	-274	4.2	16	0.4	0	250	0.3	542	0.2	42	125	313	32	7.8	0.6	906	63	2748
	0.25	-57	4.1	14	0.5	0	303	0.1	649	0.2	40	114	269	69	5.9	1.8	850	7	2962
5/12/08	1.20	-271	4.3	34	0.1	0	1321	9.7	539	0.1	513	121	261	114	4.9	0.4	1088	59	3550
	1.00	-278	4.3	13	0.1	0	837	0.3	459	0.2	398	111	221	28	3.2	0.2	913	35	2781
	0.75	-286	4.8	24	0.1	0	493	0.2	529	0.1	79	108	215	37	6.5	0.7	810	30	2430
	0.50	-271	4.1	15	0.2	0	324	0.1	796	0.2	66	105	190	45	5.1	0.5	1006	46	2966
	0.25	-45	NA	NA	NA	NA	NA	NA	NA	NA	NA	NA	NA	NA	NA	NA	NA	NA	NA
6/5/08	1.20	-271	4.3	24	0.2	0	1427	7.3	580	0.3	640	149	291	94	5.6	0.4	1046	63	3850
	1.00	-254	4.3	28	0.2	0	1017	0.4	429	0.2	248	137	254	36	5.8	0.3	989	41	2651
	0.75	-235	NA	NA	NA	NA	NA	NA	NA	NA	NA	NA	NA	NA	NA	NA	NA	NA	NA
	0.50	-188	NA	NA	NA	NA	NA	NA	NA	NA	NA	NA	NA	NA	NA	NA	NA	NA	NA
	0.25	-118	NA	NA	NA	NA	NA	NA	NA	NA	NA	NA	NA	NA	NA	NA	NA	NA	NA
7/16/08	1.20	-291	4.8	5456	0.1	0.6	641	2.1	422	0.1	278	123	156	51	4.3	0.1	761	43	2350
	1.00	-284	5.0	4545	0.1	0.4	539	0.1	370	0.1	242	98	119	14	5.9	0.2	675	24	2050
	0.75	-267	4.6	5135	0.1	0.9	350	0.1	322	0.1	61	118	132	27	10.8	0.3	561	53	1671
	0.50	-187	4.6	4720	0.2	0.5	411	0.1	273	0.1	59	81	145	29	8.0	1.3	460	11	1610
	0.25	-27	NA	NA	NA	NA	NA	NA	NA	NA	NA	NA	NA	NA	NA	NA	NA	NA	NA

Table S.B.3 Pore water and leachate composition in Treated Columns- Replicate A

Date	Depth	Eh	pH	TOC	DO	H_2S	Acidity	Al	Ca	Cu	Fe	K	Mg	Mn	Na	Zn	S	Si	SO_4
Unit	m	mv	-								(mg/L)								
7/24/08	1.20	-279	4.9	5231	0.1	0.4	303	0.1	430	0.1	104	163	191	24	8.6	0.1	746	25	2190
	1.00	-256	4.9	4279	0.1	0.6	253	0.1	296	0.1	50	110	193	15	4.8	0.2	620	20	1865
	0.75	-229	4.8	5094	0.1	0.3	214	0.0	94	0.1	27	85	105	40	5.3	0.1	621	40	1853
	0.50	-198	NA	NA	NA	NA	NA	NA	NA	NA	NA	NA	NA	NA	NA	NA	NA	NA	NA
	0.25	-103	NA	NA	NA	NA	NA	NA	NA	NA	NA	NA	NA	NA	NA	NA	NA	NA	NA
8/5/08	1.20	-295	5.0	6129	0.1	0.8	206	0.1	375	0.1	83	121	171	35	9.7	0.1	584	27	1895
	1.00	-313	4.9	4416	0.1	0.5	130	0.1	370	0.1	45	104	128	18	3.8	0.1	606	13	1811
	0.75	-212	5.0	4935	0.1	0.6	171	0.0	292	0.1	27	71	102	19	3.0	0.1	319	34	1293
	0.50	-138	4.9	3990	0.3	0.8	231	0.0	258	0.1	27	73	143	26	6.8	0.1	566	17	1345
	0.25	-76	NA	NA	NA	NA	NA	NA	NA	NA	NA	NA	NA	NA	NA	NA	NA	NA	NA
5/10/09	1.20	-365	6.5	1105	0.1	4.0	0	0.1	313	0.1	18	108	104	1	7.4	0.1	244	21	1305
	1.00	-301	6.7	1169	0.1	2.0	0	0.1	291	0.1	14	83	80	0	3.8	0.1	246	13	1090
	0.75	-159	6.7	6355	0.2	2.0	234	0.1	267	0.1	129	105	128	3	9.8	0.1	465	14	1400
	0.50	-367	6.4	6692	0.3	2.5	291	0.1	316	0.1	112	104	100	3	9.3	0.2	492	21	1470
	0.25	-61	6.5	10545	0.5	3.5	1100	0.1	615	0.1	522	112	119	20	11.0	0.5	952	8	2810
6/25/09	1.20	-265	6.7	2451	0.1	4.0	0	0.1	213	0.1	22	119	120	3	9.0	0.1	373	23	993
	1.00	-118	6.8	2588	0.1	3.0	0	0.1	260	0.1	18	100	117	0	10.6	0.2	319	27	1089
	0.75	-171	6.8	7187	0.1	4.0	96	0.1	261	0.1	81	110	116	3	12.3	0.4	404	13	1324
	0.50	-93	6.3	9260	0.2	2.5	275	0.1	240	0.1	129	118	103	8	12.8	0.2	419	5	1283
	0.25	-101	6.1	7470	0.4	4.5	150	0.1	263	0.1	32	157	185	38	11.1	1.2	494	10	1631
7/22/09	1.20	-305	6.7	2022	0.1	5.0	0	0.1	222	0.1	32	134	133	5	8.6	0.2	350	24	1135
	1.00	-243	NA	NA	NA	NA	NA	NA	NA	NA	NA	NA	NA	NA	NA	NA	NA	NA	NA
	0.75	-265	NA	NA	NA	NA	NA	NA	NA	NA	NA	NA	NA	NA	NA	NA	NA	NA	NA
	0.50	-103	NA	NA	NA	NA	NA	NA	NA	NA	NA	NA	NA	NA	NA	NA	NA	NA	NA
	0.25	-88	NA	NA	NA	NA	NA	NA	NA	NA	NA	NA	NA	NA	NA	NA	NA	NA	NA

Table S.B.4 Pore water and leachate composition in Treated Columns- Replicate B

Date	Depth	Eh	pH	TOC	DO	H_2S	Acidity	Al	Ca	Cu	Fe	K	Mg	Mn	Na	Zn	S	Si	SO_4
Unit	m	mv	-								(mg/L)								
3/6/08	1.20	-277	4	74	0.2	0	1390	12.1	530	0.2	500	121	213	52	13.6	1.8	922	41	3108
	1.00	-269	4	42	0.1	0	815	0.2	488	0.1	393	129	252	16	9.8	0.2	899	20	2976
	0.75	-278	4	43	0.2	0	607	0.3	501	0.2	264	104	191	64	18.2	0.5	768	10	2622
	0.50	-242	4	16	0.3	0	521	0.2	458	0.2	147	148	333	74	13.5	0.3	1019	12	2875
	0.25	-235	4	15	0.5	0	586	0.3	655	0.1	154	104	178	91	4.7	0.3	1002	8	2803
4/9/08	1.20	-268	4	18	0.1	0	1101	8.6	465	0.1	434	117	256	46	11.1	0.2	865	58	2881
	1.00	-284	5	20	0.2	0	533	0.2	427	0.2	217	103	241	15	5.0	0.2	812	97	2397
	0.75	-297	4	24	0.4	0	1060	0.2	409	0.2	479	133	389	34	5.6	0.8	1162	60	3658
	0.50	-236	4	24	0.6	0	415	0.2	569	0.2	115	108	210	43	4.3	2.2	726	50	2372
	0.25	-178	4	16	0.6	0	481	0.2	634	0.2	90	112	180	39	4.3	1.2	820	26	2477
5/12/08	1.20	-291	4	26	0.2	0	1001	6.4	579	0.2	470	139	224	60	12.9	2.3	968	31	3255
	1.00	-284	5	31	0.1	0	996	0.2	463	0.1	477	130	231	32	10.0	0.2	990	69	2990
	0.75	-307	4	13	0.2	0	867	0.2	434	0.2	375	139	218	34	5.6	0.2	880	21	2655
	0.50	-255	4	11	0.3	0	704	0.2	460	0.2	299	113	182	38	14.0	0.2	833	12	2501
	0.25	-158	NA	NA	NA	NA	NA	NA	NA	NA	NA	NA	NA	NA	NA	NA	NA	NA	NA
6/5/08	1.20	-295	4	18	0.2	0	1251	9.2	477	0.2	543	160	301	54	10.1	0.3	950	87	3470
	1.00	-288	4	25	0.1	0	1015	0.2	440	0.2	485	120	266	36	9.4	0.3	968	36	3071
	0.75	-256	4	13	0.1	0	NA	NA	NA	NA	NA	NA	NA	NA	NA	NA	NA	NA	NA
	0.50	-249	4	19	0.2	0	NA	NA	NA	NA	NA	NA	NA	NA	NA	NA	NA	NA	NA
	0.25	-223	3	15	0.4	0	NA	NA	NA	NA	NA	NA	NA	NA	NA	NA	NA	NA	NA
7/16/08	1.20	-263	5	6946	0.1	2.0	431	0.3	375	0.1	291	115	232	22	11.8	1.0	806	58	2433
	1.00	-264	5	5573	0.1	0.9	617	0.1	415	0.1	282	102	201	10	7.9	0.2	787	24	2351
	0.75	-249	4	4171	0.3	0.3	491	0.1	279	0.1	160	82	140	43	8.8	1.0	603	73	1785
	0.50	-119	4	4584	0.5	0.8	462	0.1	311	0.1	98	119	189	31	5.1	0.2	644	12	1941
	0.25	54	NA	NA	NA	NA	NA	NA	NA	NA	NA	NA	NA	NA	NA	NA	NA	NA	NA

Table S.B.4 Pore water and leachate composition in Treated Columns- Replicate B

Date	Depth	Eh	pH	TOC	DO	H_2S	Acidity	Al	Ca	Cu	Fe	K	Mg	Mn	Na	Zn	S	Si	SO_4
Unit	m	mv	-								(mg/L)								
7/24/08	1.20	-268	5	6168	0.4	0.7	360	0.1	391	0.1	145	102	243	19	10.2	0.1	650	62	2340
	1.00	-271	5	4498	0.2	0.2	364	0.1	307	0.1	127	93	194	6	8.8	0.1	631	29	1904
	0.75	-266	5	3948	0.3	0.8	621	0.1	383	0.0	208	89	140	38	11.8	0.2	624	43	2031
	0.50	-105	NA	NA	NA	NA	NA	NA	NA	NA	NA	NA	NA	NA	NA	NA	NA	NA	NA
	0.25	-41	NA	NA	NA	NA	NA	NA	NA	NA	NA	NA	NA	NA	NA	NA	NA	NA	NA
8/5/08	1.20	-296	5	5548	0.1	3.0	291	0.1	407	0.1	119	89	183	18	9.0	0.1	676	56	2101
	1.00	-281	5	4685	0.1	0.4	171	0.0	370	0.1	30	85	179	7	10.9	0.1	608	46	1814
	0.75	-289	5	4650	0.2	0.1	151	0.1	342	0.1	17	74	203	24	2.9	0.1	618	8	1861
	0.50	-166	5	3485	0.4	0.5	146	0.0	189	0.0	29	94	116	36	3.0	0.1	330	14	1193
	0.25	-11	NA	NA	NA	NA	NA	NA	NA	NA	NA	NA	NA	NA	NA	NA	NA	NA	NA
5/10/09	1.20	-278	7	3099	0.1	1.5	0	0.1	483	0.1	31	117	182	3	6.6	0.1	799	13	1790
	1.00	-130	6	2453	0.1	0.6	0	0.1	217	0.1	22	91	88	0	3.0	0.1	365	7	969
	0.75	-113	7	848	0.2	0.3	0	0.1	423	0.1	27	118	101	0	4.4	0.1	371	10	1238
	0.50	-128	6	7987	0.2	0.9	516	0.1	142	0.1	221	112	159	14	15.4	0.2	554	12	1317
	0.25	-155	7	5902	0.3	0.5	85	0.1	196	0.1	71	166	148	6	12.5	0.3	555	15	1265
6/25/09	1.20	-256	7	1247	0.1	2.0	0	0.1	556	0.1	19	137	219	3	8.3	0.1	714	15	2195
	1.00	-260	6	5033	0.1	0.7	0	0.1	540	0.1	52	141	274	1	8.6	0.3	815	16	2450
	0.75	-116	7	1898	0.1	3.5	110	0.1	114	0.1	56	144	195	1	12.5	0.1	412	19	1292
	0.50	-101	6	5792	0.1	2.0	775	0.1	152	0.1	410	150	146	19	15.0	0.2	501	15	1635
	0.25	-153	5	5530	0.5	1.5	67	0.1	378	0.1	21	136	142	10	13.5	0.2	354	20	1483
7/22/09	1.20	-301	7	3365	0.1	3.0	0	0.1	273	0.1	21	141	245	1	8.0	0.1	505	17	1706
	1.00	-242	NA	NA	NA	NA	NA	NA	NA	NA	NA	NA	NA	NA	NA	NA	NA	NA	NA
	0.75	-261	NA	NA	NA	NA	NA	NA	NA	NA	NA	NA	NA	NA	NA	NA	NA	NA	NA
	0.50	-220	NA	NA	NA	NA	NA	NA	NA	NA	NA	NA	NA	NA	NA	NA	NA	NA	NA
	0.25	-236	NA	NA	NA	NA	NA	NA	NA	NA	NA	NA	NA	NA	NA	NA	NA	NA	NA

Appendix C- DRAINMOD Software

Drainmod is a water management design software developed by Dr.Wayne Skaggs at the Department of Biological & Agricultural Engineering, North Carolina State University, Raleigh, NC in 1980. This model is basically a water budget model. In a thin layer of the soil, the applied water balance during time increment of Δt is:

$\Delta V_a = D + ET + DS - F$ Reaction S-C-1

ΔV_a: change in air volume (cm)

D: lateral drainage (cm)

ET: evapotranspiration (cm)

DS: deep seepage (cm)

F: infiltration (cm)

All terms in right side of the above equation will be estimated using water table elevation, soil water content, and soil properties based on the following reaction:

$P= F + \Delta S + RO$ (cm) Reaction S-C-2

P: precipitation (cm)

F : infiltration (cm)

ΔS: change in volume of water stored in the surface (cm)

RO: runoff (cm)

Fig. S.C.1 to Fig. S.C. 3 shows the applied input file for the fine grained tailings of the Ore Knob tailings pile. The Drain Vol-UpFlux and Infiltration subsection of the soil category are

automatically created based on input soil file. Depth of soil in crop subsection was assumed the minimum of 1 cm in tailings pile and up to 40 cm for vegetated watershed area.

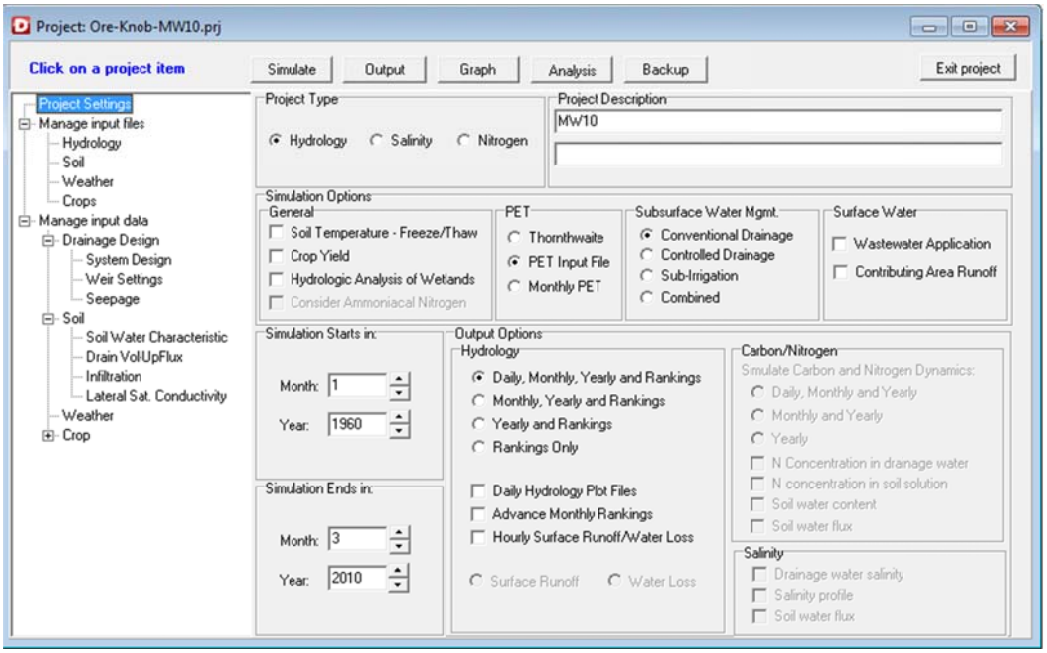

Fig. A.C.1 Drainmod input file for the fine grained tailings of the Ore Knob tailings pile

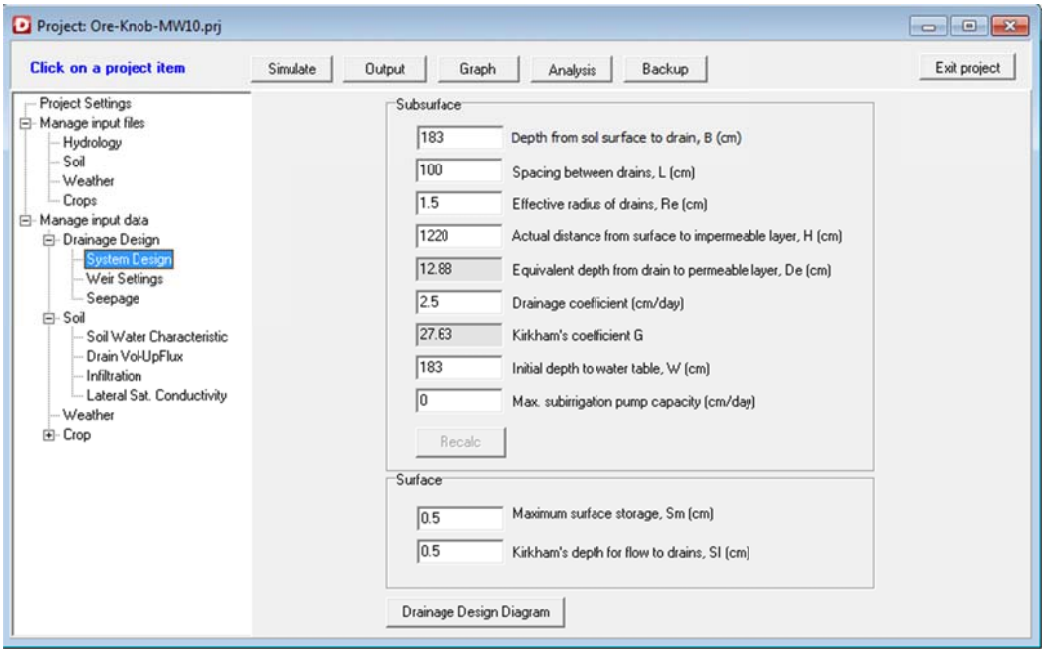

Fig. A.C.2 System design input file for the fine grained tailings of the Ore Knob tailings pile

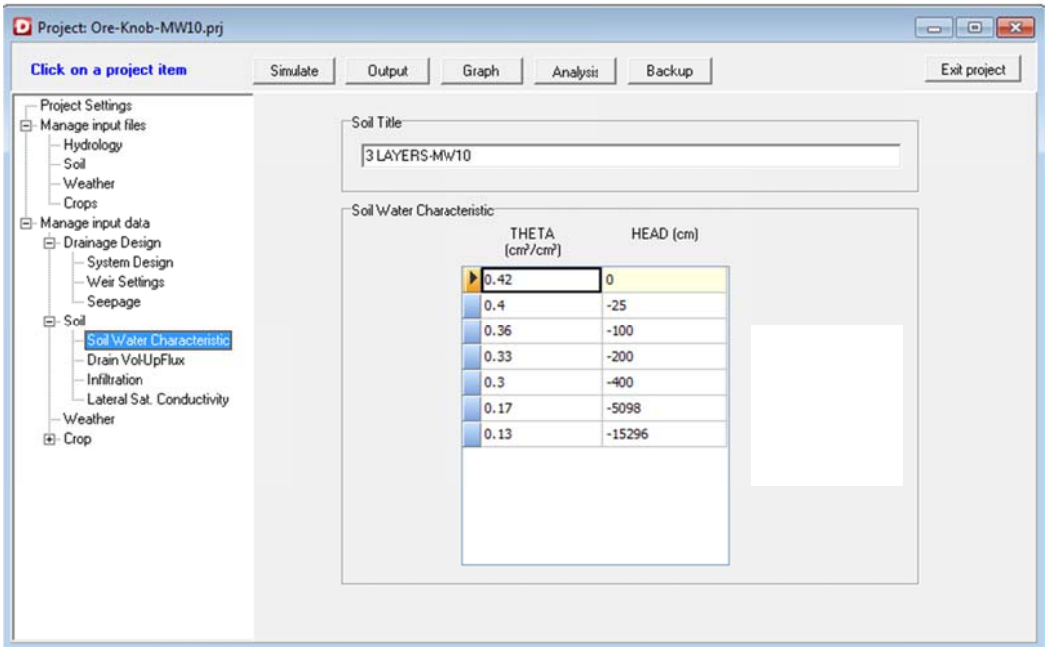

Fig. A.C.3 Soil water characteristic input file for the fine grained tailings of the Ore Knob tailings pile

Appendix D- MIN3P Software

As a part of this research, the geochemical model MIN3P was applied to simulate 1D acid mine drainage generation and treatment in the experimental columns. MIN3P is a multicomponent reactive transport model capable of simulating variably saturated flow (Mayer 1999). The model uses a local mass balance finite volume method using global implicit solution technique (Steefel and Lasaga 1994). This technique considers transport processes and reaction processes simultaneously. The model simulates batch problems and variably saturated flow models by solving coupled reactive transport equations and is capable of simulating advection-dispersion in aqueous phase and diffusion in gas phase. Aqueous ion complexation, oxidation-reduction, ion exchange, gas dissolution-exsolution and mineral dissolution-precipitation reactions can be simulated. MIN3P will always use a kinetic formulation for dissolution precipitation reactions. However, the rate expression can be set to obtain quasi-equilibrium behavior. Kinetically-controlled reactions in MIN3P are divided as reversible/irreversible and surface/transport controlled reactions (Berner 1978; Steefel and Lasaga 1994). The changes in reaction type and rate can be applied in data base file.

The MIN3P model solves the governing equation for Darcy type fluid in variable saturated media. By neglecting convective oxygen flow and assuming a passive air phase, the mass conservation equation can be written as (Mayer 2002):

$$S_w S_S \frac{\partial h}{\partial t} + \phi \frac{\partial S_w}{\partial t} - \nabla.\left[k_{rw} \overline{K} \nabla h\right] - Q_w = 0 \qquad \text{Reaction S.D.1}$$

S_w : volumetric water saturation ($m^3\ m^{-3}$)

S_s: specific storage coefficient (m^{-1})

H: hydraulic head (m)

t: time (s)

ϕ: porosity ($m^3\ m^{-3}$)

Q_w : source–sink term (s^{-1})

k_{rw} : relative permeability of the porous medium (dimensionless)

$\overline{K}$: saturated hydraulic conductivity tensor ($m\ s^{-1}$).

The nonlinear functions defining the water retention curves ($S_w - \psi$) and relative permeability functions ($k_{rw} - \psi$) are based on Van Genuchten (1980) and Wo¨sten and Van Genuchten (1988). The transport equation for advective–dispersive transport of the dissolved phase components is written as (Mayer et al. 2002):

$$\frac{\partial}{\partial t}[S_W \phi .. T_j^w] + \frac{\partial}{\partial t}[S_g \phi .. T_j^g] + \nabla[q_w T_j^w] - \nabla[S_W \phi .. D_w \nabla T_j^w] - \nabla[S_g \phi .. D_g \nabla T_j^g] - Q_j^{w,w} - Q_j^{w,s} - Q_j^{w,ext} - Q_j^{g,ext} = 0$$

J= 1 to N_c Reaction S.D.2

S_g : gas phase saturation ($m^3\ m^{-3}$),

T^w_j, T^g_j ($kg\ m^{-3}\ H_2O$): total water and gas phase concentrations of component j

q_w (m^{-1}): Darcy fluid flux

D_w, D_g ($m^2\ s^{-1}$): dispersion tensors for the water and gas phase components

$Q_j^{w,w}$, $Q_j^{w,s}$: contributions to T_{wj} from intra-aqueous and precipitation– dissolution reactions

$Q_j^{w,ext}$, $Q_j^{g,ext}$: external source–sinks for the aqueous and gas phases

Kinetically controlled reactions are approximated as reversible, elementary processes. Based on the principle of detailed balancing, rate expressions for intra-aqueous kinetic reactions, can be written as (Lasaga 1998; Lichtner 1996):

$$R_k^a = -k_k^a \prod_{\upsilon_{kj}^a<0} (\gamma_j^c C_j^c)^{\upsilon_{kj}^a} [1 - \frac{IAP_k^a}{K_k^a}] \qquad \text{Reaction S.D.3}$$

k_k^a : rate constant of the forward reaction

IAP_k^a : ion-activity product of the reaction

K_k^a: equilibrium constant

This rate expression is valid for elementary reversible reactions (Lasaga 1998).

The general rate expression for surface controlled dissolution-precipitation reaction can be expressed as:

$$R_k^{ms} = -S_i k_k^m [\underbrace{\prod_{\substack{j=1 \\ \sigma_{kj}^{mt}\neq 0}}^{N_c} (T_j^a)^{\sigma_{kj}^{mt}}}_{\text{fractional order } T_j^a} \underbrace{\prod_{\substack{j=1 \\ \sigma_{kj}^{mc}\neq 0}}^{N_c} (\gamma_j^c C_j^c)^{\sigma_{kj}^{mc}}}_{\text{fractional order } C_j^a} \underbrace{\prod_{\substack{j=1 \\ \sigma_{kj}^{mx}\neq 0}}^{Nx} (\gamma_j^x C_j^x)^{\sigma_{kj}^{mx}}}_{\text{fractional order } C_j^x} \underbrace{\prod_{\substack{j=1 \\ K_{kj}^{m,mo}}}^{Nc} \frac{T_j^a}{K_{kj}^{m,mo} + T_j^a}}_{\text{Monod } T_j^a} \underbrace{\prod_{\substack{j=1 \\ K_{kj}^{m,in}}}^{Nc} \frac{K_{kj}^{m,in}}{K_{kj}^{m,in} + T_j^a}}_{\text{Inhibition } T_j^a}] \underbrace{[1 - \frac{IAP_k^m}{K_k^m}]}_{\text{Affinity term}}$$

Reaction S.D.4

R_k^{ms} (mol dm^{-3} porous medium s^{-1}): reaction rate for the k^{th} surface-controlled dissolution-precipitation reaction

Si (m^2mineral dm^{-3}): reactive surface area corresponding to the mineral phase A_i^m

k_k^m : rate constant for dissolution of the mineral

σ_{kj}^{mt}, σ_{kj}^{mc}, σ_{kj}^{mx} : reaction orders with respect to the total aqueous component concentrations and the activities of the dissolved species

$K_{kj}^{m,mo}$ and $K_{kj}^{m,in}$: the half saturation constants and inhibition constants

Affinity terms can be excluded for irreversible dissolution- precipitation problem. Details on rate expressions of various rate expressions for mineral dissolution-precipitation and transport controlled modeling are presented in Mayer et al. 1999 and 2002.

Steady state variably saturated flow with reactive transport condition was simulated during 593 days of columns performance. Eighteen primary aqueous components (H_4SiO_4, H^{+1}, $O_2(aq)$, Fe^{+2}, Ca^{+2}, Mg^{+2}, Na^{+1}, Cu^{+2}, Cu^{+1}, Zn^{+2}, K^{+1}, Al^{+3},Fe^{+3}, HS^{-1}, CO_3^{-2}, Mn^{+2}, Mn^{+3}, SO_4^{2-}) were included in the simulation. Mineral composition was applied based on the XRD identified minerals. Sulfide minerals oxidation rate (e.g., pyrrhotite and pyrite) was assumed to be diffusion controlled based on the shrinking core model (Davis and Ritchie 1986). Columns were simulated as four homogenous layers of tailings over the gravel layer with each layer containing five control volumes. Physical hydrological parameters of the tailings in the model were based on the water retention curve of the parent material. Background chemistry of the tailings was set as the columns leachate at the start of monitoring (Behrooz and Borden 2012). Recharge water chemistry was set to the rainwater chemistry based on Mayer 2002.

For flow simulation, a second type (Neumann-constant flux) boundary condition was applied to the columns top. Amount of infiltrated water was obtained based on the amount of

drained water during sampling period. A first type (Dirichlet- constant head) boundary was applied to the bottom of columns representing the initial head in the columns.

The model initial conditions were established by first equilibrating the pore water with the solid phase assuming the column was completely saturated. Once the aqueous phase was in equilibrium, the boundary condition on the column bottom was changed causing water to drain out the bottom and air to enter the top. This resulted in a dramatic change in geochemical conditions within the simulated column. These dramatic changes resulted in numerical instability and the model crashed. A variety of different approaches were attempted to resolve this problem including forcing the model to use a very short time step, altering the unsaturated flow parameters, and changing the mineral components entered into the model. Unfortunately, none of these approaches were successful. Future work should explore two potential approaches: (1) evaluating alternative numerical methods to solve the model equations; and (2) using a smaller number of mineral species in the model simulations.